UNIVERSITÀ DEGLI STUDI DI GENOVA

DIME/TEC

Dipartimento di Ingegneria Meccanica Energetica Gestionale e dei Trasporti

Sezione di Termo-Energetica e Condizionamento Ambientale

Dottorato in Ingegneria Meccanica Energetica e Gestionale
Curriculum Fisica Tecnica

XXXI Ciclo

Ing. Ermanno Lo Cascio

Energy management and guidelines to digitalisation of integrated natural gas distribution systems equipped with expander technology

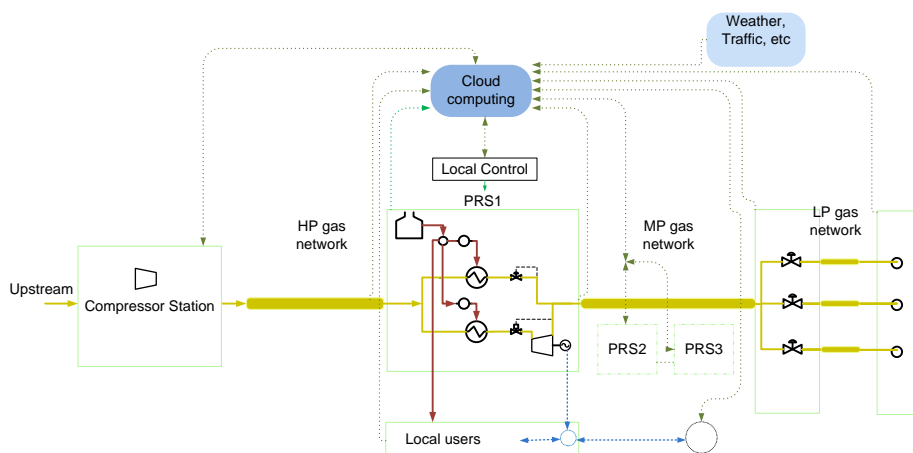Tutor: Prof. Ing. Corrado Schenone

Aprile 2019

To the Ambiguity.
The only reason for which we are here.

"It is important to realize that in physics today, we have no knowledge of what energy is."

Richard Feynman, 1964.

Abstract

In a swirling dynamic interaction, digital innovation, environment and anthropological evolution are swiftly shaping the smart grid scenario. Integration and flexibility are the keywords in this emergent picture characterised by a low carbon footprint. Digitalisation, within the natural limits imposed by the thermodynamics, seems to offer excellent opportunities for these purposes. Of course, here starts a new challenge: how digital technologies should be employed to achieve these objectives? How would we ensure a digital retrofit does not lead to a carbon emission increase? In author opinion, as long as it remains a generalised question, none answer exists: the need to contextualise the issue emerges from the variety of the characteristics of the energy systems and from their interactions with external processes. To address these points, in the first part of this research, the author presented a collection of his research contributions to the topic related to the energy management in natural gas pressure reduction station equipped with turbo expander technology. Furthermore, starting from the state of the art and the author's previous research contributions, the guidelines for the digital retrofit for a specific kind of distributed energy system, were outlined. Finally, a possible configuration of the ideal ICT architecture is extracted. This aims to achieve a higher level of coordination involving, natural gas distribution and transportation, local energy production, thermal user integration and electric vehicles charging. Finally, the barriers and the risks of a digitalisation process are critically analysed outlining in this way future research needs.

Contents

1. Preface

1.1. Digitalization of the energy sector

During the past two years, the 90 % of the data in the world were created [1]. 2.5 quintillion bytes of data created every day [1]. Advances in computing power and efficiency have enabled more powerful and sophisticated analytics, such as artificial intelligence and automation [2]. For example, advanced analytics enable sophisticated control of building and industrial process equipment [2].

In this context, the electricity sector is becoming more decentralized with the proliferation of distributed energy resources connected directly to local distribution grids [2]. Digitalization is allowing customers to become more active in adapting their own electricity production, use and storage [2]. This rise of small-scale, distributed generation allows consumers to increasingly have the choice to buy electricity from a retailer or to produce at least part of it themselves, becoming "prosumers" [2]. Then, withdrawals and injections of electricity from and into the grid can be actively managed using new digital technology.

In the same way, energy system integration could lead to higher degree of flexibility which could lead to optimized energy conversion and management at local level if appropriate digital technology is employed.

However, due to the fragmented nature of the natural gas distribution sector, the digitalization process of natural gas pressure reduction stations integrated with external users might require a "case-by-case" design approach to be accomplished.

1.2. Gas distribution in Europe and Italy

The global demand for natural gas (NG) is expected to grow by up to 50% by 2040 according to the International Energy Agency, and NG is considered the most promising fossil fuel of the 21st century [3]. Therefore, the European natural gas transmission infrastructure has been continuously expanding over recent decades to satisfy new territory needs. For instance, the total Italian infrastructure length has growth approximately 4% in less than 9 years [4]. A similar evolution was noticed worldwide, with the global demand growing by more than 30% over the last 15 years [5]. According BP statistics [6], in 2017 the total World production is about 3680.4 billion cubic meters of which 951.5 were produced by North America while central America counts 179 billion cubic meters. In Europe, the NG production in 2017 was about 241.9 billion cubic meter. Middle East and Asia counts about 659.9 and 607 billion cubic meter respectively. The NG supply chain consist in different parts: upstream, midstream and downstream. After the exploration and production (upstream), the midstream activities involves the natural gas import in as liquid (LNG via ships) or gas phase (via pipeline). In this last case the NG pressure is increased for transmission purposes by means of the compressor stations while the LNG is regasified before being injected in the pipeline system. Finally, the NG pressure is lowered in city gate stations (pressure reduction stations) to be

distributed to users. The entire supply chain is owned by different operators. Normally, upstream, midstream and downstream activities are conducted by different companies. For example, in Italy the upstream activities are managed by ENI while the midstream activities are conducted by SNAM and finally, the distribution is done by IREN, HERA, etc. and other similar companies.
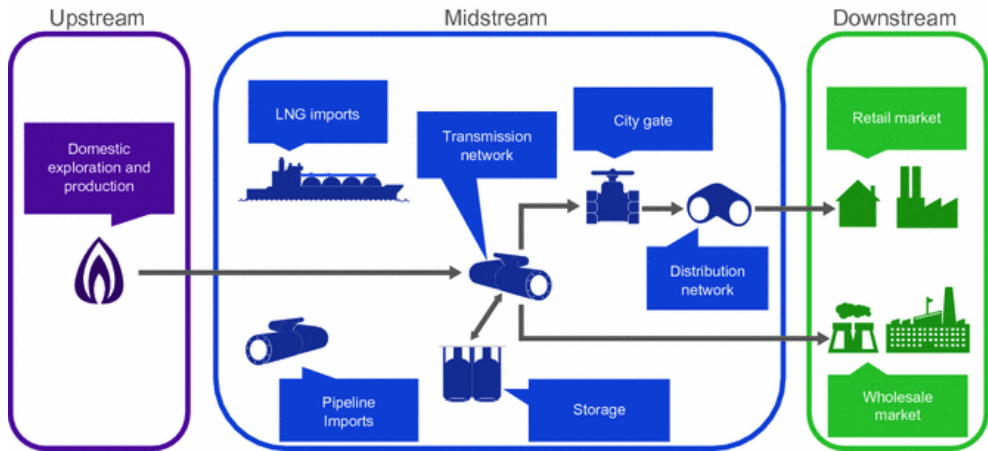
Figure 1. Natural gas supply chain [7].

More in details, as regard to the transmission infrastructure, it is generally composed of different subparts: compression stations, transportation, storage, pressure regulation stations (PRSs) and distribution. The role of PRSs is to ensure a certain pressure drop between the transportation and distribution nodes. NG pressure regulation is commonly achieved by throttling valves. However, it is possible to upgrade this process, enabling energy recovery from the pressure drop by implementing turbo expander (TE) technology or different type of gas expanders (screw, piston etc). The pressure drop along the NG pipelines is used to generate electricity that can be stored locally or returned to the utility grid. In this case, the NG preheating process, which is fundamental to avoid the formation of methane hydrate, would require higher thermal energy

than that of the dissipative process. In Italy, the overall pipeline length is about 34628 km [9]. *SNAM* company, covering 93% of NG transportation grid, counted 8962 redelivery points in 2015 [9].

EU natural gas flows
2017, % | bcm

Algeria 7.91% | 32.3bcm
LNG 11.61% | 47.4bcm
Netherlands 10.18% | 41.6bcm
Norway 27.28% | 111.5bcm
Russia 40.32% | 164.8bcm

Belgium 5.50% | 22.47bcm
France 11.21% | 45.82bcm
Germany 19.81% | 80.95bcm
Italy 15.97% | 65.27bcm
Netherlands 7.44% | 30.41bcm
Other 29.78% | 121.72bcm
United Kingdom 10.29% | 42.04bcm

9.4bcm
23.9bcm
3.7bcm
17.9bcm
6.8bcm
1.4bcm
5.6bcm
4.0bcm

■ Libya ■ Other ■ Turkey

■ Other: all the remaining EU countries (so excluding France, Italy, Germany, UK, Belgium, and Netherlands)

Figure 2. Natural gas flows [7]

REFERENCES

[1]   2.5 quintillion bytes of data created every day. How does CPG & Retail manage it?   Available   online: https://www.ibm.com/blogs/insights-on-

11

business/consumer- products/2- 5-quintillion-bytes- of-data-created-every-day-how-does-cpg-retail- manage-it/ (accessed 19/09/2018).

[2]   Digitalization & Energy, International Energy Agency. October 2017. Available online: http://www.iea.org/digital/, (accessed 19/09/2018).

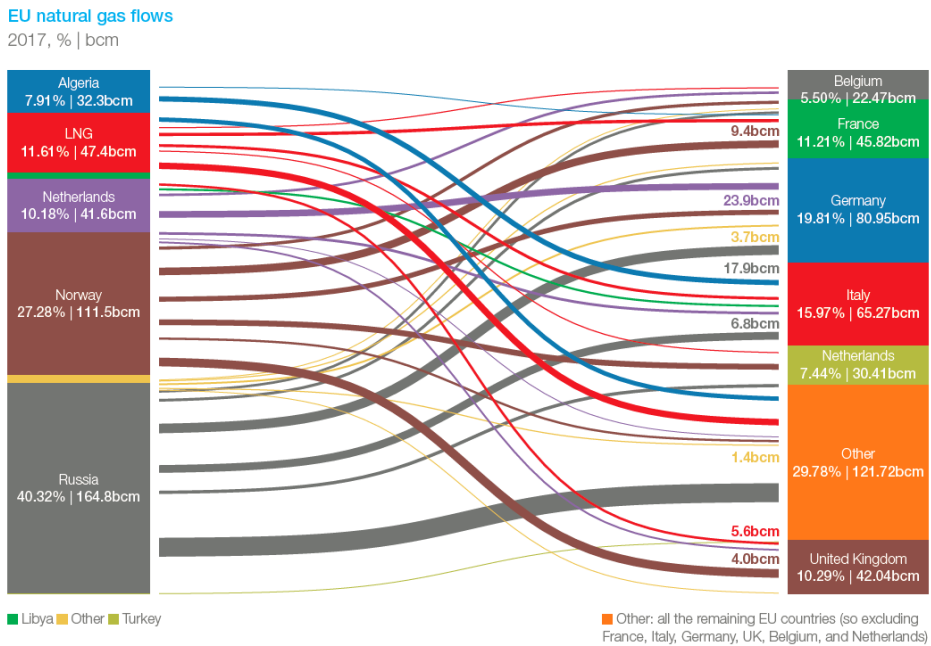[3]   W. E. Outlook 2016,   available   online: http://www.worldenergyoutlook.org/publications/weo-2016/   (accessed 23/03/2017).

[4]   Capacita' di trasporto, available online: http://www.snamretegas.it/it/servizi/Anno-termico_2016_2017/Capacita_trasporto/ (accessed 06/04/2017).

[5]   A. Toscano, F. Bilotti, F. Asdrubali, C. Guattari, L. Evangelisti, C. Basilicata. Recent Trends in the World Gas Market : Economical , Geopolitical and Environmental Aspects. Sustainability 2030; pp. 1:24, (2016).

[6]   BP Statistical Review of World Energy. June 2018. Available online: https://www.bp.com/content/dam/bp/business-sites/en/global/corporate/pdfs/energy-economics/statistical-review/bp-stats-review-2018-full-report.pdf (accessed 11/03/2019).

[7]   Shell International and The Development Research Center, Ishwaran M., King W., Haigh M., Lee T., Nie S. (2017) An Overview of International Regulatory Experience. In: Shell Centre, The Development Research Center (DRC) of the State Council of the People's Republic of China (eds) China's Gas Development Strategies. Advances in Oil and Gas Exploration & Production. Springer, Cham (11/03/2019).

[7]   The European Gas Market in 10 charts. Available online: https://www.mckinseyenergyinsights.com/insights/the-2017-european-gas-market-in-10- charts/, (accessed 19/09/2018).

[8]   Gas transportation companies. Available online http://www.autorita.energia.it/it/dati/elenco_dati.htm (accessed 24/07/2017).

[9]   Redelivery points - SNAM. Available online: http://www.snamretegas.it/en/services/New_Delivery_Redelivery_Points/

(accessed 24/07/2017)

1.3. Aim and scope of the work

The aim of this work consists in the definition of technical guidelines for the digitalization of a specific kind of distributed, integrated energy system comprising natural gas distribution, district heating networks and power production. To design the technical guidelines, the author mainly employed his previous research contributions, and used a holistic approach to identify the implementation of a digital retrofit. In fact, all the possible latest system configurations, management strategies and energy technologies are taken in consideration; thus, ensuring the digitalization process to be properly accomplished: the proper ICT architecture is identified and key process parameters have been investigated. To be more precise, the numerical models employed have been created and properly validated based on real data deriving from a demonstrator constructed within the European CELSIUS project framework [1]. Finally, the previous research contributions of the author mainly involved the formalization of the research question and the modeling activity, while the actual contribution of this work with respect to the author's previous research outcomes can be summarized in the following points:

● An in-depth analysis of the most recent pressure reduction station configurations, management strategies and energy technologies.

● The identification of the key parameters involved in the digitalization process, at system and global level based on an advanced modeling activity.

● The preliminary design of the ICT architecture to enable integrated control and optimisation.

● An insight relatives to the barrier and risks of the digitalization of the gas distribution sector.

● A discussion relative to the regulatory framework and the possibility of new business models.

As shown in figure 3, this work is organized in six main phases. The first one is related to a critical, in-depth review of the state-of-the-art in order to identify the most common system configurations that can be employed during a PRSs retrofitting projects. Starting from literature and the author previous research contributions, the author identify the key process parameters to be monitored and the external information to be acquired to enable an optimal system management and an ideal coordination with external processes (phase 2). Based on these information, the ICT architecture is designed (phase 3). Further, the measuring and verification strategy is presented. This post activity, is based on dynamic modeling of the system (phase 4). Finally, a new business model based on a cooperative approach is introduced (phase 5). Concluding, a discussion and recommendation section is presented (phase 6).

1	• In-depth analysis of the state of the art
2	• Identification of the key paramenters for control optimization starting from previous research contribution of the author
3	• Preliminary design of the ICT architecture
4	• Performance monitoring and verification
5	• New business model identification
6	• Discussion, reccomendation and best practices.
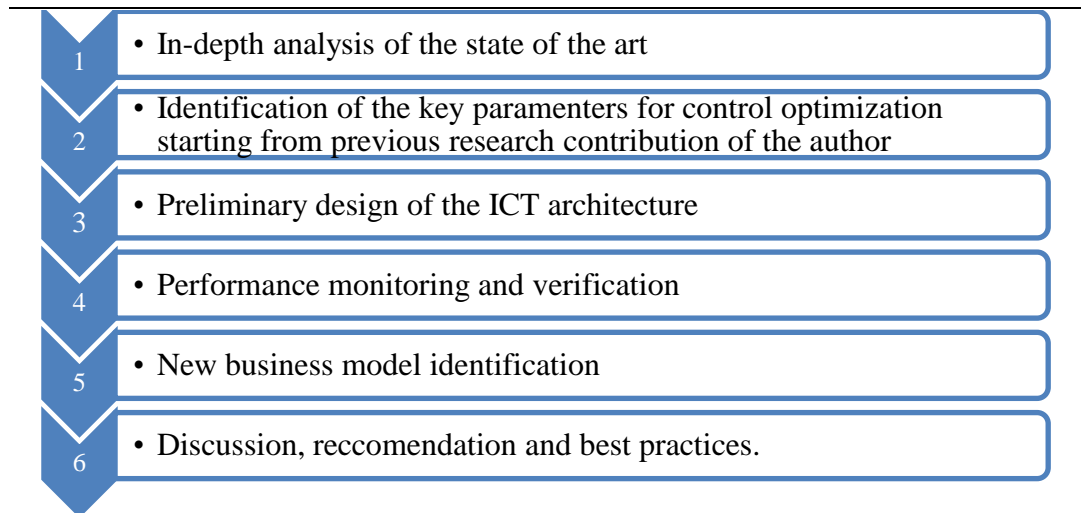
Figure 3. Work structure.

REFERENCES

[1] CELISUS Smart Cities, available online: http://celsiuscity.eu/, (accessed 04/10/2018).

2. Literature Review

In the following sections, the author provide a state-of-the-art overview and an insight of the most recent researches related to the modeling activity conducted.

2.1. State of the art overview

In the world's transition to a sustainable energy scenario, natural gas will keep playing a key role for residential and commercial sectors for most countries [1]. After being gathered and processed, the main phases for natural gas are transportation, storage, and distribution. Normally, the natural gas pressure is raised to 70 bars by means of compressor stations for a proper transportation through the transnational and national

pipelines until the distribution nodes. At this stage, so-called pressure reduction stations (PRS) are responsible for metering and reducing the gas pressure to the desired set-point for distribution purposes. Here, the natural gas pressure drop is normally induced by employing Joule-Thomson valves, thus, dissipating the gas energy. To prevent methane hydrates from being formed [2], the natural gas is normally preheated to temperatures that range between 40ºC and 60ºC depending on system operating conditions and the natural gas composition. In order to obtain a more sustainable process, a smart technological solution consists of the use of a turbo-expander (TE) instead of the Joule-Thomson valves, where the aim of the TE is to harvest energy from the gas pressure drop.

The potential energy that might be recovered from PRSs has become an interesting issue for the research community. This aspect is also emphasized by the growing number of PRS; for instance, in Turkey, according to Neseli et al. [3], the number of PRS increased from 274 in 2010 to 320 in 2012, and in [3], for a single PRS, a potential electricity recovery of 4.11 GWh/year was estimated for an annual natural gas mean flow rate of approximately 4.953 kg/s, with a maximum of 6.36 GWh/year for the highest natural gas flow scenario. Borelli et al. [4] used numerical dynamic simulations to calculate a potential energy recovery of approximately 2.9 GWh/year for a total preheating need of approximately 3.1 GWh/year. In general, the energy recovery depends on the natural gas flow rate, the component characteristics and the pressure drop, as clearly highlighted in the literature [5], [6], [7] and [8].

Technological innovations in natural gas networks with energy recovery have been increasingly demonstrated by recent studies in which different system configurations have been analysed. Howard et al. [9] investigated a hybrid version of a TE application in which a portion of the preheating energy was provided by a molten carbonate fuel cell working with natural gas. The results showed that the maximum efficiency of a 12.000 scm per hour TE increased by

approximately 10% after implementing the fuel cell. In this case, the total power production was approximately 0.934 GWh/year. To decrease the fuel consumption, Farzaneh-Gord et al. [10] considered the possibility of employing a geothermal heat exchanger to boost the preheating process. However, this configuration does not consider the use of TE technology for waste energy recovery (WER). Arabkosarh et al. [11] investigated the possibility of coupling solar thermal collectors and PRSs. Here, simple payback periods of 2.3 years and 6.3 years were estimated with and without implementation of the TE. Kostowski et al. [12] reported the integration of a PRS with a cogeneration unit to propose a thermo-economic analysis, and the results seemed to show economic advantages over boilers. Farzaneh-Gord et al. [13], [14] studied the feasibility of employing uncontrolled and controlled linear heaters with a solar system in PRSs. Another study was presented by Farzaneh-Gord et al. [15], who focused on the possibility of employing vertical ground-coupled heat pumps and modelled the system by writing energy and thermal equations. Economic analysis was then adopted for selecting the most efficient layout of the geothermal system. In [16], with the same method, the authors identified the technical criterion for economic justification of employing combined heat and power (CHP) technologies in PRSs. In a similar manner, Arabkoohsar et al. [17] provided an energetic and economic analysis for PRSs coupled with CHP. The thermodynamic deterministic model was subsequently linked to an economic cost benefit analysis to evaluate the efficiency of the considered system configurations and, therefore, the optimal design. Robust traditional methods proved to be effective in guiding the integration of energy recovery from PRSs with different renewable energy sources, although they were challenging to develop. Finally, in [18], the possibility of reducing the water process temperature was investigated; this is a key aspect to exploit, for instance, with regard to low-temperature waste heat. Kostowski et al. [19] used a thermodynamic model of a PRS to define the thermoecological cost of

electricity production; this cost has the advantage of providing a complete picture that includes not only the analysed system but also the production process of the resources consumed by that system, as well as the emission of pollutants. The optimization of the system control was also investigated in other studies. A timing optimization model of a single-stage, single-acting, reciprocating expansion engine was presented in [20]. Pellegrino and Villecco [21] proposed an optimal control approach based on a fuzzy logic system; in this research, the proposed widely used optimization and control method was specifically applied for the first time to energy recovery in PRSs. Without delving into the physics of the phenomenon, the fuzzy control achieved good results, with negligible investment costs, a calculated energy recovery larger than 15% and a decrease in the maintenance costs of approximately 15%. In [22], Lo Cascio et al. proposed a multi-objective mathematical model for PRS optimal control where the electrical energy produced by the TE was differentiated based on how the preheating phase was accomplished (renewable sources or fossil-fuel-based production). Their model is based on dynamic modelling through an operational formulation involving costs, environmental impact and the form of energy.

The optimal design issue of the PRSs was investigated by Sanaye and Nasab in [23], who proposed a relatively fast method to select the size and number of components for PRSs using an objective function defined as the sum of the income and expenses. Subsequently, the optimum values of nine decision variables were obtained by maximizing the objective function using the genetic algorithm optimization technique. According to the authors, this hybrid semi-empirical procedure permits efficiently calculating the optimal configuration for a wide range of operating parameters. However, the variability of the WER potential, which is dependent on the NG flow patterns for a given TE, was not considered in this study.

Recent studies, focused on optimal design of integrated natural gas pressure reduction stations [24], integration with parabolic trough solar collectors [25]. In addition, a technique to increase the energy production flexibility, called gas bagging, has been recently introduced by the author inb [26].

The performance assessment of the system in comparison with a baseline process, have been analysed in [27].

REFERENCES

[1]   W. E. Outlook 2016, available online: http://www.worldenergyoutlook.org/publications/weo-   2016/ (Accessed 21/03/2018).

[2]   J. Chen, J. Liu, G. Chen, C. Sun, M. Jia, B. Liu, S. Si, N. Ren Insights into methane hydrate   formation, agglomeration, and dissociation in water + diesel oil dispersed system   Energy Conversion and Management 86, pp. 886–891, (2014).

[3]   M. Alparslan, O. Ozgener, L. Ozgener. Energy and exergy analysis of electricity generation from natural gas pressure reducing stations. Energy Conversion and Management 109, pp.120-93, (2015).

[4]   Borelli, F. Devia, E. Lo Cascio, C. Schenone, and A. Spoladore. Combined Production and Conversion of Energy in an Urban Integrated System. Energies 1, pp. 17-9 (2017).

[5]   E. Ashouri, F. Veysi, E. Shojaeizadeh, M. Asadi. Journal of Natural Gas Science and Engineering The minimum gas temperature at the inlet of

regulators in natural gas pressure reduction stations (CGS) for energy saving in water bath heaters. Journal Natural Gas Science; 230, pp. 240-21 (2014).

[6] I. Andrei, T. Valentin, T. Cristina,T. Niculae. Recovery of Wasted Mechanical Energy from the Reduction of Natural Gas Pressure. Procedia Enginerring 986, pp. 990-69, (2014).

[7] D. Borelli, F. Devia, M. Marré Brunenghi, C. Schenone, A. Spoladore. Waste energy recovery from natural gas distribution network: Celsius project demonstrator in Genoa. Sustainability 16703, pp. 16719-7, (2015).

[8] I. Fletcher,C.S. Cox, W.J.B. Arden, A. Doonan. Modelling of a two-stage high-pressure gas reduction station. Applied Mathematical Modelling; 741, pp. 749-20, (1996).

[9] C. Howard, P. Oosthuizen, and B. Peppley. An investigation of the performance of a hybrid turboexpander-fuel cell system for power recovery at natural gas pressure reduction stations. Applied Thermal Enginering 2165, pp. 2170-31 (2011).

[10] M. Farzaneh-gord, R. Ghezelbash, A. Arabkoohsar, L. Pilevari, L. Machado. Employing geothermal heat exchanger in natural gas pressure drop station in order to decrease fuel consumption. Energy 164, pp. 176-83, (2015).

[11] A. Arabkoohsar, M. Farzaneh-gord, M. Deymi-dashtebayaz, L. Machado. A new design for natural gas pressure reduction points by employing a turbo expander and a solar heating set. Renewable Energy 239, pp. 250-81, (2015).

[12] W. J. Kostowski and S. Usón. Thermoeconomic assessment of a natural gas expansion system integrated with a co-generation unit. Applied Energy 101; pp. 58:66 (2013).

[13] M. Farzaneh-gord, A. Arabkoohsar, M. D. Dasht-bayaz, V. Farzaneh-kord. Feasibility of accompanying uncontrolled linear heater with solar system in natural gas pressure drop stations. Energy 41; pp 420:428, (2014).

[14]   M. Farzaneh-gord, A. Arabkoohsar, M. D. Dasht-bayaz, and L. Machado. Energy and exergy analysis of natural gas pressure reduction points equipped with solar heat and controllable heaters. Renewable Energy 72; pp. 258:270, (2014).

[15] M. Farzaneh-gord, R. Ghezelbash, M. Sadi, A. Jabari. Integration of vertical ground-coupled heat pump into a conventional natural gas pressure drop

station : Energy , economic and CO 2 emission assessment. Energy 112; pp. 998:1014, (2016).

[16]   V. Farzaneh-kord, A. B. Khoshnevis, A. Arabkoohsar, M. Deymi-dashtebayaz. Defining a technical criterion for economic justi fi cation of employing CHP technology in city gate stations. Energy 111, pp. 389:401, (2016).

[17]   A. Arabkoohsar, Z. Gharahchomaghloo, M. Farzaneh-gord, R. N. N. Koury. An energetic and economic analysis of power productive gas expansion stations for employing combined heat and power. Energy 133; pp. 737:748, (2017).

[18]   D. Borelli, F. Devia, E. Lo Cascio, C. Schenone.Energy recovery from natural gas pressure reduction stations : Integration with low temperature heat sources. Energy Conversion Management 159; pp. 274:283, (2018).

[19]   W. J. Kostowski, S. Usón, W. Stanek, P. Bargiel. Thermoecological cost of electricity production in the natural gas pressure reduction process. Energy 76; pp. 10:18, (2014).

[20]   M. Farzaneh-gord and M. Jannatabadi. Timing optimization of single-stage single-acting   reciprocating expansion engine based on exergy analysis. Energy Conversion Management   105; pp. 518:529, (2015).

[21]   Arcangelo Pellegrino and Francesco Villecco. Design Optimization of a Natural Gas Substation with Intensification of the Energy Cycle. Mathematical Problem Engineeing 2010; Article ID 294102; doi:10.1155/2010/294102.

[22]   E. Lo Cascio, D. Borelli, F. Devia, C. Schenone.Future distributed generation : An   operational   multi-objective optimization model for integrated small scale urban electrical,   thermal and gas grids. Energy Conversion and Management 143; pp. 348:359, (2017).

[23]   S. Sanaye and A. M. Nasab. Modeling and optimizing a CHP system for natural gas pressure reduction plant. Energy 40; pp. 358:369, (2012).

[24]   E. Lo Cascio, M.P. Von Friesen, C. Schenone. Optimal retrofitting of natural gas pressure reduction stations for energy recovery. Energy 153, pp. 387-399, (2018).

[25]   E. Lo Cascio, Z. Ma, C. Schenone. Performance assessment of a novel natural gas pressure reduction station equipped with parabolic trough solar

collectors. Renewable Energy 128, pp. 177-187, (2018).

[26]   E. Lo Cascio, E., B. De Schutter, C. Schenone. Flexible energy harvesting from natural gas distribution networks through line-bagging. Applied Energy 229, pp. 253-263, (2018).

[27]   E. Lo Cascio, D. Borelli, F. Devia, C. Schenone. Key performance indicators for integrated natural gas pressure reduction stations with energy recovery. Energy Conversion and Management 164,pp. 219-229, (2018).

3. Research contributions

3.1. CHP integration and optimal control

The integration of cogeneration units into PRS process issue, has been deeply analyzed by the research community during the recent years. In fact, Lazzaretto et al. presented an optimization procedure based on symbolic exergeconomic methodology for a system comprising a CHP and TE units in [1]. Sanaye et al. defined a relatively quick method to find optimal nominal component sizes for PRSs retrofits in [2]. Among all the possible PRSs configurations, Howard et al. investigated the possibility of accomplishing the pre-heating phase by using a molten carbonate fuel cell in [3]. Results show how the hybrid system (TE/fuel cell) may increase the efficiency by about 10 percent for certain cases. Kostowski et al. define a thermodynamic and economic analysis of TE application providing an interesting case study in [4].

In [5], the integration of cogeneration and its control has been investigated. In fact, here a multi-objective mathematical model for the control optimization of retrofitted PRSs integrated with thermal users. Referring to the pressure regulation process, the NG preheating phase could exploit fossil fuels, renewables or a mix of them. Depending on the system configuration, the proposed optimization model enables a proper differentiation based on how the NG preheating process is

expected to be accomplished in the following time intervals. This differentiation is achieved by weighting the electricity produced by the TE and linking it to customized energy remuneration tariffs. In the following sections, a generic formulation of the multi-objective model is given. Finally, the effectiveness of the model has been tested on an existing integrated urban system in the city of Genoa. Here, the thermal energy is provided by means of two redundant gas-fired boilers and a cogeneration unit. Furthermore, the whole system in thermally integrated with a district heating network. A numerical model, created with the software Honeywell UniSim Design Suite, is presented. Results have been compared with the optimal solutions achieved.

3.1.1 Methodology

The study has been carried out by following the methodology shown in figure 4. A mathematical model has been preliminarily developed and an existing integrated grid has been used as a case study. Based on this system configuration, a numerical dynamic model has been implemented by using commercial software *UniSim Design Suite* [6]. The numerical model created, allows users to analyze systems' transients. The *Peng-Robinson* state equation package has been used for this analysis. Furthermore, the current control logic of the existing system has been implemented within this model. Finally, a case scenario has been simulated. Results in terms of economic performance and environmental emissions have been compared with the optimal solution identified by the multi-objective model.

Figure 4. Methodology

3.1.2. Integrated micro-grid reference configuration

The proposed mathematical model refers to a generic integrated system configuration whose components are shown in figure 5. Here, the NG pressure drop is accomplished by means of throttling valves which are located in parallel to a TE, whose function is to recover energy. A CHP units and the gas-fired boilers are included in this system configuration, to provide the necessary heat to the process. Finally, the reference configuration is thermally integrated with a nearby DHN or, more generally, with an industrial process. The model refers to a given pressure drop which has to be maintained constant during the system operation. Finally, with appropriate modifications, the proposed model could be applied to different system configurations that may include non-dispatchable production units.
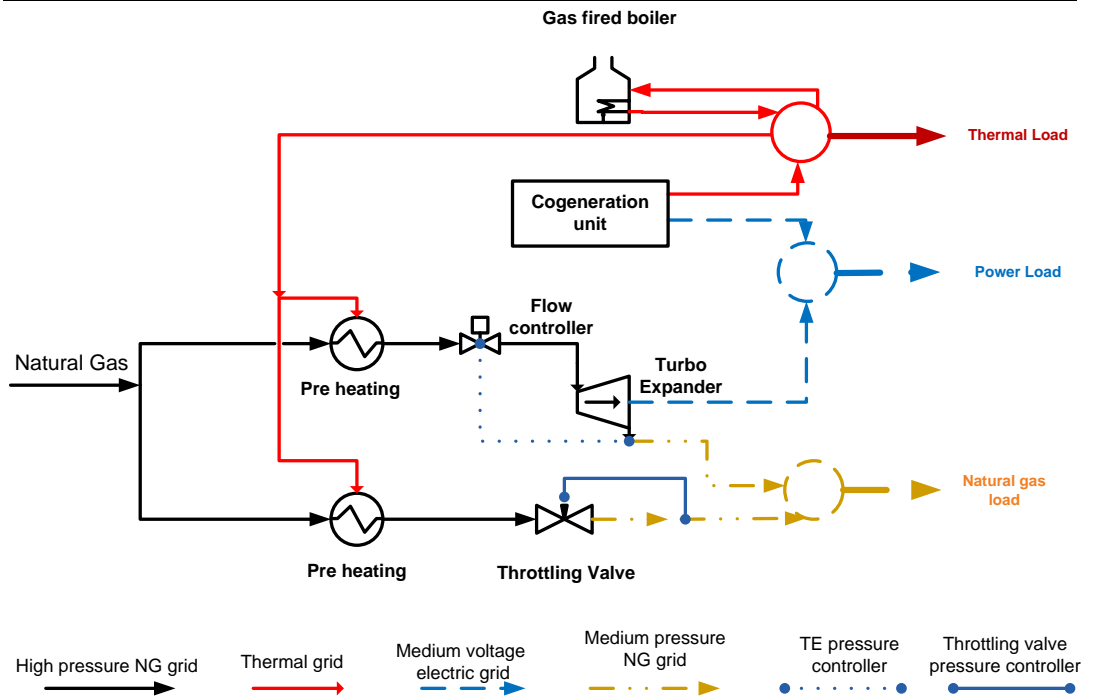
Figure 5. Integrated micro-grid generic conceptual structure

3.1.3. Modelling and optimization

In the following sections, an economic and environmental problem formulation will be presented.

CHP economic problem formulation

The non-linear convex function [7] of the total cost of the cogeneration units is represented by:

$$C_{\text{chp},j}(t) = \alpha_j + \beta_j P_{\text{chp,j}}(t) + \gamma_j P_{\text{chp,j}}(t)^2 + \delta_j Q_{\text{chp,j}}(t) + \varepsilon_j Q_{\text{chp,j}}(t)^2 \qquad (1)$$
$$+ \xi_j P_{\text{chp,j}}(t) Q_{\text{chp,j}}(t)$$

The output of unit j is assumed to lie in a region in the P_j Q_j plane bounded by n_i lines [7]. The lines are defined by equation 2:

$$a_{ji}P_i + b_{ji}Q_i \geq c_{ji}; j = 1, \ldots, n_i \qquad (2)$$

where the coefficient αj, represents fixed operational costs of unit j. More precisely, in this study, capital cost were not considered. The βj, γj, δj, εj, represent the operational cost of unit j and finally, ξj represents the well-known coupling term [8]. a_{ji}, b_{ji} and c_{ji} are the coefficients of the equations, which represent the boundaries of the feasible heat-power region of each cogeneration unit.

Thermal unit economic problem formulation

The non-linear convex function of the total cost of the thermal units is represented by:

$$C_{b,i}(t) = \alpha_i + \beta_i Q_{b,i}(t) + \gamma_i Q_{b,i}(t)^2 \qquad (3)$$

with the following inequality constraints upon thermal power

$$Q_{b,i}^{\min} \leq Q_b(t) \leq Q_{b,i}^{\max} \qquad (4)$$

Turbo-expander economic problem formulation

The operational cost of the TE can be formulated by using a linear equation as follows:

$$C_{te,k}(t) = \alpha_k + \beta_k N_{te,k}(t) + \gamma_k P_{te,k}(t) \qquad (5)$$

subjected to the linear equality constraint:

$$P_{\text{te,k}}(t) = \rho_k N_{\text{te,k}}(t) \tag{6}$$

where ρ_k is the NG/ power correlation factor.

with the local constraints:

$$N_{\text{te},k}^{\min} \geq N_{\text{te,k}}(t) \geq N_{te,\text{k}}^{\max} \text{ and } P_{\text{te},k}^{\min} \leq P_{\text{te,k}}(t) \leq P_{\text{te},k}^{\max} \tag{7}$$

Throttling valve economic problem formulation

The operational cost of the throttling valves is formulated as follows:

$$C_{\text{vlv},s}(t) = \alpha_s + \beta_s N_{\text{vlv},s}(t) \tag{8}$$

subjected to the inequality constraints:

$$N_{\text{vlv},s}^{\min} \leq N_{\text{vlv,s}}(t) \leq N_{\text{vlv},s}^{\max} \tag{9}$$

Electric and thermal grid economic problem formulation

The operational cost due the withdrawal and the injection of power with the electric national grid is:

$$C_{\text{grid}}^{\text{el}}(t) = \alpha_g P_{\text{withdrawal}}(t) - w_j(t)\sigma_{\text{grid},j}^{\text{el}} P_{\text{sold}}(t) - w_k(t)\sigma_{\text{grid},k}^{\text{el}} P_{\text{sold}}(t) \tag{10}$$

Instead, the operational cost for the local thermal grid is defined as:

$$C_{\text{grid}}^{\text{th}}(t) = -w_t(t)\sigma_{\text{grid},j}^{\text{th}} Q_u(t) - w_r(t)\sigma_{\text{grid},i}^{\text{th}} Q_u(t) \tag{11}$$

where w_j and w_k are respectively the electricity price factors for cogeneration and waste energy recovery. Moreover, $Q_u(t)$ is the thermal demand at time t that corresponds to the district heating network thermal demand at time t. Instead, w_t represents the thermal power cost and the electric and thermal weights are defined as:

$$\sigma_{\text{grid},j}^{\text{el}} = \frac{P_{\text{chp,j}}(t)}{P_{\text{chp,j}}(t) + P_{\text{te,k}}(t)} \quad \sigma_{\text{grid},k}^{\text{el}} = \frac{P_{\text{te}}(t)}{P_{\text{chp,j}}(t) + P_{\text{te,k}}(t)} \tag{12}$$

$$\sigma_{\text{grid},j}^{\text{th}} = \frac{Q_{\text{chp,j}}(t)}{Q_{\text{chp,j}}(t) + Q_{b,i}(t)} \quad \sigma_{\text{grid},i}^{\text{th}} = \frac{Q_{b,i}(t)}{Q_{\text{chp,j}}(t) + Q_{b,i}(t)} \tag{13}$$

Mixed thermal production and electricity recovery

For those system configurations where the thermal energy is provided by both fossil-fuel based units and renewable technologies, e.g. solar flat plate collectors or solar thermodynamics, it becomes necessary to add some further considerations regarding the electricity recovered by the TE. More precisely, it is necessary to define two different tariffs in order to properly incentivize the energy produced by the TE. This means to distinguish the fraction of the heat, used for preheating, which fully derives from fossil-fuel from the one which derives from renewables. For this purpose, during a control optimization procedure, at each time interval, the electricity produced by the TE should be properly weighted and linked to the appropriate tariff. With these considerations, referring to a system where the thermal production is provided by means of flat plate solar collectors and boilers (no CHP units), the electrical grid problem is defined as:

$$C_{\text{grid}}^{\text{el}}(t) = \alpha_g P_{\text{withdrawal}}(t) - P_{\text{sold}}(t) \tag{14}$$

where:

$$P_{\text{sold}}(t) = w_{k1}(t)\sigma_{\text{grid},n}^{\text{th}} P_{\text{te}}(k,t) + w_{k2}(t)\sigma_{\text{grid},i}^{\text{th}} P_{\text{te,k}}(t) \tag{15}$$

and $\sigma_{\text{grid},n}^{\text{th}}$ and $\sigma_{\text{grid},i}^{\text{th}}$ are defined as:

$$\sigma_{\text{grid},n}^{\text{th}} = \frac{Q_{\text{sol,n}}(t)}{Q_{\text{sol,n}}(t) + Q_{b,n}(t)}; \ \sigma_{\text{grid},i}^{\text{th}} = \frac{Q_b(t)}{Q_{\text{sol,n}}(t) + Q_{b,i}(t)} \tag{16}$$

where $Q_{\text{sol}}(t)$, represents the thermal energy generated by the solar flat plate collectors at time t.

Tariffs structure and legislation

The proposed thermal weighting functions are useful tools for assessing the proper incentivization of the recovered energy in a control optimization procedure. It worth to remind that it is up to the legislators to define the structure of incentives to address this problem.

National Incentives problem formulation

Referring to the cogeneration unit, the electricity produced is normally subjected to national incentives, which are usually based on the total effective energy produced in cogeneration asset. The Italian regulations [9] envisage clear instructions about how to calculate the economic value of the incentive for different cases and conditions[8]. More precisely, the value of the incentive is defined as:

$$C_{\text{incentive},j}(t) = -\text{WC} * b(t) \tag{17}$$

where b is the economic value of the so-called "white certificate" WC:

$$\text{WC} = \text{RISP}(t) * 0.086 * K \tag{18}$$

and RISP is defined as:

$$\text{RISP}(t) = \frac{E_{\text{chp,j}}(t)}{\eta_{\text{el,rif}}} + \frac{H_{\text{chp,j}}(t)}{\eta_{\text{th,rif}}} - F_{\text{chp}}(t) \tag{19}$$

With the constraint relative to the Primary Energy Saving (PES) index:

$$PES(t) \geq \vartheta \tag{20}$$

where $0 \leq \vartheta \leq 0.1$ depending of the type of cogeneration technology considered [8].

PES is defined as:

$$PES(t) = \left(1 - \frac{1}{\frac{H_{chp,j}(t)}{F_{chp,j}(t)} + \frac{E_{chp,j}(t)}{F_{chp,j}(t)}} \right) \times 100 \tag{21}$$

where: $H_{chp,j}(t)$, $F_{chp,j}(t)$, $E_{chp,j}(t)$ are respectively, the thermal energy, the fuel consumption and the electricity produced/consumed in cogeneration asset [9].

Moreover, it is necessary to define the quantities:

$H_{non_{chp,j}}(t)$, $F_{non_{chp,j}}(t)$, $E_{non_{chp,j}}(t)$ which are respectively thermal energy, fuel consumption and the electricity produced/consumed in non-cogeneration asset [9].

Finally, it is possible to define:

$$Q_{chp,j}(t) = H_{chp,j}(t) + H_{non_{chp,j}}(t) \tag{22}$$

$$P_{chp,j}(t) = E_{chp,j}(t) + E_{non_{chp,j}}(t) \tag{23}$$

$$\dot{m}_{fuel,j}(t)\text{LHV} = F_{non_{chp,j}}(t) + F_{chp,j}(t) \tag{24}$$

Economic objective function

Finally, it is possible to define the economic objective function as

$$\min C = \sum_j C_{\text{chp},j}(t)$$

$$+ \sum_i C_{b,i}(t)$$

$$+ \sum_k C_{\text{te},k}(t) + \sum_s C_{\text{vlv},s}(t) + \sum_j C_{\text{incentive},j}(t) + C_{\text{grid}}^{\text{th}}(t)$$

$$+ C_{\text{grid}}^e(t)$$

$$(25)$$

Global constraints

Thermal energy balance:

$$Q_u(t) + \sum_s \left(\frac{Q_{\text{vlv},s}^{\text{preheating}}(t)}{\varepsilon_{\text{HE},s}} \right) + \sum_k \left(\frac{Q_{\text{te},k}^{\text{preheating}}(t)}{\varepsilon_{\text{HE},k}} \right) - \sum_i Q_{b,i}(t)$$

$$- \sum_j Q_{\text{chp,j}}(t) = 0$$

$$(26)$$

Power balance:

$$P_u(t) + P_{\text{sold}}(t) - P_{\text{withdrawal}}(t) - \sum_j P_{\text{chp,j}}(t) - \sum_k P_{\text{te,k}}(t) = 0 \qquad (27)$$

Natural gas energy balance:

$$N_u(t) - \sum_k N_{\text{te},k}(t) - \sum_s N_{\text{vlv},s}(t) = 0 \tag{28}$$

CHP environmental problem formulation

The GHG emissions from the CHP units can be considered proportional to the thermal power generated. The emissions can be represented by the following linear function:

$$e_{\text{chp},j}(t) = a_j Q_{\text{chp}}(t) \tag{29}$$

Thermal unit environmental problem formulation

The GHG emissions from the thermal units alone are proportional to the thermal power generated. The emission is represented by the following linear function:

$$e_{b,i}(t) = a_i Q_{b,i}(t) \tag{30}$$

Turbo-expander environmental problem formulation

The GHG related to the TE operation have to be considered as the avoided grid emission due to the added local electricity production. i.e. the emission that would be generated if the same quantity of electricity, generated by the TE, were to be acquired from the national grid. Finally, the emission model for TE operation can be formulated as follows:

$$e_{\text{te},k}(t) = -w(t) \sum_k P_{\text{te,k}}(t) \tag{31}$$

where w(t) is the national electricity emission factor.

Throttling valves environmental problem formulation

The GHG related to the throttling valves operation have to be considered as the emissions due to the not added local electricity production since the same quantity of gas could be released potentially by a TE unit, so, a potential part of waste energy has not been recovered.

$$e_{\text{vlv},s}(t) = 0 \tag{32}$$

Electric and thermal grid environmental problem formulation

$$e_{\text{grid}}^{\text{el}}(t) = w(t)P_{\text{withdrawal}}(t) \tag{33}$$

$$e_{\text{grid}}^{\text{th}}(t) = 0 \tag{34}$$

Environmental objective function

$$\min e = \sum_j e_{\text{chp},j}(t) + \sum_i e_{b,i}(t) + \sum_k e_{\text{te},k}(t) + \sum_s e_{\text{vlv},s}(t) + e_{\text{grid}}^{\text{el}}(t) \tag{35}$$

Multi-objective function

$$\min\{\sigma C + (1 - \sigma)\Gamma e\} \tag{36}$$

where $0 \leq \sigma \leq 1$.

3.1.4. Case study

The case study proposed is located in Genoa city (Latitude:44.3435; Longitude: 8.959). The area includes different industrial activities, residential buildings and offices as shown in figure 6.
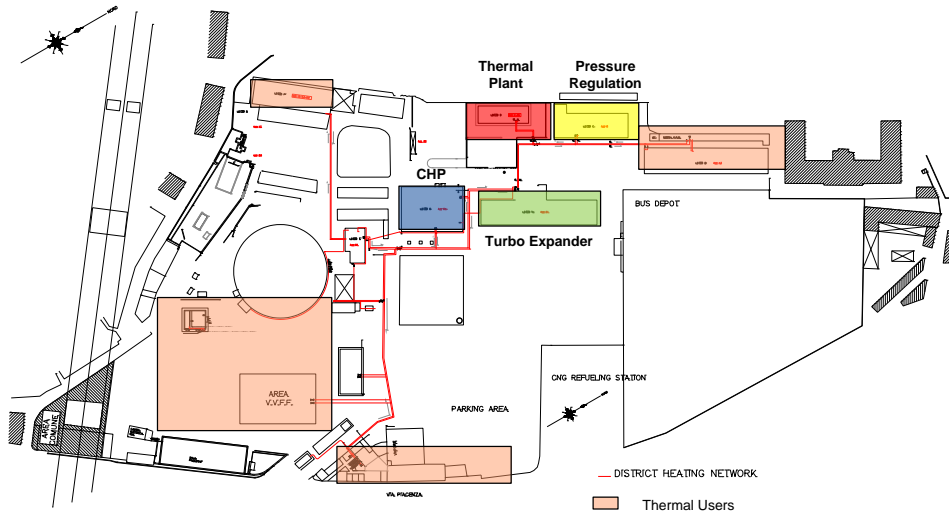

Figure 6. Site overview

Integrated system and process description

As shown in figure 7, the case-study involves a multiple energy carriers integrated system where the NG, which arrives from the national grid at 24 bars, is expanded down to 5 bars, through 3 parallel throttling valves with a nominal capacity of about 60,000 Sm^3/h each. A parallel line brings

NG to a TE of about 550 kW of nominal mechanical power and 22,500 Sm^3/h. The thermal energy necessary for the NG preheating process is provided by two gas-fired boilers of about 950 kW_{th} each. Another part of the heat is provided by a cogeneration unit. More precisely, the CHP unit is a gas-fired internal combustion turbocharged engine. The machine is capable of delivering, at nominal conditions, 550 kW_{el} and 630 kW_{th}. Finally, a small scale DHN provides thermal power to the local users. Currently, the CHP control logic is based on a thermal load tracking

34

strategy. The CHP and the boiler units are not feed by the amount of NG processed. They have a dedicated line.
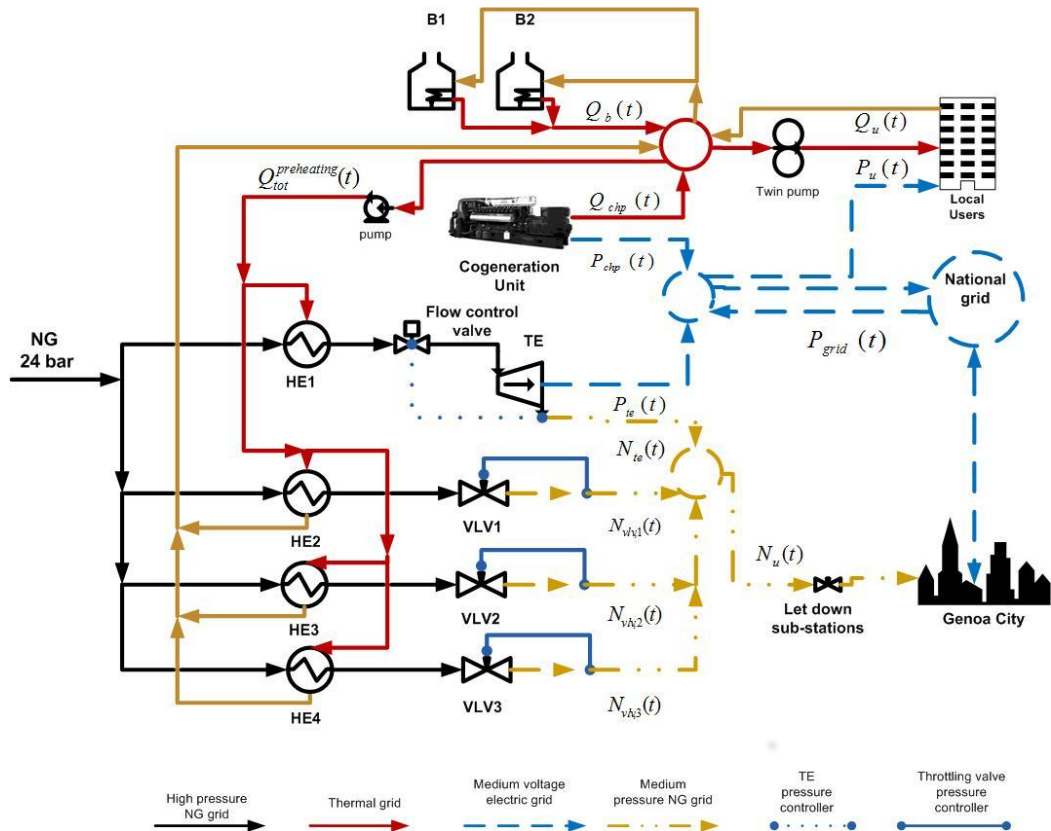
Figure 7. Case study integrated system.

UniSim Design Suite Numerical Model

In order to evaluate the potential energy and environmental benefits of the proposed mathematical model, the integrated grid has been modeled in dynamic regime by using *UniSim* software. *UniSim* is a process modeling software that allows to create steady-state and dynamic models for plant design, performance monitoring, troubleshooting, business planning, and asset management [6]. In

figure 8, it is possible to appreciate the system process and flow diagram. Here, very few simplifications have been made: in the reality, the two gas-fired boilers have a local control logic which manages the starts and stops of the two thermal units in order to achieve the most efficient working conditions. For simplicity reasons, an equivalent single thermal generation unit has been implemented in the model as shown in figure 8. Possible thermal losses in the headers and in all other components have not been considered in this study. The model has been built after intensive on site surveying and component analysis. The cogeneration unit has been modeled considering a simple thermal unit. Its control is based on the hot water temperature (whose set point is 82ºC) at the inlet in the hydraulic circuit relative to the district heating network and the pre-heating systems. Figure 9 represents the non-dimensional hourly volume flow of NG used for this case study.
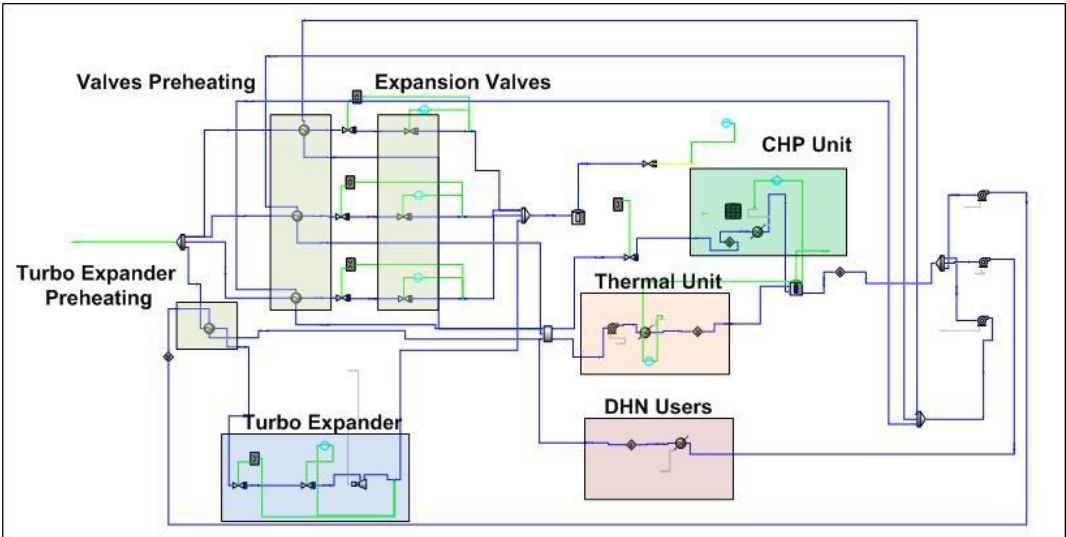

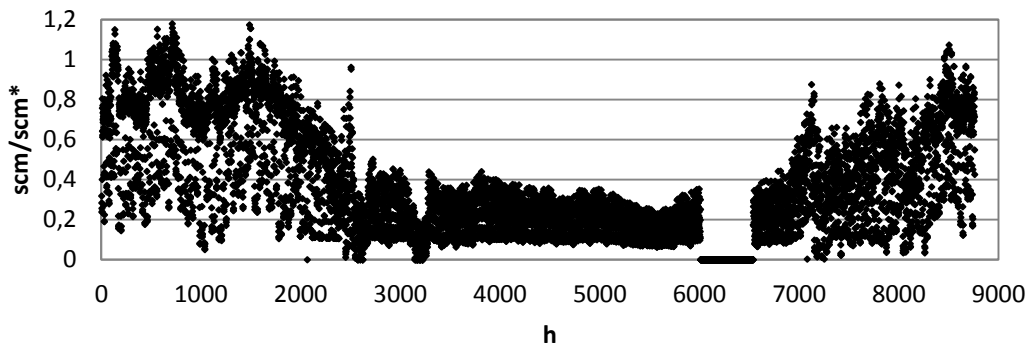Figure 8. *UniSim Design Suite* integrated system process flow diagram

Figure 9. Hourly volume flow of natural gas released in 2012

Solution methods

The optimal results have been calculated by using *Matlab* software. Here, two different algorithms, available in *Matlab*, have been used to solve the optimization problem. They are respectively the *Fmincon* and *Genetic Algorithm* (GA). This one has been set to a population size of about 200 individuals, with a function tolerances of about $1x10^{-6}$ and a constrain tolerances of about $1x10^{-3}$ .The Generation was set at 1700. After different tests, it has been possible to observe that the *Fmincon* solver allows one to find only a local optimal solution. On the other hand, the GA seems to be more effective allowing one to reach global optimal solutions in most cases. At this stage, it might be important to highlight that the first algorithm was able to achieve solutions faster than the GA. More precisely, the *Fmincon* solver took an average of 50 iterations to reach a solution. GA iterations instead range from 125 to 500 depending on the case examined. Some similarities have been identified in other optimization studies: [10], [11], and [12].

Discrete scenario evaluation

In order to test the effectiveness of the proposed model, a typical winter scenario has been considered. Figure 10 describes the hourly trend of the thermal, electrical and NG demand for a typical winter day on a 24-hour scale.
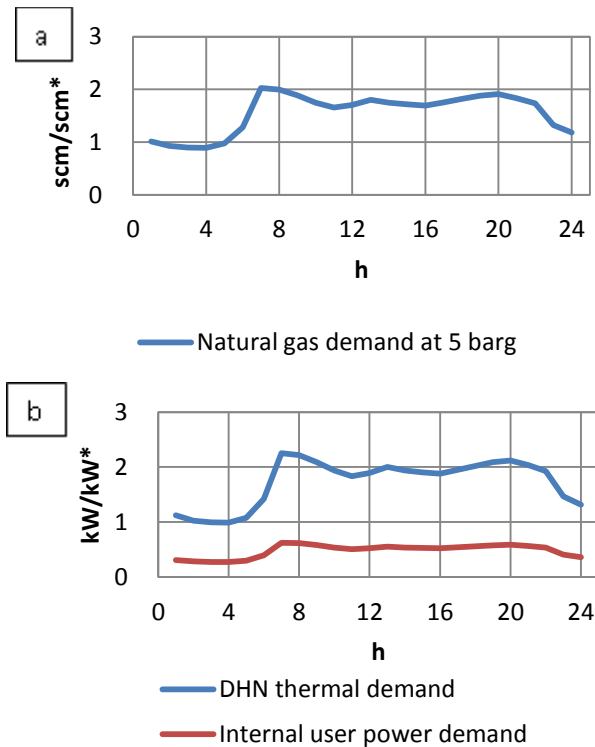

Figure 10. Case scenarios a) NG demand b) Thermal and electrical power demand

3.1.5. Results and conclusions

The economic and environmental optimization results for the above-mentioned case scenario are presented in table 1 in comparison with the thermal load tracking control logic. Referring to the economic optimization where the weight σ has been

set equal to 1 (fully economic optimization), the best performing solution is given by the GA where a global optimum has been reached. Here, a potential daily operational cost reduction of about 17% could be achieved with respect to the thermal load tracking strategy. Instead, for the same case scenario, considering the environmental emissions, it is possible to observe a better performance for the thermal load tracking control logic with carbon emission recovery of about 1. Considering the environmental optimization (σ=0), the most effective results have been identified by the *Fmincon solver* where a potential daily reduction of about 20% of the operational cost could be achieved with a carbon emission recovery 3.32 times higher than the thermal load tracking strategy.

Table 1. Optimization normalized results.

Economic Optimization σ=1				Environmental Optimization σ=0				Thermal load tracking	
operational cost		environmental emissions		operational cost		environmental emissions		operational cost	environmental emissions
Fmincon	GA	Fmincon	GA	Fmincon	GA	Fmincon	GA		
Euro*	Euro*	kg*	kg*	Euro*	Euro*	kg*	kg*	Euro*	kg*
0.93	0.83	- 0.71	- 0.83	0.80	0.87	- 3.32	- 2.80	1.00	- 1.00
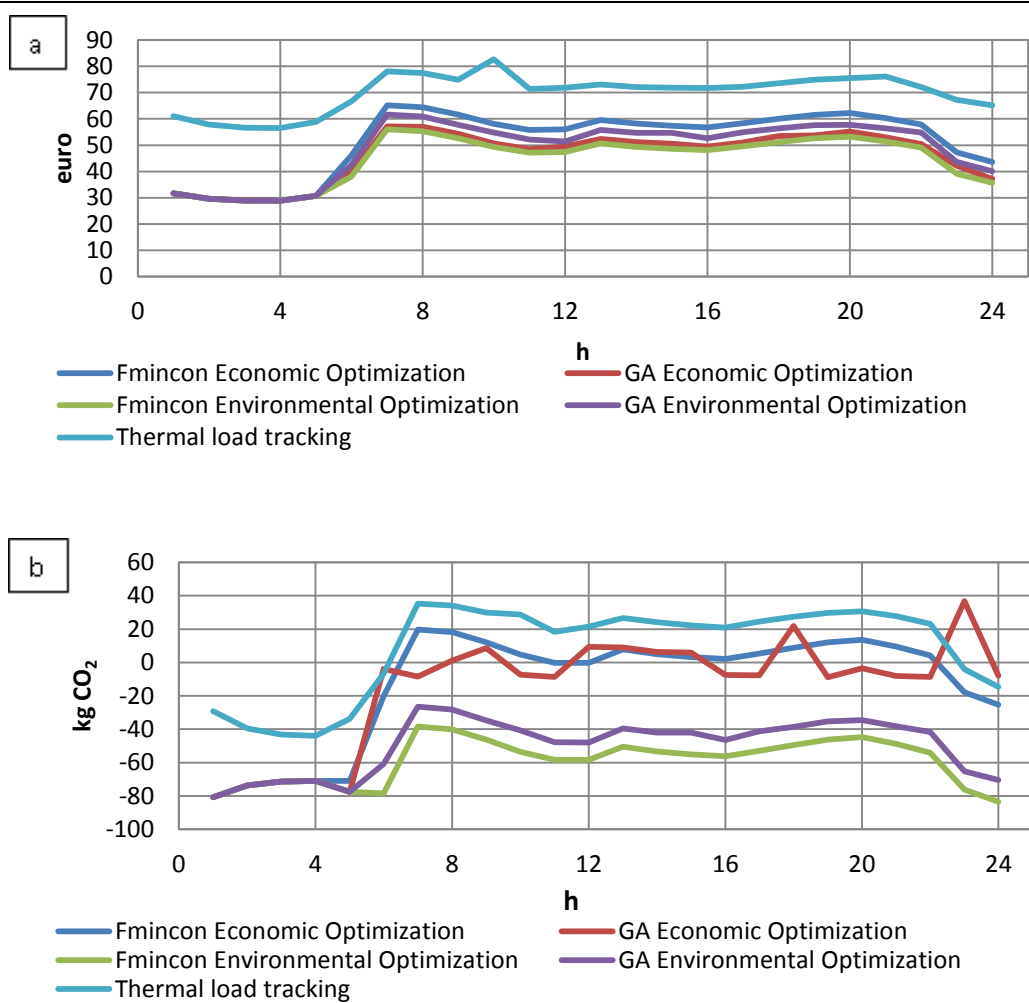
Figure 11. Method comparison: a) Operational costs b) Carbon emissions
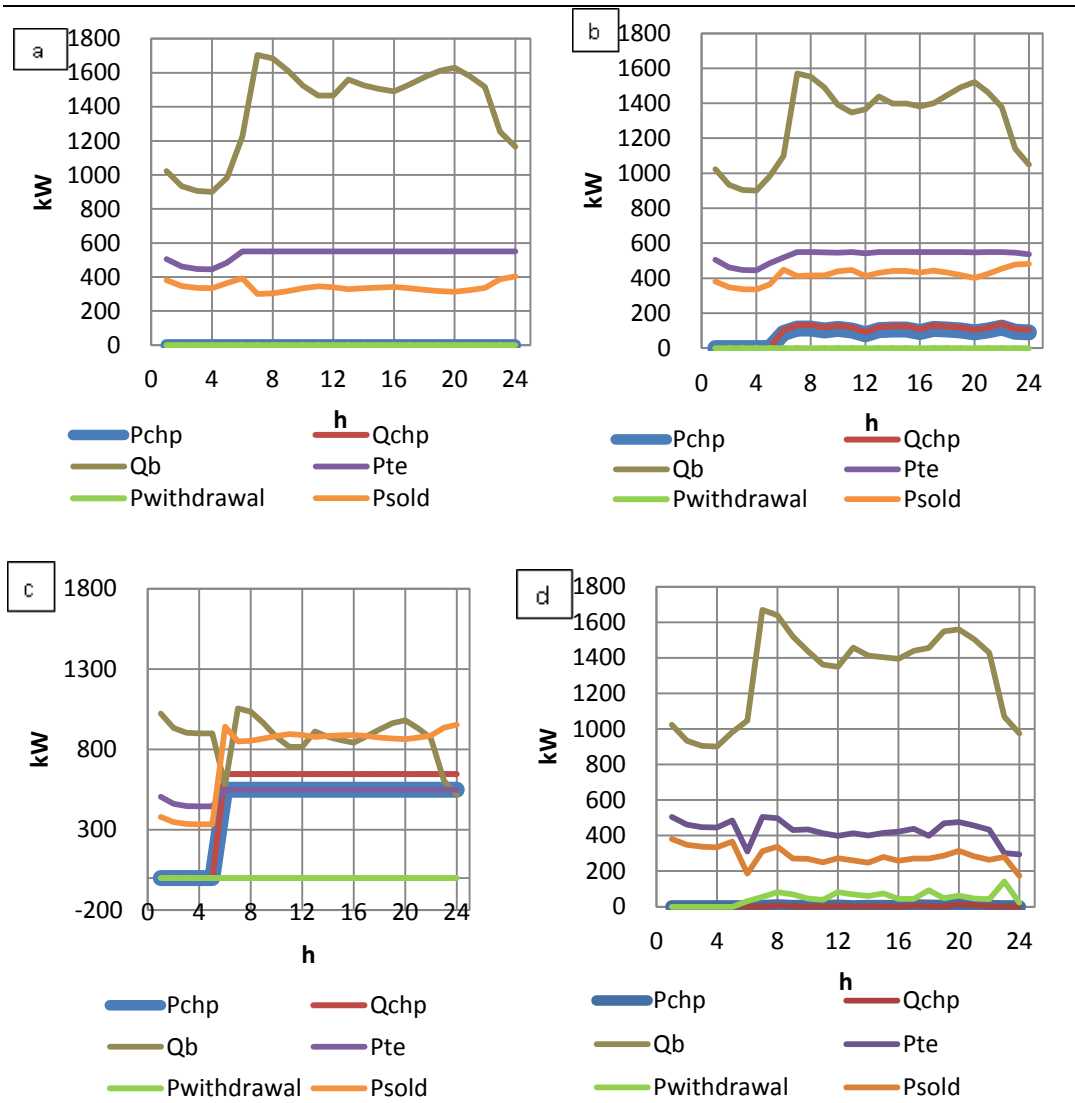
Figure 12. Operational configuration comparison: a-b) Environmental optimization, Fmincon and GA

c-d) Economic optimization, Fmincon and GA

In figure 12-d, it is possible to appreciate that, in this specific case (i.e economic optimization, GA), the cogeneration unit should be always switched off and the thermal energy need would be entirely supplied by the thermal unit. Besides, a

41

small percentage of electricity should be purchased from the national grid. The alternative local optimum proposed by the *Fmincon solver* foresees the startup of the cogeneration unit at 100% load from 07.00 till 00.00. Referring to figure 12-b, the peak that is possible to observe at h 19.00 h 23.00 is due to an optimal solution that foresees important slowdowns of the TE which is responsible for the carbon emission recovery. Of course, this would not affect the respective operational cost whose trend is shown in figure 11-a.

Referring to the most effective environmental solution figure 12-a, the *Fmincon* solver identifies an working configuration where the cogeneration unit should still be off 24 h. Here, no electricity is purchased from the national electric grid. Moreover, the solution provided by the GA would foresee a not feasible working condition for the cogeneration unit since it should work under its technical lower limit of 293 kW$_{el.}$ Therefore, this solution would not work in reality.

The effectiveness of the model, in terms of economic and environmental performances, has been quantified and good results have been achieved. In fact, it has been possible to observe that for a typical winter day scenario, the mathematical model allows to achieve a daily operational cost reduction of about 17% with respect to the case in which the cogeneration unit control logic is based on thermal load tracking strategy. The same reduction can be achieved in daily carbon emissions. Referring to the fully environmental optimization, a 20% reduction on the daily carbon emissions can be achieved. The multi-objective model seems to provide a good compromise between carbon emissions and operational costs reduction, even when fully economic optimization mode was selected (σ=1).

However, generally speaking, slight changes on the NG demand may affect the optimal solution. Then, it might be quite easy to identify different optimal working conditions for different case scenarios. This is due to the system complexity and

the high number of factors involved in the control optimization calculation. That makes difficult to achieve general conclusion about what should be the best working conditions for this type of system. Then, the usefulness of such model become fundamental for optimal system operations.

NOMENCLATURE

$b(t)$ national incentive value [€/tep]

$C_{b,i}(i,t)$ thermal unit i, operational cost [€/h] at time t ϵ T

$C_{\mathrm{chp},j}(j,t)$ cogeneration unit j, operational cost [€/h] at time t ϵ T

$C_{\mathrm{grid}}^{\mathrm{el}}(t)$ electrical grid, operational cost [€/h] at time t ϵ T

$C_{\mathrm{grid}}^{\mathrm{th}}(t)$ thermal grid, operational cost [€/h] at time t ϵ T

$C_{\mathrm{incentive},j}(j,t)$ incentive   value   [€/h]   at   time   t   ϵ T

$C_{\mathrm{te},k}(k,t)$ energy recovery unit k, operational cost [€/h] at time t ϵ T

$C_{\mathrm{vlv},s}(s,t)$ expansion   valve   s,   operational   cost   [€/h]   at   time   t   ϵ T

$E_{\mathrm{chp}}(j,t)$ cogeneration unit j, active power in cogeneration asset [MW] at time t ϵ T

$E_{\mathrm{npn_{chp}}}(j,t)$ cogeneration unit j, active power in non-cogeneration asset [MW] at time t ϵ T

$e_{b,i}(i,t)$ thermal unit j, environmental carbon emissions [kg/h] at time t ϵ T

$e_{\mathrm{chp},j}(j,t)$ cogeneration unit j, environmental carbon emissions [kg/h] at time t ϵ T

$e_{\mathrm{te},k}(k,t)$ energy recovery unit k, environmental carbon emissions [kg/h] at time t ϵ T

$e_{\mathrm{vlv},s}(s,t)$ expansion valve s, environmental carbon emissions [kg/h] at time t ϵ T

$e_{\mathrm{grid}}^{\mathrm{el}}(t)$ national electrical grid, environmental carbon emissions [kg/h] at time t ϵ T

$e_{\mathrm{grid}}^{\mathrm{th}}(t)$ thermal grid, environmental carbon emissions [kg/h] at time t ϵ T

$F_{\mathrm{chp}}(j,t)$ cogeneration unit j, fuel consumption in cogeneration asset [MW] at time t ϵ T

$F_{\text{non}_{\text{chp}}}(j, t)$ cogeneration unit j, fuel consumption in non-cogeneration asset [MW] at time t ϵ T

$H_{\text{chp}}(j, t)$ cogeneration unit j, thermal power in cogeneration asset [MW] at time t ϵ T

$H_{\text{non}_{\text{chp}}}(j, t)$ cogeneration unit j, thermal power in non-cogeneration asset [MW] at time t ϵ T

i generic thermal unit

j generic cogeneration unit

k generic turbo expander

K correction factor

LHV lower heating value [MW/kg]

$\dot{m}_{\text{fuel}}(j, t)$ cogeneration unit j, total fuel mass flow [kg/h] at time t ϵ T

$N_{\text{te}}(k, t)$ energy recovery unit k, delivered NG [kW] at time t ϵ T

$N_{\text{te},k}^{\min}$ technical deliverable NG minimum of unit k [kW]

$N_{t,\text{ke}}^{\max}$ technical deliverable NG maximum of unit k [kW]

$N_{\text{vlv}}(s, t)$ expansion valve s, delivered NG [kWh] at time t ϵ T

$N_{\text{vlv},s}^{\min}$ technical deliverable NG minimum of unit s [kW]

$N_{\text{vlv},s}^{\max}$ technical deliverable NG maximum of unit s [kW]

PES primary energy saving index

$PES(t)$ Primary energy saving index at time t ϵ T

$P_{\text{chp}}(j, t)$ cogeneration unit j, power [kW] at time t ϵ T

$P_{\text{te}}(k, t)$ energy recovery unit k, power [kW] at time t ϵ T

$P_{\text{te},k}^{\min}$ technical power minimum of unit k [kW]

$P_{\text{te},k}^{\max}$ technical power maximum of unit k [kW]

$P_{\text{withdrawal}}(t)$ power withdrawal [kW]

$Q_b(i, t)$ thermal unit i, thermal power [€/h] at time t ϵ T

$Q_{b,i}^{\min}$ technical thermal power minimum of thermal unit i [kW]

$Q_{b,i}^{\max}$ technical thermal power maximum of thermal unit i [kW]

$Q_{\mathrm{chp}}(j,t)$ cogeneration unit j, thermal power [kW] at time t ϵ T

$Q_{\mathrm{te}}^{\mathrm{preheating}}(k,t)$ energy recovery unit k, pre-heating thermal power at time t ϵ T

$Q_{\mathrm{vlv}}^{\mathrm{preheating}}(s,t)$ expansion valve s, pre-heating thermal power at time t ϵ T

$RISP(t)$ energy saving [MW] at time t ϵ T

s generic throttling valve

T set of time intervals considered in the daily period

t single time interval length

WC number of incentives accumulated [tep]

$w_j(t)$ cogenerated electricity tariff at time t ϵ T

$w_k(t)$ recovered electricity tariff at time t ϵ T

$w_{k1}(t)$ recovered electricity tariff (fully renewable) [€/kWh] at time t ϵ T

$w_{k2}(t)$ recovered electricity tariff (fully fossil fuel) [€/kWh] at time t ϵ T

$w_r(t)$ conventional thermal power tariff [€/kWh] at time t ϵ T

$w_t(t)$ cogenerated thermal power tariff [€/kWh] at time t ϵ T

$w(t)$ national electricity cost factor [€/kWh] at time t ϵ T

Greek letters

$\varepsilon_{\mathrm{HE},s}$ expansion valve s, heat exchanger effectiveness

$\varepsilon_{\mathrm{HE},k}$ energy recovery unit k, heat exchanger effectiveness

$\eta_{\mathrm{el,rif}}$ average electrical national grid efficiency

$\eta_{\mathrm{th,rif}}$ average thermal national grid efficiency

ρ_k NG/ power correlation factor unit k

$\sigma_{\mathrm{grid},j}^{\mathrm{el}}$ cogeneration unit j, electrical weight

$\sigma_{\mathrm{grid},k}^{\mathrm{el}}$ recovery unit k, electrical weight

$\sigma_{\mathrm{grid},j}^{\mathrm{th}}$ cogeneration unit j, thermal weight

$\sigma_{\mathrm{grid},i}^{\mathrm{th}}$ thermal unit i, thermal weight

$\sigma_{\mathrm{grid},n}^{\mathrm{th}}$ thermal unit n, thermal weight

σ energy policer decision weight

Γ avoided carbon emissions incentive factor (euro/kg)

Abbreviations

CHP combined heat and power

DHN district heating network

NG natural gas

TE turbo expander

WER waste energy recovery

REFERENCES

[1] Lazaretto, A., Macor, A., Mirandola, A., & Reini, M. "Analytical-symbolic method of thermoeconomic optimization of an energy recovery and cogeneration system," ASME, . NEW YORK, NY(USA), pp. 183-190, (1992).

[2] S. Sanaye and A. M. Nasab. Modeling and optimizing a CHP system for natural gas pressure reduction plant. Energy 40; pp. 358:369, (2012).

[3] C. Howard, P. Oosthuizen, and B. Peppley. An investigation of the performance of a hybrid turboexpander-fuel cell system for power recovery at natural gas pressure reduction stations. Applied Thermal Enginering 2165, pp. 2170-31 (2011).

[4] W. Kostowski, "The Possibility of Energy Generation within the Conventional Natural Gas Transport System," Strojarstvo: časopis za teoriju i praksu u strojarstvu 52.4; pp. 429-440, (2010).

[5] E. Lo Cascio, D. Borelli, F. Devia, C. Schenone.Future distributed generation : An operational multi-objective optimization model for integrated small scale urban electrical, thermal and gas grids. Energy Conversion and Management 143; pp. 348:359, (2017).

[6] Honeywell Process Solutions, UniSim® Design Suite R450. UniSim® is a registred trademark of Honeywell Process Solutions, https://www.honeywellprocess.com, 2016.

[7] P. S. N. Rao. Combined heat and power economic dispatch: A direct solution. Electric Power Components and Systems, 34(9); pp. 1043-1056, (2006).

[8]   Rooijers, Frans J., and Robert AM van Amerongen. "Static economic dispatch for co-generation systems." IEEE Transactions on Power Systems 9.3 (1994): 1392-1398.

[9]   CAR's High Efficiency Cogeneration Guide. (Guida alla Cogenerazione ad Alto Rendimento CAR, in Italian), 2012, available at http://www.gse.it/it/salastampa/GSE_Documenti/Guida%20CAR.pdf

[10]   M. Geidl, "Integrated Modeling and Optimization of Multi-Carrier Energy Systems," Ph.D. no. 17141, TU Graz, 2007.

[11]   M. Novac, E. Vladu, O. Novac, and M. Gordan, "Aspects Regarding the Optimization of the Induction Heating Process using Fmincon , Minimax functions and Simple Genetic Algorithm," Journal of Electrical and Electronics Engineering 2(2): pp. 64–70,(2009).

[12]   S. Katuli and M. Cehil, "A novel method for fi nding the optimal heat storage tank capacity for a cogeneration power plant,"Applied Termal Engineering, vol. 65, pp. 530–538, (2014).

3.2. Key Performance Indicators

If a certain expertise was developed in operatively increasing the efficiency of the PRS recovery systems through the integration with RES or CHP, the topic of the assessment of the global energy efficiency of the process has not yet been thoroughly explored. It is obvious that the characteristics of the heat source chosen for NG pre-heating affect the efficiency of the recovery process, and that the above mentioned thermal integrations enhance its performance. In the same time, it is definitely more complicated to assess in a quantitative way how the hybrid conversion process and the energy recovery are influenced by the several thermodynamic parameters involved, starting with the features of the pre-heating energy source.

Kostowski addressed in some papers the definition of figures of merit in order to assess the efficiency of the recovery systems and to compare the performance of alternative configurations. In [1] energy and exergy analysis of the expansion plant was developed and indicators have been proposed to evaluate the corresponding CO_2 emissions. Several different performance indicators have been defined, calculated and discussed in [2], where both energy and exergy efficiency parameters were presented in order to compare different possible set-ups. Performance Ratio, Incremental Performance Ratio and Local Differential Efficiency refer to energy balances, while several formulations of exergy efficiency ratio are based on the 2nd Law of Thermodynamics. A comparative analysis of electricity generation in PRSs based on thermo-ecological cost was proposed in [3], aiming to a thermodynamic evaluation of energy resources management. The assessment method considered both the interrelation of irreversibility for the analyzed system and its influence related to the depletion of non-renewable resources.

However, there is still a vagueness in the analysis of Waste Energy Recovery (WER) in PRSs. On one hand, the WER efficacy is intimately related to system design, NG flow rate, pressure drop, control technique and operating conditions, and this dependence needs to be clearly assessed. On the other one, an operative reference to conventional processes without energy recovery is necessary, aiming to evaluate the benefit coming from the upgraded system. More precisely, for given system configurations and operating conditions, proper Key Performance Indicators (KPIs) are required to estimate, with an acceptable degree of confidence, the effectiveness of the energy recovery process in terms of energy savings and carbon emissions reduction.

Thus, in order to bridge that gap, in this paper, specific Key Performance Indicators (KPIs) for the assessment of WER in PRSs are introduced and discussed. The proposed KPIs aim to provide a quantitative comparison between the operational

performance for WER process, with TE, and the one for conventional process, where the NG expansion is achieved by means of standard throttling valves. Those indicators can guide the operational management of the recovery system, since real-time estimation is available, as well as its design phase. Differently from previous research, the present paper deals with the dynamic behavior of the energy recovery system, developed through a time domain analysis, so that the performance is calculated and assessed in a dynamic scenario, taking into account the effect on the system dynamics due thermal integration. Considering this dynamic approach, preheating load prediction models are also presented, based on system configurations and operating characteristics that are commonly used in PRSs and considering different pressure drops. Finally, an application to a case study is presented and the effectiveness of the prediction model is assessed by means of numerical dynamic simulations.

3.2.1. KPIs definition

The proposed KPIs are based on physical parameters that are usually known in the pre-design phase, and are aimed at quantitatively evaluating the energy and environmental benefits from energy recovery in PRSs. Moreover, definition of the following KPIs is derived with the intention of making them easily applicable to real systems. Hence, the strong point of such indicators resides in their fast and reliable implementation for real-time performance monitoring. As shown in the following, the KPIs can be adapted to different system configurations with slight modifications. In particular, the proposed indicators take into account the possibility of integrating PRSs with external thermal users, e.g. district heating networks, and/or of employing cogeneration units. The possibilities and limitations of extending the use of indicators to those system configurations where renewable energy is integrated will also be discussed in this section.

KPIs have been defined considering the case study reported in fig. 13. The layout represents a typical PRS plant in which energy recovery is achieved through a TE, functioning in parallel with Throttling Valves (TV). The pressure drop needed to regulate the gas network can be produced by both devices, through the TE recovering the energy or through the TV with a mere dissipation, depending on flow rate conditions. This means that the TV only operates under extreme flow conditions, i.e. it works when gas flow rates exceed the top or the bottom of the TE operating range and then allows the flow to by-pass the TE. When the mass flow rate is below the TE functioning range, the total NG flow passes through the TV. When the mass flow rate is above the TE functioning range, only the exceeding part by-passes the system through the TV. The TE is able, through a heat supply, to convert part of the mechanical energy of the gas into electricity. The gas flow rate preheating, addressed to avoid excessive reduction of gas temperature and methane-hydrate formation, is done by boiler-feed water heat exchangers that, in the present layout and in many real plants, also feed a heating network. Two heat exchangers in parallel supply the gas flow rates passing through the TE or the TV. Expansion through the TE requires more heat if compared to the throttling process, but it is able to recover a noticeable quantity of energy. Besides, as above, Q_{TE} and $Q_{tot}^{preheating}$ are quantities that can both differ or be the same, depending on the operating conditions as explained above. This configuration has been assumed as a reference, since it represents a standard layout and contains all the items that characterise a PRS with energy recovery. It must be highlighted that the preheating process can be alternatively supplied by other thermal energy sources (CHP, solar heat, heat pumps, geothermal, etc.) without altering the validity of the illustrated design and so of the proposed approach.

The recovery process described is simple, but it is not trivial to assess its thermodynamic efficiency, or the actual overall energy saving and carbon emissions reduction. This evaluation also impacts on the economic and financial

budget, and in the end on the feasibility of any existing system upgrade or new construction. KPIs have generally been built with the goal of evaluating the benefits coming from energy recovery in PRS in comparison with a reference condition represented by the pressure drop in a traditional PRS with TV. This assumption implicitly considers the transformation of existing stations like the major area of application of the proposed methodology. In KPI definition particular attention has been paid to the use of waste heat recovery for natural gas pre-heating, always on the basis of a leading trend in technology. The diverse meaningful energy and environmental elements have then been considered and for each one of them a specific performance indicator has been introduced, as reported below.
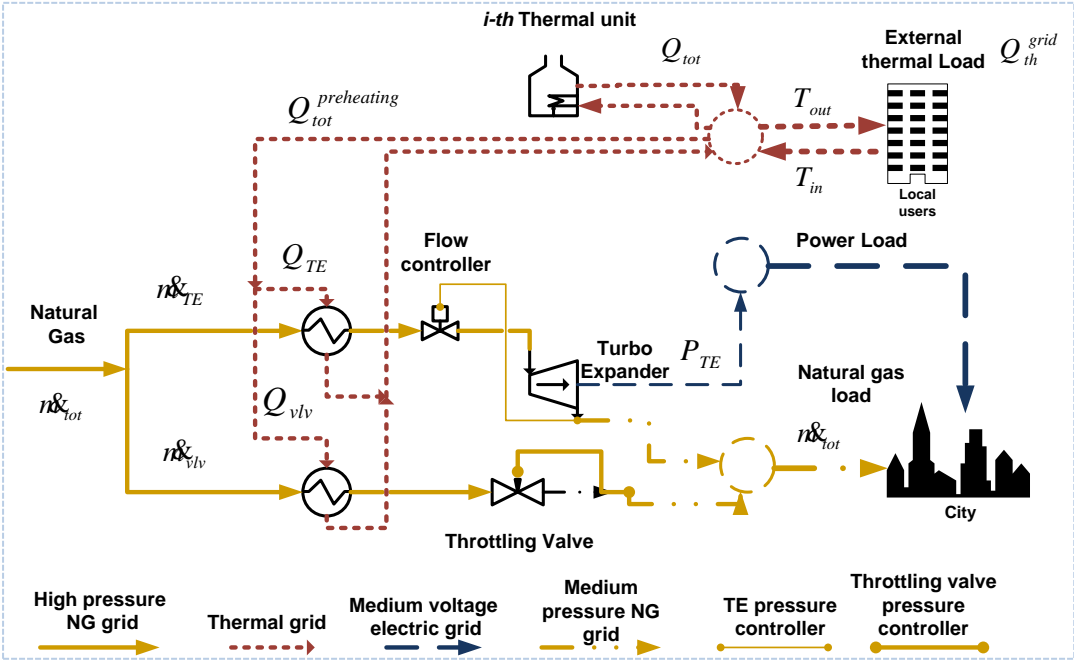

Figure 13. Case study, system overview.

3.2.2. Power-to heat ratio

With reference to figure 13 system configuration, it is possible to define the instantaneous power/heat ratio (PQ) as:

51

$$PQ = \frac{P_{TE}}{Q_{tot}^{preheating}} \tag{1}$$

where

$$Q_{tot}^{preheating} = \left(Q_{tot} - Q_{th}^{grid}\right) \tag{2}$$

P_{TE} is the TE power output and Q_{tot} represents the net heat flow rate produced by the PRS thermal plant units. It is defined as:

$$Q_{tot} = \sum_i \left(\dot{m}_{fuel_{WER}} LHV \eta_{th}\right)_i \tag{3}$$

where $\dot{m}_{fuel_{WER}}$ and η_{th} are respectively the fuel mass flow rate and the thermal efficiency of the ith unit, and LHV represents the i-fuel lower heating value. At this stage it is worth recalling that the PQ ratio, under certain operating conditions, could be higher than the unit depending on the water preheating temperature set-points and the actual boiler and TE efficiency. Generally speaking, the higher the PQ ratio, the better.

3.2.3. Thermal integration

In case of integrated PRS [4], Q_{th}^{grid} represents the instantaneous heat demand required by the thermal users, e.g. the District Heating Network (DHN), which is defined as:

$$Q_{th}^{grid} = \dot{m}_{grid} c_p (T_{in} - T_{out}) \tag{4}$$

where $\dot{m}_{grid}, c_p, T_{in}, T_{out}$ are respectively the mass flow rate of the energy vector used to feed thermal users, its specific heat and inlet and outlet temperatures.

Similarly, for a given time length, the average power/thermal power ratio $\overline{PQ}$, is formally defined as:

$$\overline{PQ} = \frac{1}{(t - t_0)} \int_{t_0}^{t} \frac{P_{TE}}{Q_{tot}^{preheating}} dt \tag{5}$$

Instead, the instantaneous Effective Power/heat ratio (PQ_{eff}) is defined as:

$$PQ_{eff} = \frac{P_{TE}}{Q_{TE}} \tag{6}$$

where Q_{TE} represents the TE preheating need.

For a given time length (t-t_0), the average Effective power/heat ratio ($\overline{PQ}_{eff}$) is formally defined as:

$$\overline{PQ}_{eff} = \frac{1}{(t - t_0)} \int_{t_0}^{t} \frac{P_{TE}}{Q_{TE}} dt \tag{7}$$

3.2.4. Recovery ratio

The Recovery ratio (R) provides the information related to the status of the recovery process of the PRS.

This is defined as:

$$R = \frac{\dot{m}_{TE}}{\dot{m}_{tot}} \tag{8}$$

Here, $\dot{m}_{TE}$ and $\dot{m}_{tot}$ are the NG mass flow rates flowing through the TE and through the entire station respectively. R indicates whether the station is recovering energy or not. For instance, once the TE upper flow limit is passed, throttling

valves will open, in support of the expansion process, reducing R to values below the unit.

Similarly, for a given time length, the average Recovery ratio $\bar{R}$, can be formally defined as:

$$\bar{R} = \frac{1}{(t - t_0)} \int_{t0}^{t} \frac{\dot{m}_{TE}}{\dot{m}_{tot}} dt \tag{9}$$

3.2.5. Waste energy recovery

Finally, it is possible to define the instantaneous Waste Energy Recovery index (*WER*), which is fundamental to assessing system performance. It is defined as:

$$WER = \left(\frac{E_{rel} - E_{WER}}{E_{rel}} \right) \tag{10}$$

where E_{rel} represents the energy that would be required to expand the same amount of natural gas by means of a 100% Joule-Thomson-based process and to produce the same TE power output by means of centralised production, while E_{WER} is the energy required for the real process, where energy recovery occurs.

E_{rel} is defined as:

$$E_{rel} = \frac{Q_{rel}^{preheating}}{\eta_{th}} - \frac{Q_{th}^{grid}}{\eta_{th}} + \frac{P_{TE}}{\bar{\eta}_{el\_grid}} \tag{11}$$

where η_{th} represents the thermal efficiency of the plant thermal supply system, $\bar{\eta}_{el\_grid}$ the average national electricity production efficiency [5] and:

$$Q_{rel}^{preheating} = \sum_i \left(\dot{m}_{fuel_{rel}} LHV \right)_i$$

(12)

is the primary energy consumption related to fuel combustion.

Instead, E_{WER} is defined as:

$$E_{WER} = \sum_i \left(\dot{m}_{fuel_{WER}} LHV \right)_i - \frac{Q_{th}^{grid}}{\eta_{th}}$$

(13)

where $\left(\dot{m}_{fuel_{WER}} LHV \right)_i$ is the thermal power of the ith unit.

The $Q_{rel}^{preheating}$ represents the relative thermal power that would be required if the total NG flow was expanded through a conventional PRS (no TE implemented) for the same boundary conditions. It is important to point out that, for a given NG flow rate, $Q_{rel}^{preheating}$ depends on the characteristics and operating conditions of the system considered, e.g. ambient temperature or process water temperature set points and type of system layout and control. This issue will be examined in more depth in the following and a method to evaluate the $Q_{rel}^{preheating}$ will be introduced. Lastly, for a given time length (t-t_0), the average $\overline{WER}$ can be formally defined as:

$$\overline{WER} = \left(\int_{t_0}^{t} \frac{(E_{rel} - E_{WER})}{E_{rel}} dt \right) \times \frac{1}{(t - t_0)}$$

(14)

3.2.6. Carbon emissions reduction

Analogously for *WER*, it is possible to define the Carbon Emission Recovery index (*CER*) as:

$$CER = \left(\frac{e_{rel} - e_{WER}}{e_{rel}}\right) \tag{15}$$

where:

$$e_{rel} = \sum_i \left[\delta\left(\dot{m}_{fuel\_rel} LHV\right)\right]_i - \delta\left(\frac{Q_{rel}^{preheating}}{\bar{\eta}_{th}}\right) + \gamma\left(\frac{P_{TE}}{\bar{\eta}_{el\_grid}}\right) \tag{16}$$

$$e_{WER} = \sum_i \left[\delta\left(\dot{m}_{fuel\_WER} LHV\right)\right]_i - \delta\left(\frac{Q_{th}^{grid}}{\bar{\eta}_{th}}\right) \tag{17}$$

where δ and γ are the emission factors associated with the PRS thermal plant and national grid respectively.

Similarly, the average Carbon Emission Recovery index can be formally defined as:

$$\overline{CER} = \left[\int_{t_0}^{t} \frac{e_{rel} - e_{WER}}{e_{rel}} dt\right] \times \frac{1}{(t - t_0)} \tag{18}$$

Finally, due their definitions, *CER* and *WER* indexes could be considered equivalent with an acceptable degree of confidence if, as a first approximation, the emission factors δ and γ are considered constant.

3.2.7. Handling 100 % solar-based or waste energy preheating

Since the only real energy contribution to the recovery system is due to gas preheating, it is interesting to consider a free thermal energy input, so that an active energy supply is no longer required. Therefore, it is important to point out that, for those cases where the required heat is fully provided by means of solar collectors or waste energy sources, the *WER* index defined in equation 10 diverges since no fuel consumption would be involved. In such scenarios, WER and $\overline{WER}$ are defined as:

$$WER = \left(\frac{P_{TE}/\bar{\eta}_{el\_grid} - P_{TE}}{P_{TE}/\bar{\eta}_{el\_grid}} \right) \tag{19}$$

$$\overline{WER} = \left(\int_{t_0}^{t} \frac{\int\left(P_{TE}/\bar{\eta}_{el\_grid} - P_{TE}\right)}{P_{TE}/\bar{\eta}_{el\_grid}} dt \right) \times \frac{1}{(t - t_0)} \tag{20}$$

Also, CER and $\overline{CER}$ indexes can be substituted by instantaneous Avoided Emission (*AE*) index as:

$$AE = -\gamma \left(P_{TE}/\bar{\eta}_{el\_grid}\right) \tag{21}$$

and by the average Avoided Emission index ($\overline{AE}$), formally defined as:

$$\overline{AE} = -\frac{\gamma}{(t - t_0)} \int \left(P_{TE}/\bar{\eta}_{el\_grid}\right) dt \tag{22}$$

3.2.8. Preheating prediction

As mentioned above, the term $Q_{rel}^{preheating}$ represents the theoretical preheating needed for expansion in a TV, to be compared with the actual preheating for TE pressure drop, for assigned and common boundary conditions. This quantity not only depends on NG begin/end thermodynamic states, but is influenced by operating and external conditions. Ashouri et al. [6], for their case study, demonstrated that 43% energy savings can be achieved by maintaining the minimum process water temperature with appropriate system control, thereby highlighting the wide variations in $Q_{rel}^{preheating}$ values as a function of the actual plant operating conditions. Thus, the preheating thermal energy, for an assigned NG mass flow, can change from station to station, depending on the above-mentioned items. For this purpose, numerical simulations are helpful tools to assess the heat needs for given PRS and operating conditions, which are needed to evaluate the WER indicator.

In order to enable the online estimation of $Q_{rel}^{preheating}$ for real plant operations, a semi-empirical correlation has been developed based on numerical simulations performed for the reference system and several different conditions inspired by real data. Modelling was implemented through Honeywell's *UniSim® Design Suite* software. Dissipative expansion was simulated considering expansion ratios equal to 4.8, 6, 7.5 and 15, as these values proved to be the most common after the data analysis described below. A simple control logic based on supply water temperature tracking was assumed while, for simplicity, heat losses to the ambient were neglected. Numerical and real data observations showed that the preheating demand can be approximated as a logarithmic function of the NG flow.

The preheating prediction correlation that best suits the trend is represented by equation 23:

$$Q_{rel}^{preheating} = a \log(\dot{m}_{tot})^b \tag{23}$$

where coefficients *a* and *b* are reported in Table 1 for diverse expansion ratios. Coefficients were defined for NG mass flow rate ranging from 5000 to 30000 kg/h, which is a typical range for PRSs located in urban areas. The model proposed in equation 23 was chosen based on real data records to be further extrapolated for different operating pressure drops based on numerical simulation conducted with *UniSim® Design Suite* software. At this stage, it is worth recalling that, equation 23 was selected due to its application simplicity in plant real operations. However, other different forecasting approaches could lead to more accurate results. Indeed, neural-network-based approaches might be suitable for this purpose due the large amount of data available that are required for the net training [7].

Data used in calculations refer to the Italian case. Nevertheless, because of the strong standardisation in the gas sector, these assume a general meaning, at least extended to the continent [8]. In Italy, the overall pipeline length is about 34628 km [9]. *SNAM* company, covering 93% of NG transportation grid, counted 8962 redelivery points in 2015 [10]. Each type of redelivery point is characterised by pressure, minimum contractual pressure, NG available, booked and maximum mass flow rate. Not all redelivery points are suitable for *WER* since, for very small expansion flow rates, TE technologies are not appropriate for NG pressure reduction. In figures 14a-d a general characterisation of the redelivery points is presented for different types of users and for Italian geographical areas respectively, North West (NW), North East (NE), South East (SE), South West (SW) and Deep South. Input regarding the pressure gap available for energy recovery and the expansion ratio was obtained from the reported data, and then used in the numerical model for the purpose of achieving an accurate predictive correlation for $Q_{rel}^{preheating}$.

Table 2. $Q_{rel}^{preheating}$ prediction model.

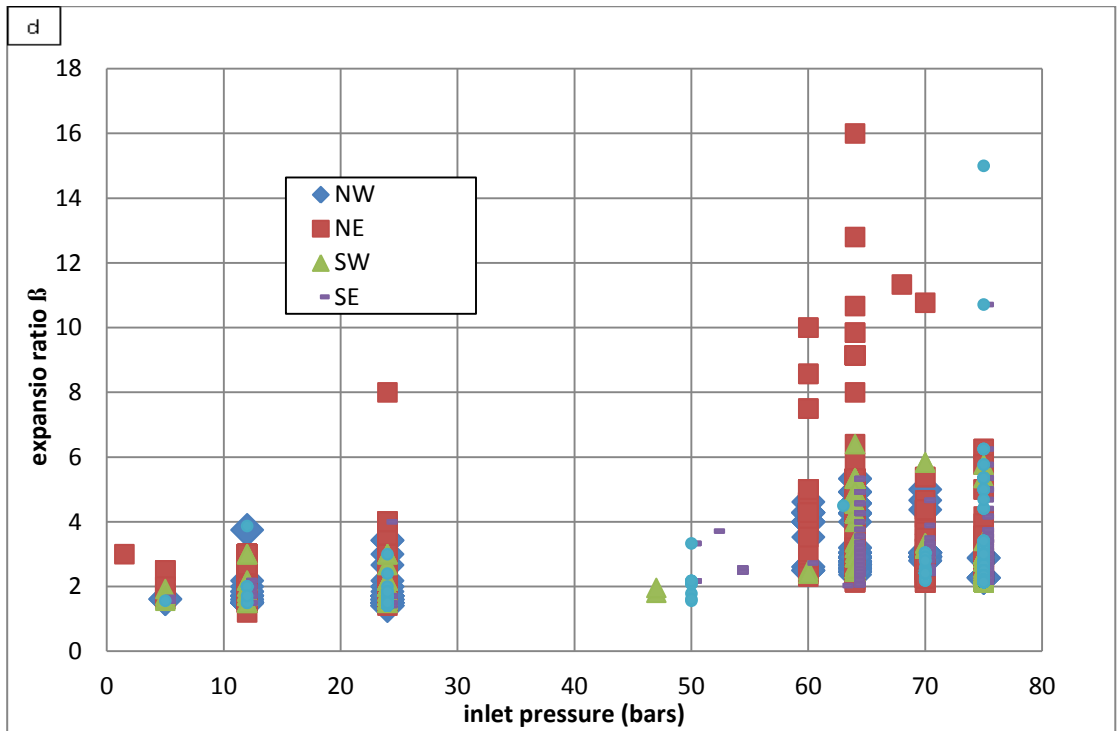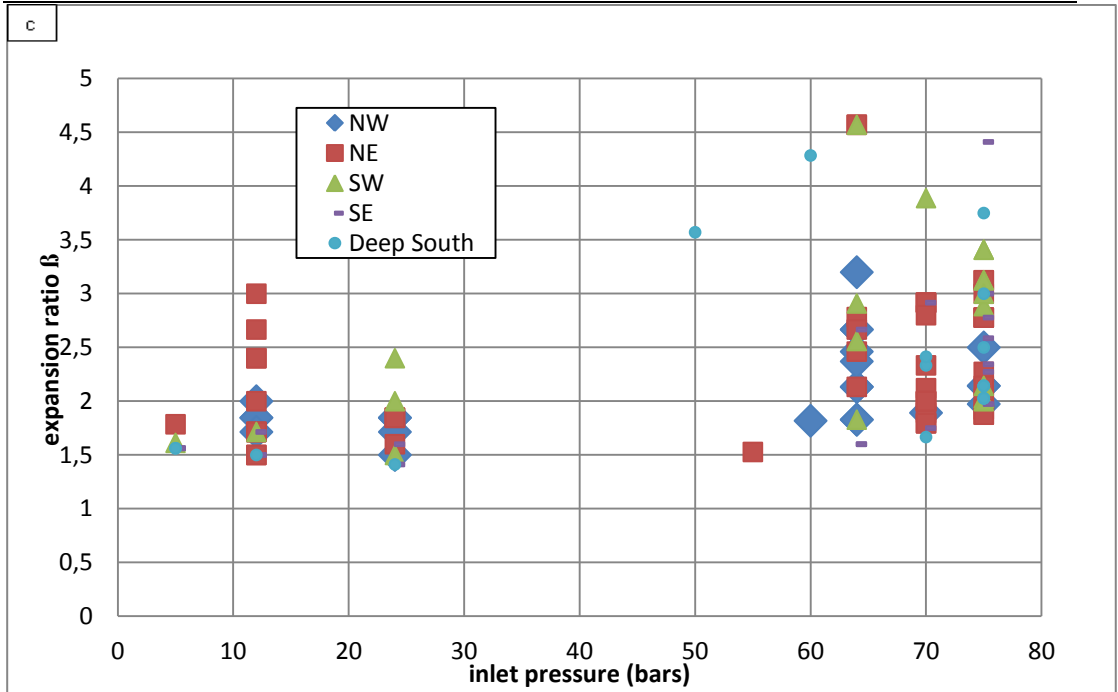| Expansion ratio (β)	Inlet pressure (bars)	Max set point (ºC)	a	b
4.8	24	75-89	0.04078	3.489
6	60	55-95	0.02395	3.912
7.5	65	55-95	0.08205	3.415
15	65	55-95	0.000625	5.526
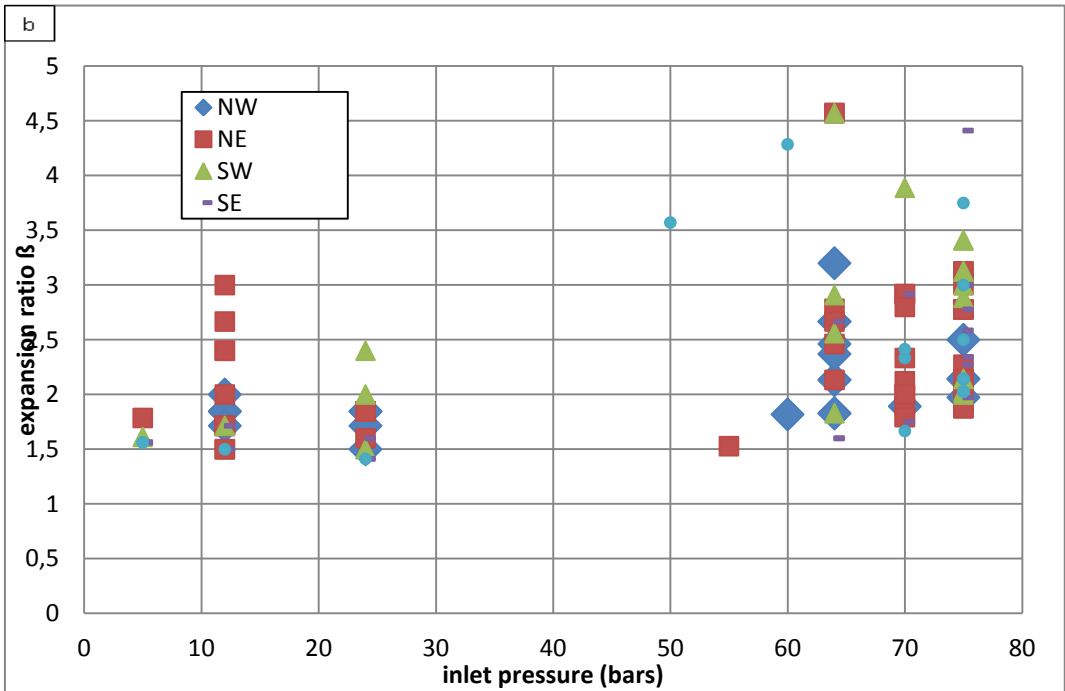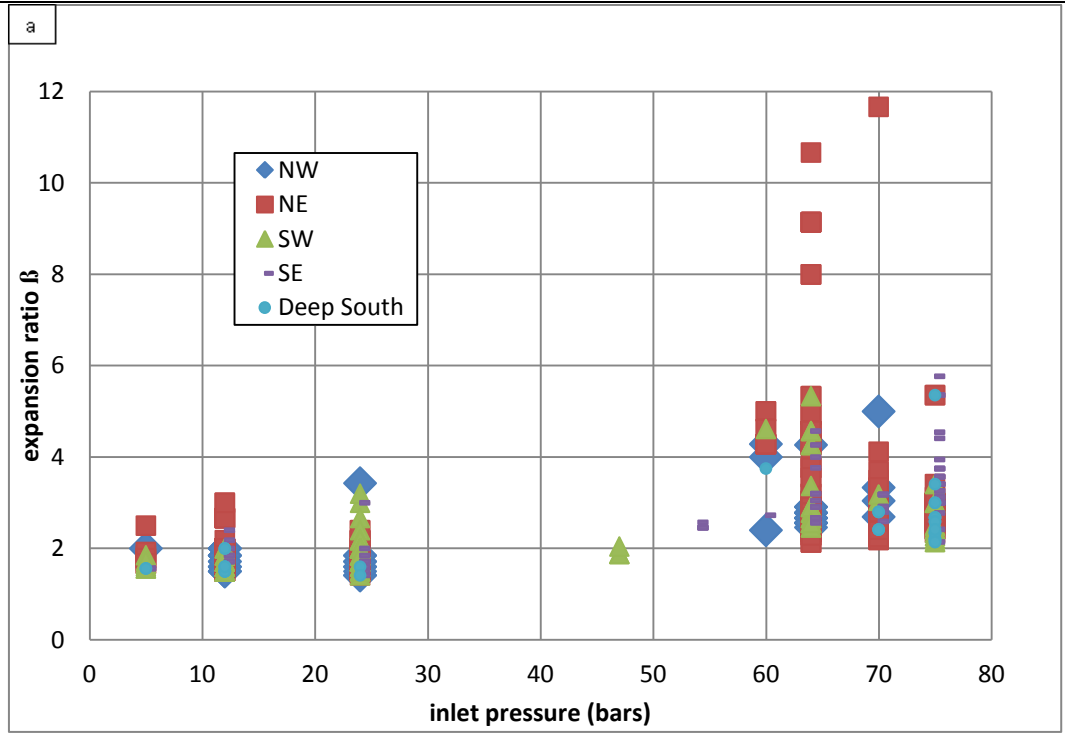
Figure 14. Redelivery points (source SNAM [11]: (a) Transportation users (b)
Industrial users (c) Thermoelectric users (d) Distribution

3.2.9. KPIs application

The purpose of using KPIs is to support the selection of the most convenient set-up and, after that, of the most convenient operation for the PRSs. For this reason, a set of several dynamic simulations of real PRSs was accomplished to calculate the energy recovery and the related performance, in order to evaluate the KPIs' capability of representing actual savings as well as the distinct and particular features of each proposed KPI.

Dynamic modelling has allowed prediction of time histories for the various system parameters, with different boundary conditions and operating procedures. Finally, energy quantities needed to evaluate KPIs have been calculated, thereby assessing their effectiveness and accuracy.

At first, the most common system configuration was considered as a reference, with the purpose of assessing the most conventional plant configuration. More precisely, with reference to the lay-out in figure 13, the thermal energy is provided by means of two conventional gas-fired boilers, which produce the hot water necessary to accomplish the NG preheating process. Here, the NG is preheated by process water, the temperature of which ranges from 55ºC to 90ºC, in a shell and tube heat exchanger with heat transfer coefficient (UA) of about 1.94 kW/K. Upstream of the TE, there is a flow control valve that enables NG mass flow regulation.

In order to test the accuracy of the prediction models, which are essential to enable online estimation of the indexes, a comparison was made between two different numerical simulations. The two system configurations (the one with TE and the one with TVs only) were implemented in *UniSim® Design Suite* software. In the first plant, the entire NG mass flow rate flows through the TV while, in the other, the mass flow rate is split into the TE and the TV. To make analysis of the

results easier, the simulation of the two PRSs was conducted in parallel, to be sure that the same operating conditions were shared. The thermal production was controlled by means of a simple proportional controller the proportional gain (p) of which was set equal to 5 kW and its process variable was the boiler outlet water temperature. The set points were established to maintain the minimum admissible NG temperature at the TE outlet. Figures 15a and b, represent the boiler and TE characteristics respectively. The KPIs were assessed for NG mass flow rates ranging from 5000 kg/h to 30000 kg/h. These values are typical for PRS [10].
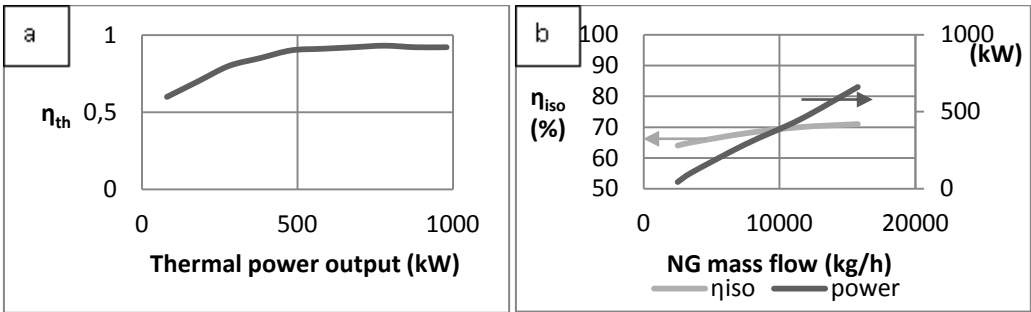

Figure 15. System characteristics: (a) Boiler's thermal efficiency; (b) turbo expander efficiency

It is worth recalling that the effect of heat losses along the pipelines are not explicitly taken into account in calculation of the performances and of the KPIs. More precisely, the thermal losses, which depend both on the system characteristics and on climatic conditions, could have a slightly lower impact on conventional PRS since the temperature set point, for this kind of plant configuration, can be set to lower values, with respect to the PRS with TE implemented (e.g. 55ºC versus 85ºC), and this would result in lowering the thermal losses of conventional plant, if the system is wisely managed. The effect of neglecting thermal losses from connection piping could generate a minor mismatch between the actual performances of the plants and those calculated, since these account for a small percentage of main heat flow rates. Indeed, the heat losses through piping shell

could account for a not trivial amount of energy. Nevertheless, the precise calculation of these heat losses has not been included in this study for the following reasons.

Heat losses strongly depend on the real insulation of plant, besides the combined effect of the external temperature and of feed water temperature, on heat losses which could be up to 40% of a small percentage of the gross heat flow rates and, thus, these do not definitely shift the global results.

3.2.10. Discussion and conclusions

This section describes the outcome that can be obtained by using the proposed KPIs, with specific focus on WER and CER, to exemplify to what extent the performance indicators are useful for assessing the energy recovery from PRSs as well as the environmental benefits. Finally, preheating model accuracy and limitations are analysed together with the possible thermal grid integration.
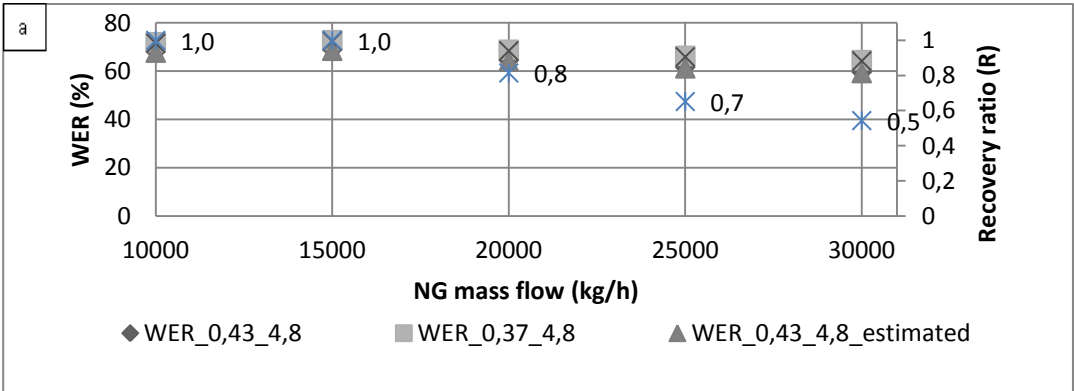
KPI assessment

The WER index was calculated by means of numerical dynamic simulations for 0.43 and 0.37 electric grid efficiency and for different expansion ratios (WER_0.43_4.8-15) and (WER_0.37_4.8-15) respectively. The same indexes were lastly estimated by using the prediction models (WER_0.43_4.8-15_estimated) and (WER_0.37_4.8-15_estimated).

From figures 17a-d, when the system is working at nominal conditions, the WER could achieve a maximum value of about 69.03 % by considering the national electric efficiency at 43%. WER values range from 45% to 69% depending on system operating conditions and characteristics. NG flow rate influences WER and R values as well, but the trend changes depending on β, showing the crucial role played by the flow conditions in determining the effects of recovery process.

Obviously, the national electric power system characteristics influence the WER and CER indexes. More precisely, the higher the conversion factor the lower the WER. Eventually, the same considerations are true for the CER index due to its definition.

The R drop does not influence the WER index at all. However, by considering β=4.8 with a single stage expansion process (figure 17a), it seems that as the R value drops, the WER is slightly dragged down. This should not be misunderstood since the WER drop is entirely linked to the system efficiency curves. Figure 18 instead, shows a comparison between the CER and WER indexes for a β=4.8. Here, CER and WER index have the same trend actually due to their definition. The curves show a trend with a peak value at 10000 kg/h or 15000 kg/h and a smooth slope at higher values.

It is worth recalling that there might exist certain operating conditions where the WER and CER indexes become very low or close to negative values. This might be quite frequent in those systems where transients at low NG flow rates i.e. low system efficiency, are not properly handled with an appropriate automatic control.
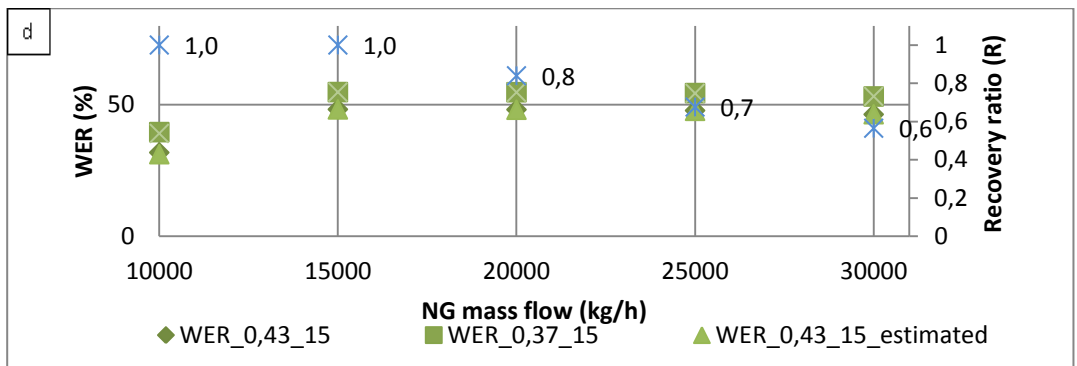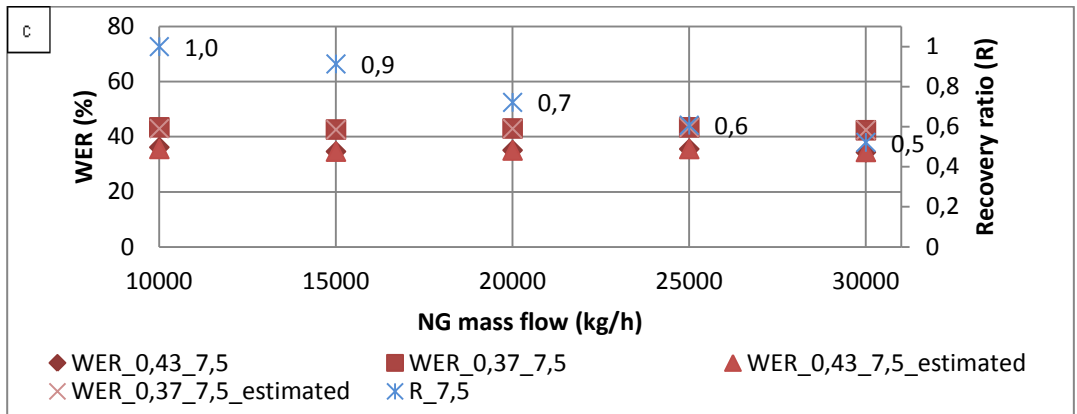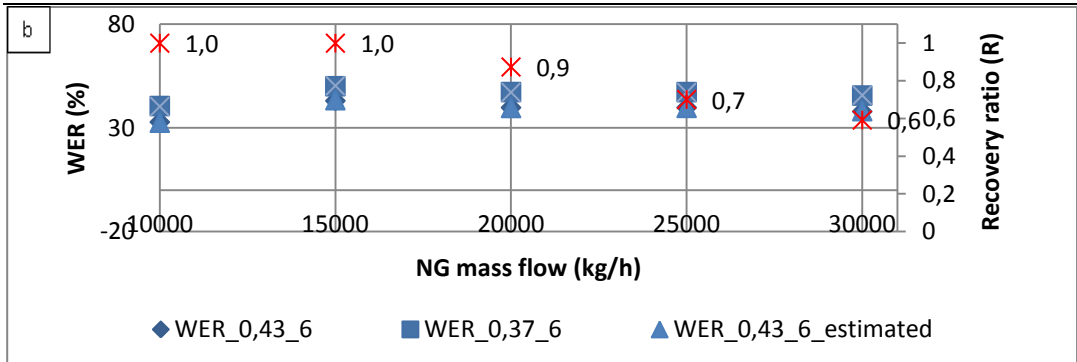
Figure 16. Waste Energy Recovery (WER) index assessment. (a) β=4.8, single stage (b) β=6, double stage (c) β=7.5, double stage (d) β=15, double stage.
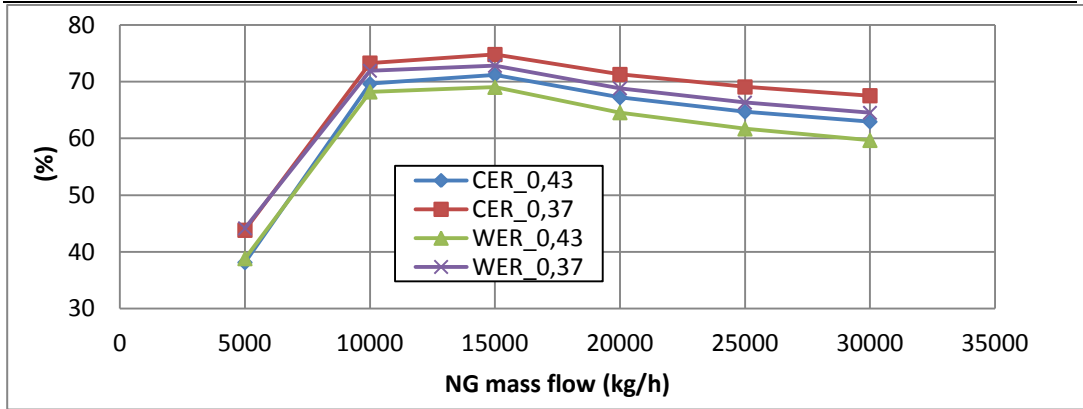
Figure 17. CER and WER index comparison for β=4.8.

Prediction model accuracy and limitations

The percentage relative difference and the absolute error [11] were evaluated comparing the results of the prediction model with the ones obtained by means of the detailed dynamic simulation, made with *UniSim®*. Figure 19a shows the percentage relative difference of the models, while figure 19b reports the absolute error.

The results shown in figures 18a-b point out that the model has good reliability, particularly at the higher NG flow values. Indeed, a maximum over estimation of about 15% is observed in figure 18a for low NG flow rates. Similarly, the absolute error is less than 1 for all mass flow rates, except for 5000 kg/h (Fig. 18b). However, the accuracy is generally satisfactory even for that functioning condition. Both graphs in figures 18a-b suggest a certain sensitivity to the β values, but the effect changes its direction according to the flow rate range. In the end, the model uncertainty is definitely acceptable for the present purpose, which is to test the efficacy of the proposed KPIs.

Some limitations might be found in utilisation of such prediction models. Since these were defined based on specific operating conditions, the percentage error

might become not negligible for NG inlet pressure transients or set point variations. Normally, such variations influence the system performance modestly, resulting in slight variations of the percentage error of such prediction models. This implies variation of the accuracy of WER and CER indexes. However, for an inlet pressure variation of about ± 5%, the effect on such indexes could be considered negligible.

Finally, for colder climate zones, the effect of heat losses should be considered in definition of the heat prediction models in order to avoid not negligible overestimation of the WER and CER indexes. On this basis, it is possible to conclude that the prediction models shown in table 2, used to estimate $Q_{rel}^{preheating}$, seem to be quite accurate.
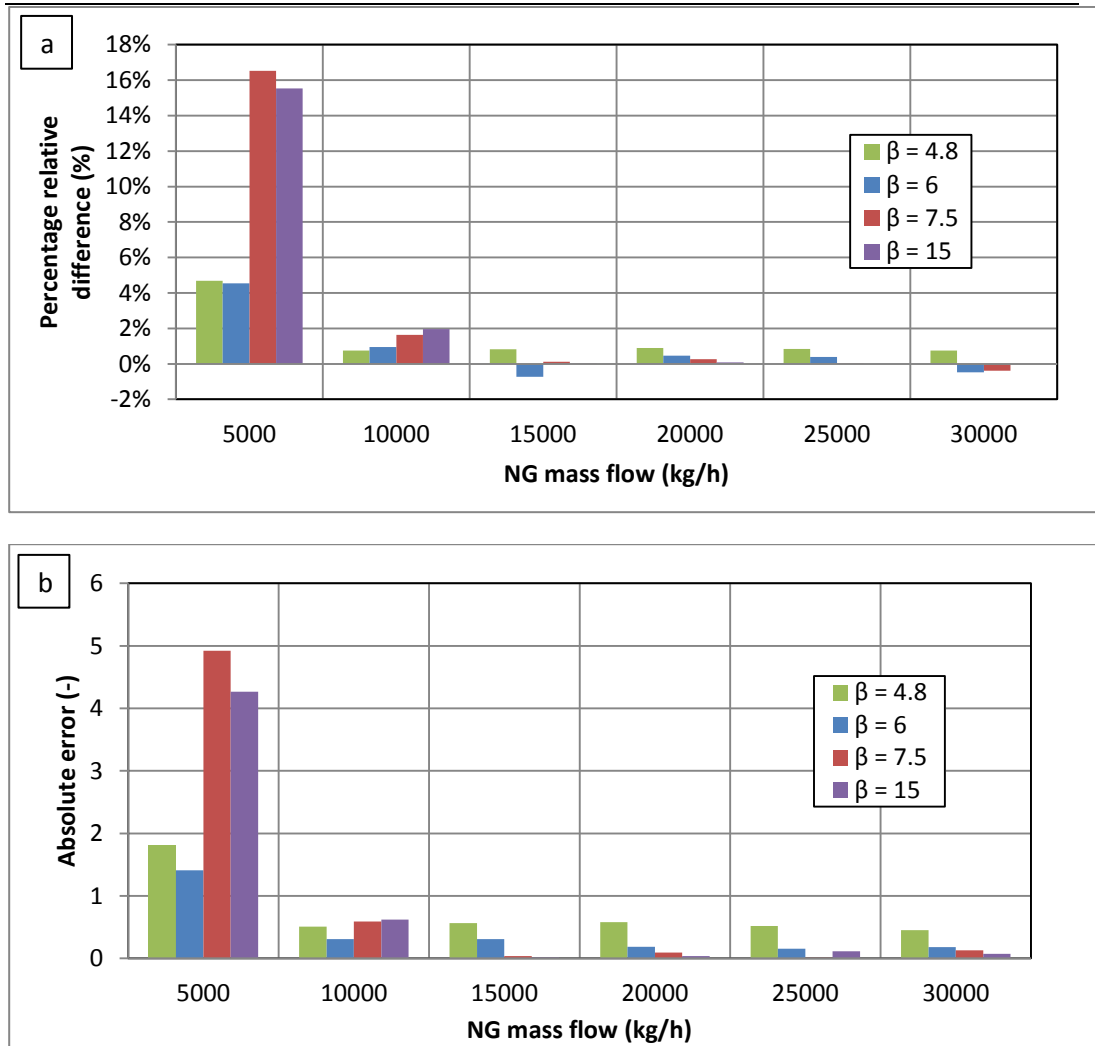
Figure 18. Prediction model accuracy: (a) percentage relative difference; (b) absolute error.

Effect of thermal grid integration

Recently, the possibility of integrating PRSs with external thermal users e.g. district heating networks, was presented [12]. PRS thermal integration represents an opportunity to achieve higher primary energy conversion efficiencies if appropriate system control is used [4]. In this section, the effect of the integration on the WER index is quantitatively assessed. By thermal integration, the author refers to the plant connection to any thermal user such as a district heating network.

In this case, the thermal energy required by the network would be supplied by the boilers of the PRS. For this purpose, the two system configurations were implemented in *UniSim® Design Suite* and a simulation was conducted for different external heat loads (Q_{th}^{grid}) at different NG flow rates. The results are reported in figures 19a - 19e in comparision with the case where the thermal user (district heating) requires no heat ('No demand'). Here, it is possible to appreciate how the WER index varies based on the system operational status when thermal integration is enabled. To be more precise, by considering a 5000 kg/h NG flow, the WER index relative to the case with thermal integration is higher by about 10.14%, 11.4% and 8.72% at 100, 300 and 500 kW respectively. Instead, at 700 and 900 kW this difference becomes negative (-10.02% and -12.76% respectively). This effect is strongly linked to the characteristic curves of efficiency of the thermal efficiency of the production units (figure 4) and, in particular, it is mainly due to their non-linearity. The performance of the system greatly depends on the control system of the gas preheat temperature and on its ability to control the valves and the TE gas outlet temperature. In particular, this is influenced by the size and the thermal inertia of the hydraulic circuits, and by the characteristics of the heat exchangers.

In some conditions, especially at lower flow rates, the effectiveness of the control system decreases considerably, and this results in efficiency reductions in the entire system. This phenomenon is more relevant at the lowest flow rates and during transients, especially in rapid ones: these effects can also be seen looking at the results of the simulation model, which often fail to converge in such cases. For this reason, an analysis of the results in these situations will be the subject of a forthcoming in-depth analysis.

Finally, figure 20 shows the WER difference for different heat loads and NG flow rates. Referring to figure 20, both negative and positive values would suggest the

71

possibility of optimising the system control achieving higher WER index during system operation. This might involve the use of thermal storage and appropriate optimisation algorithms. When the mass flow rate increases, errors tend to reduce, always maintaining a set of positive and negative values of ΔWER.
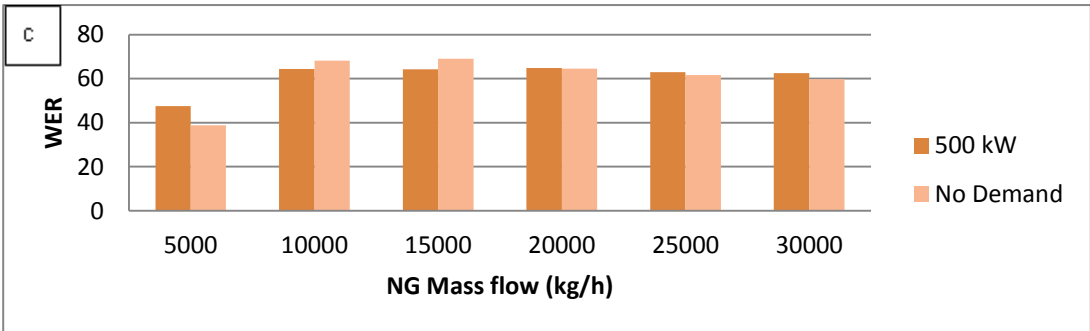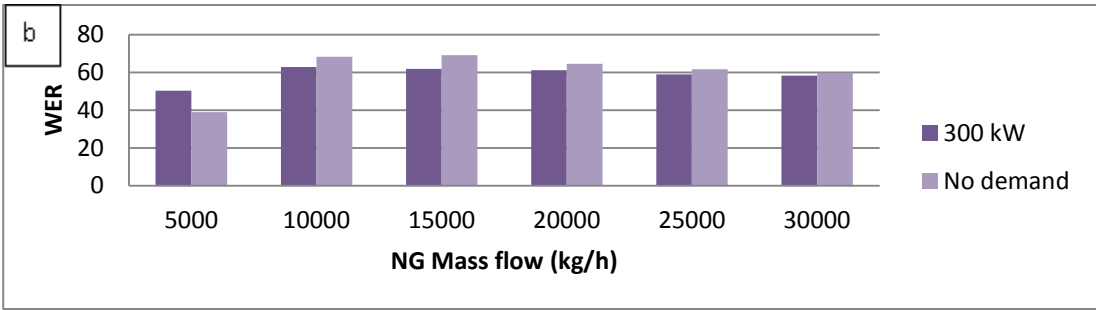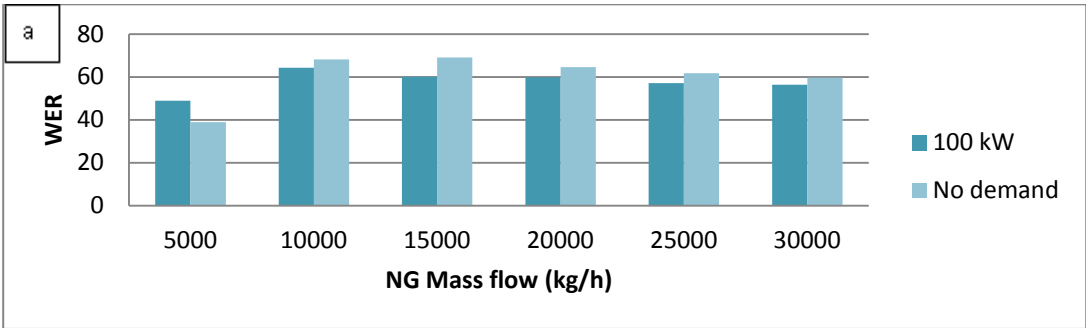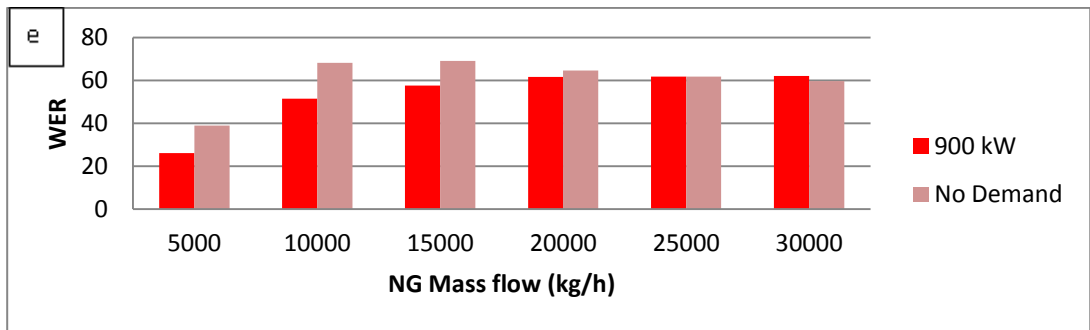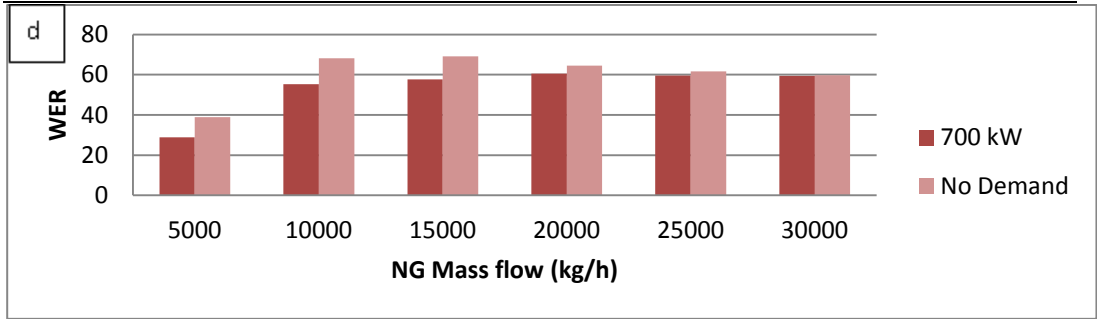
Figure 19. Effect of thermal integration on WER. a) 100 kW; b) 300 kW; c) 500 kW; d) 700 kW; e) 900 kW.

	5000	10000	15000	20000	25000	30000
■ 100 kW	10,14	(3,92)	(8,88)	(4,72)	(4,60)	(3,34)
■ 300 kW	11,40	(5,40)	(7,27)	(3,39)	(2,72)	(1,48)
■ 500 kW	8,72	(3,90)	(4,85)	0,26	1,21	2,76
■ 700 kW	(10,02)	(13,02)	(11,41)	(4,08)	(2,20)	(0,28)
■ 900 kW	(12,76)	(16,79)	(11,54)	(2,93)	0,08	2,43

Figure 20. WER difference assessment.

Key performance indicators to guide sustainable energy actions

Sustainable energy planning often suffers from a lack of prioritisation criteria, able to guide energy policy towards optimised or, at least, effective choices. Objective indicators are needed in order to select the best practices and maximise the impact of economical investments. In this framework, the proposed KPIs can play a role for initiatives aimed at energy saving in NG grids. In fact, the indicators permit assessment of the actual benefits coming from a certain action and comparison of different options, to select the best. Policymakers must be aware of the damage that improvised decisions or wrong presumption-based ones make in sustainable energy planning, with a huge waste of resources and credibility.

Currently, the incentives for energy recovery from the NG transportation and distribution grid have not yet been properly designed to account for novel and unconventional technologies [4]. Normally, from the CELSIUS project experience emerged that the energy produced by the TE is remunerated based on readapted incentive mechanisms e.g. in some cases, for those PRS equipped with solar thermal panels, incentives of photovoltaic are adapted to remunerate the electricity produced by the TE. Instead, the energy recovered by the TE should be incentivised with a proper methodology based on objective indicators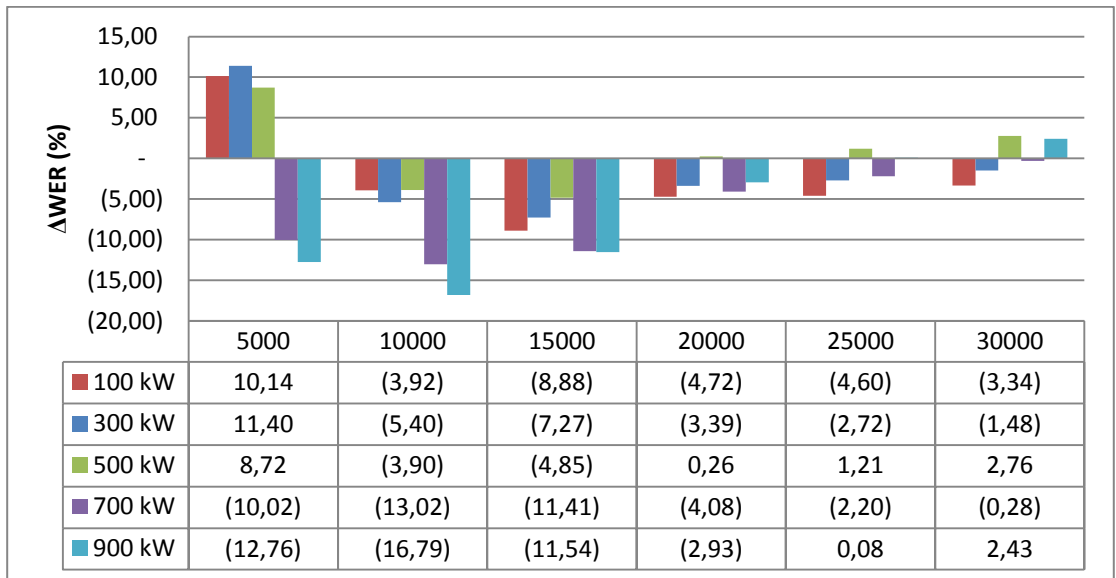, such as those introduced in this paper. The use of such performance indicators can play a fundamental role in the incentive mechanism decision process, for policy makers. In fact, the proposed KPIs allow you to understand the real efficiency of the recovery process and to facilitate energy incentive design and distribution.

In this study, key performance indicators for integrated natural gas pressure reduction stations with energy recovery have been proposed. In spite of their simplicity, or specifically for this reason, they can drive sustainable energy initiatives at both public and industrial level. In particular, the research conducted

can be important for the natural gas industry, in which energy can be recovered instead of wasted by throttling valves.

The KPIs introduced cover the different aspects of energy recovery in PRS. The Waste Energy Recovery (WER) index is fundamental to assess the efficiency of the recovery process. Other indicators such as the Recovery ratio (R) and the Carbon Emission Recovery index (CER) provide information related to the status of the recovery process and to carbon emission reduction, respectively. KPI values have been calculated for a reference configuration and confirm the possibility of achieving an effective energy recovery from the natural gas transportation grid. In general, the proposed KPIs permit avoidance of non-performing interventions and allow you to see the potential of the design and operation optimisation. Moreover, they are able to quantify the potential to minimise the environmental impact of gas networks through pressure drop capitalisation.

Furthermore, the effect of the integration of pressure regulation stations with external thermal grids has been assessed. By using the KPIs, it was possible to quantify the potential benefits that can be achieved from this integration. More precisely, the WER index can be potentially improved by providing heat to the thermal grid, especially at low natural gas flow rate. Indeed, this would let the system work at its nominal conditions, with higher efficiency, thereby enabling the possibility of achieving effective energy recovery from the natural gas grid as well as what would otherwise be lost.

Finally, the test cases which have been analysed in this paper show that the proposed KPIs represent a fundamental supporting tool to conduct efficient system operations and avoid risky energy and economic mismatches. The simplicity and the strength of the performance indicators make their implementation and interpretation easy for system operators. Besides, they can easily be implemented in management software for real time control, thereby improving system operation.

As a general conclusion, it is possible to state that these KPIs may be fundamental to properly designing fair incentive mechanisms for policy makers and/or energy performance contracting.

Looking at future developments, the use of KPIs for turbo-expanders in NG PRSs can play a large role in the development of integrated smart grids, facilitating the diffusion of sustainable distributed generation. However, some issues still deserve to be investigated. The unclearness linked to the energy remuneration policies for the different possible system configurations, for instance solar based stations, needs to be properly addressed to encourage the use of this technology. The impact of the high investment cost on the financial sustainability is to be better analysed. Moreover, a proper assessment of global and local energy recovery potential is still missing, and should be undertaken possibly through an international coordinated cooperation involving NG transportation and distribution companies, research organisations and policy makers. For all these issues the availability of accurate and reliable KPIs is a necessary condition.

NOMENCLATURE

AE Instantaneous avoided carbon emissions (kg/h)

$\overline{AE}$ Average avoided carbon emissions (kg)

CER Instantaneous carbon emission recovery (%)

$\overline{CER}$ Average carbon emission recovery (%)

c_p Thermal grid energy vector's heat specific value (kJ/kgK)

E_{rel} Recovery process power production (kW)

e_{rel} Relative process carbon emission (kW)

E_{WER} Recovery process power production (kW)

e_{WER}	Recovery process carbon emissions (kg/h)
$\dot{m}_{fuel_{WER}}$	Fuel mass flow for recovery process (kg/s)
$\dot{m}_{grid}$	Thermal grid water energy vector flow rate (kg/s)
$\dot{m}_{TE}$	Turbo expander natural gas flow rate (kg/s)
$\dot{m}_{tot}$	Total natural gas flow rate (kg/s)
P_{TE}	Turbo expander power output (kW)
PQ	Power/heat ratio
$\overline{PQ}$	Average power/heat ratio
PQ_{eff}	Effective power/ heat ratio
$\overline{PQ}_{eff}$	Average effective power/heat ratio
Q_{TE}	Instantaneous turbo expander preheating load (kW)
$Q_{rel}^{preheating}$	Instantaneous relative preheating load (kW)
Q_{th}^{grid}	Instantaneous thermal grid heat load (kW)
$Q_{tot}^{preheating}$	Instantaneous total preheating need (kW)
Q_{tot}	Instantaneous heat load (kW)
R	Recovery factor
$\bar{R}$	Average recovery factor
t_0	Time lower bound (s)
t	Time upper bound (s)
T_{in}	Thermal grid inlet temperature (K)
T_{out}	Thermal grid outlet temperature (K)
WER	Waste Energy Recovery index (%)

Abbreviations

CHP	Combined Heat and Power
DHN	District Heating Network
LHV	Lower Heating Value
NG	Natural Gas
PRS	Pressure Reduction Station
RES	Renewable Energy Sources
TE	Turbo Expander
TV	Throttling Valve

Greek letters

β	Expansion ratio
γ	National electric grid emission factor (kg_{CO2}/kWh)
δ	Thermal unit carbon emission factor (kg_{CO2}/kWh)
$\bar{\eta}_{el\_grid}$	National electricity production efficiency
$\bar{\eta}_{th}$	Thermal unit, average thermal efficiency
η_{th}	Thermal unit, thermal efficiency

REFERENCES

[1]   W. J. Kostowski and S. Usón. Thermoeconomic assessment of a natural gas expansion system integrated with a co-generation unit. Applied Energy 101; pp. 58:66 (2013).

[2]   W. J. Kostowski, S. Usòn. Comparative evaluation of a natural gas expansion plant integrated with an IC engine and an organic Rankine cycle, Energy Conversion and Management 75; pp. 509-516,(2013).

[3]   W. J. Kostowski, S. Usón, W. Stanek, P. Bargiel. Thermoecological cost of electricity production in the natural gas pressure reduction process. Energy 76; pp. 10:18, (2014).

[4]   E. Lo Cascio, D. Borelli, F. Devia, C. Schenone. Future distributed generation : An   operational   multi-objective optimization model for integrated small scale urban electrical,   thermal and gas grids. Energy Conversion and Management 143; pp. 348:359, (2017)

[5]   Piano d'Azione Italiano per l ' Efficienza Energetica, 2014. Available online: https://ec.europa.eu/energy/sites/ener/files/documents/2014_neeap_it_italy.p df (accessed 24/07/2017)

[6]   E. Ashouri, F. Veysi, E. Shojaeizadeh, M. Asadi. Journal of Natural Gas Science and Engineering The minimum gas temperature at the inlet of regulators in natural gas pressure reduction stations (CGS) for energy saving in water bath heaters. Journal Natural Gas Science; 230, pp. 240-21 (2014).

 [7]   Hagan, M. T., Demuth, H. B., Beale, M. H., De Jesús, O. (2014). Neural network design. Martin Hagan, Stillwater.

[8]   ETSONGMap.Available online:http://www.gie.eu/download/maps/2016/ENTSOG_SYSDEV_2015-2016_1600x1200_online.pdf (accessed 24/04/2017)

[9]   Gas transportation companies. Available online http://www.autorita.energia.it/it/dati/elenco_dati.htm (accessed 24/07/2017).

[10] Redelivery points - SNAM. Available online:
      http://www.snamretegas.it/en/services/New_Delivery_Redelivery_Points/
      (accessed 24/07/2017)

[11] Törnqvist, L., Vartia, P., & Vartia, Y. How Should Relative Changes Be
      Measured? The American Statistician, 39(1), 43-46, (1985).

[12] Borelli, F. Devia, E. Lo Cascio, C. Schenone, and A. Spoladore. Combined
      Production and Conversion of Energy in an Urban Integrated System.
      Energies 1, pp. 17-9 (2017).

3.3. Optimal design approach

The optimal design issue of the PRSs was investigated by Sanaye and Nasab in [1], who proposed a relatively fast method to select the size and number of components for PRSs using an objective function defined as the sum of the income and expenses. Subsequently, the optimum values of nine decision variables were obtained by maximizing the objective function using the genetic algorithm optimization technique. This hybrid semi-empirical procedure permits efficiently calculating the optimal configuration for a wide range of operating parameters. However, the variability of the WER potential, which is dependent on the NG flow patterns for a given TE, was not considered in this study.

In general, the abovementioned studies show that different techniques can be adopted to optimize the design of systems for energy recovery from PRSs, although, the current methods for system synthesis problems, clearly described by Frangopolus et al. in [2], do not appear to be completely adequate for PRS

retrofitting because of their complexity or inaccuracy. Therefore, this part of the research introduces the structured retrofitting approach (SRA) that intends to guide system designers and engineers during the entire PRS retrofitting process for energy recovery. While the traditional approach oscillates between heuristic methods and numerical analyses that, with difficulty, lead to a practical project assessment, the new proposed method allows quick and accurate determination of the optimal plant size.

The proposed SRA envisions a model for component dimensioning, which includes novel key aspects that emerge during the PRS retrofitting, such as the variability of the energy recovery potential and the system thermal integration. For this purpose, a non-smooth constrained optimization problem based on the minimization of the levelized cost of energy (LCOE) was developed. Finally, the SRA promotes a series of post-retrofit activities to emphasize project continuity and dissemination for practical knowledge capitalization.

3.3.1. Structured retrofitting approach

As shown in figure 21, different factors of different nature, should be taken into consideration to achieve a successful retrofit project. for this reason, a structured retrofitting approach becomes fundamental during the whole retrofitting process.
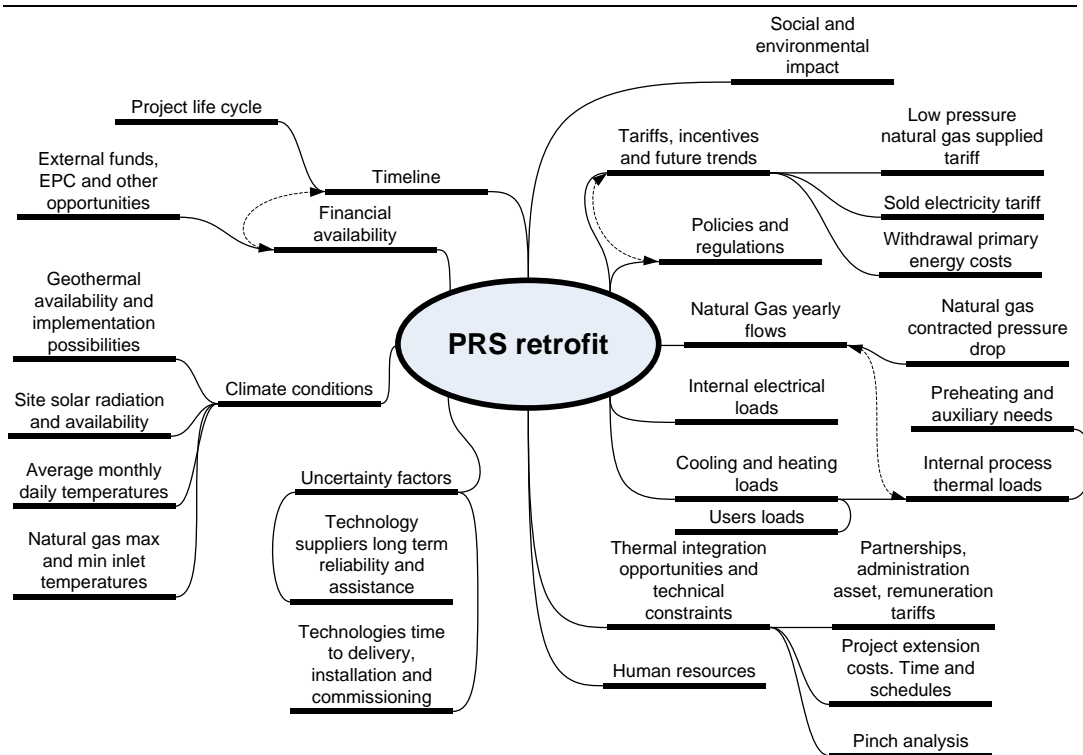
Figure 21. Factors affecting the retrofit project.

Figure 22 illustrates the key steps of a general PRS structured retrofitting approach (SRA). The overall procedure, based on a long-term approach, is divided into four main temporal phases: pre-retrofit activities, preliminary and executive project design, implementation and commissioning and post-retrofit activities. For each phase, a given set of sequential tasks is defined, and the respective information, tools and consideration needs are highlighted.

The proposed SRA has been designed to include long-term objectives and collateral activities. In fact, it emphasizes dissemination activities for project continuity and suggests considerations about the opportunity to involve research institutes and universities, of which the purpose is to boost and

strengthen different key actions of the process, including dissemination, numerical model setup and validation, operational control model design and tests, forecasting, data analytics, performance assessment, analysis via numerical dynamic simulations, etc. These activities are fundamental for replicability and reference dataset definitions for similar future project implementations.

The main task of the *pre-retrofit activities* consists of local data acquisition. Here, it is necessary to collect different types of specific information related to the PRS and its surrounding conditions: past NG annual flow rates, internal and external thermal and electrical loads, analysis of the potential integration opportunities with neighbouring processes, etc.

Furthermore, the *preliminary and executive project design phase* is schematized as a sub-iterative process where the first task consists of identifying a set of potential system configurations. Uncertainty factors (technology supplier long-term reliability, time to delivery, installation and time-to-commissioning) are fundamental to be considered at this stage since they might cause the PRS project to not completely succeed within the planned time schedules. Moreover, considering the magnitude of a single PRS retrofit, the lower contractual strength with respect to technology providers and industries, if compared to larger projects, could emphasize the negative effects of those uncertainty factors.

Once the configuration set has been identified, the second step of the process involves the optimal component design. Here, the component dimensioning will be based on the information acquired during the preliminary phase. For this purpose, an optimal design approach will be presented in the following section. Furthermore, once the optimal component size has been defined, it is possible to start the executive PRS project. At this stage, the numerical dynamic simulation represents a powerful tool to understand the system behaviours of Hazardous and Operability (HAZOP) and "What if" analysis, energy performance assessment and transient analysis.

An optimal economic design must guarantee that a cost-effective configuration has been achieved. However, an economic analysis and risk assessment are still necessary to properly evaluate component implementation schedules, control strategies and operational planning and, eventually, energy performance contracting, target definition and baseline assessment. As is commonly known, many tools are available for this purpose: levelized cost of energy (LCOE), net present value (NPV), internal rate of return (IRR), profitability index (PI), discounted payback period (DPBP), lifecycle assessment (LCA), etc.

Furthermore, during the *implementation and commissioning phase*, the custom optimal control strategy definition is fundamental to ensure energy savings and carbon emission minimization. At this stage, it is important to highlight that the optimal system design and the optimal control strategy should not be considered as two different and unconnected issues. In fact, the identified optimal design conditions, i.e., the average energy production required to guarantee the validity of the optimal design conditions, must be taken into consideration during the optimal control strategy definition. This is fundamental to keep the optimal design points valid during the system lifecycle. In contrast, the design conditions identified during the preliminary and executive project design phase can no longer be considered optimal in the further phases. In this study, this problem is addressed by defining the OEP index.

During the *commissioning phase*, the system performance data will be acquired, stored and further disseminated. These data are important to proceed with a parallel numerical model validation. Numerical model validation is a fundamental step to be properly achieved to proceed with system performance forecasting. This task is important to consolidate the system operation strategies of optimal control adjustments, operation and maintenance schedule settings, etc.

After these activities are completed and the implementation and commissioning phase ends, the *post-retrofit activities* must be conducted. For this purpose, the key

task consists of measurement and verification activities (M&V). Finally, once the process has been completed, the retrofit report should be prepared and frequently updated.
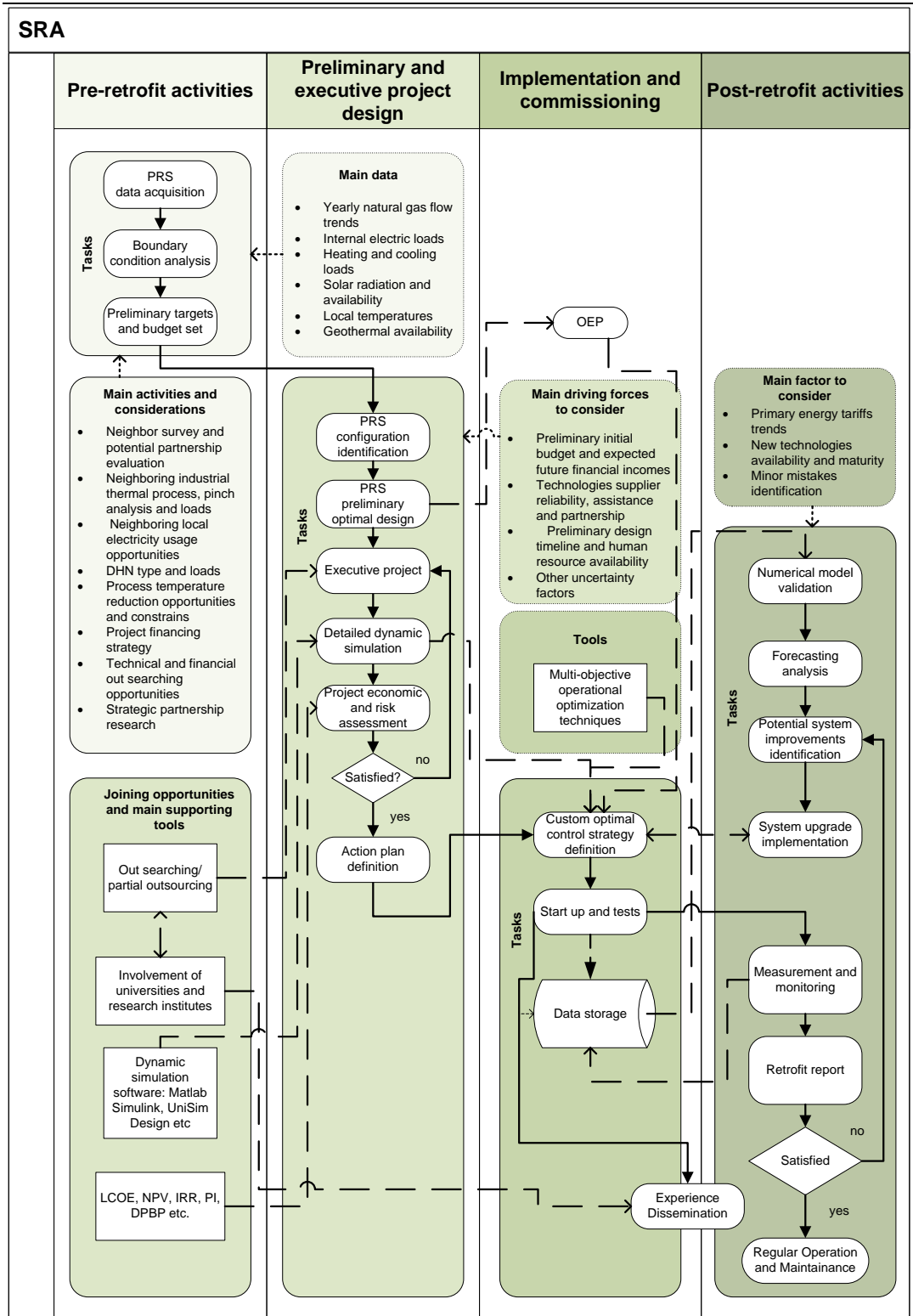
SRA

Pre-retrofit activities	Preliminary and executive project design	Implementation and commissioning	Post-retrofit activities

Tasks

PRS data acquisition

Boundary condition analysis

Preliminary targets and budget set

Main data
- Yearly natural gas flow trends
- Internal electric loads
- Heating and cooling loads
- Solar radiation and availability
- Local temperatures
- Geothermal availability

Main activities and considerations
- Neighbor survey and potential partnership evaluation
- Neighboring industrial thermal process, pinch analysis and loads
- Neighboring local electricity usage opportunities
- DHN type and loads
- Process temperature reduction opportunities and constrains
- Project financing strategy
- Technical and financial out searching opportunities
- Strategic partnership research

Joining opportunities and main supporting tools

Out searching/ partial outsourcing

Involvement of universities and research institutes

Dynamic simulation software: Matlab Simulink, UniSim Design etc

LCOE, NPV, IRR, PI, DPBP etc.

Tasks

PRS configuration identification

PRS preliminary optimal design

Executive project

Detailed dynamic simulation

Project economic and risk assessment

Satisfied? — no

yes

Action plan definition

OEP

Main driving forces to consider
- Preliminary initial budget and expected future financial incomes
- Technologies supplier reliability, assistance and partnership
- Preliminary design timeline and human resource availability
- Other uncertainty factors

Tools

Multi-objective operational optimization techniques

Tasks

Custom optimal control strategy definition

Start up and tests

Data storage

Main factor to consider
- Primary energy tariffs trends
- New technologies availability and maturity
- Minor mistakes identification

Tasks

Numerical model validation

Forecasting analysis

Potential system improvements identification

System upgrade implementation

Measurement and monitoring

Retrofit report

Satisfied — no

yes

Regular Operation and Maintainance

Experience Dissemination

Figure 22. Structured Retrofitting Approach (SRA).

86

3.3.2. Optimal design model

The design optimization during the *preliminary and executive project design* is an essential piece of the SRA and a key element in the proposed methodology, and a relevant part of the SRA success depends on this aspect. For this reason, a novel mathematical model has been developed, which is based on the minimization of the levelized cost of energy (LCOE) defined by Equation 1:

$$LCOE = \frac{\dfrac{\sum_{t=1}^{n}(I_t + M_t + F_t)}{(1+r)^t}}{\dfrac{\sum_{t=1}^{n}E_t}{(1+r)^t}} \tag{1}$$

where I_t, M_t and F_t are, respectively, the investment expenditure, maintenance and operation costs, and fuel expenditure in the year t. Then, r and n are, respectively, the discount rate and the expected lifetime of the components or systems, and E_t is the energy generated by the system.

Distinct from Sanaye and Nasab [1], this original model was designed by considering the variability of the WER potential, which mainly depends on the NG flow pattern and the size of the selected TE. For this purpose, the model was structured as a non-smooth constrained optimization problem. Moreover, the optimization model was designed considering the system thermal integration opportunities with the neighbouring users as well. As is known [3], this is a key aspect for strategic PRS retrofitting and for efficient energy exploitation in urban districts. Finally, the model is also easily scalable for system configurations where

two TEs are normally implemented in a series due to a higher expansion ratio or for water-process temperature reduction.

The proposed optimization approach is given in the system configuration shown in figure 23. This layout represents a reference configuration for energy recovery from natural gas PRSs. The chosen system configuration involves two gas fired boilers, a gas fired CHP unit and a single TE with its heat exchanger, working in parallel with the throttling valves, which operate at very low or high mass flow rates to manage the turbine functioning range. The thermal plant is also connected to a group of buildings through a district heating network, which is supplied by the CHP and boilers.

These boilers have an integrative function for peak heat loads and perform a supplementary function during CHP downtime. Though the model is applied to this reference layout, which has a standard energy recovery from the PRSs, it can be extended to diverse configurations. Likewise, the results obtained from the proposed optimization method have a general validity and are suitable for wide generalization.

The design approach is based on a few main global constraints, depending on the system considered. The first constraint is related to the amount of total recoverable energy $E_{total}^{recoverable}$ from the turbo expander for a time length t. Generally, the total amount of recoverable energy for a certain PRS and TE is strictly dependent on the NG flow rates, pressure drop, temperature conditions, system configuration, and the type of system control. Another four constraints refer to maximum size, redundancy condition, overall thermal energy balance and TE synchrony (for TEs in series). From the results of the design optimization process, the optimal sizes of the nominal components and the respective average optimal energy production

(OEP) will be known for a given time length t and for each component considered. In a future stage, once the system process and instrumentation diagram (P&ID) has been defined, the OEP conditions should be considered to properly address the system control optimization problem, as previously mentioned. In the following section, the optimization problem will be formulated with reference to the system configuration shown in figure 23. However, it can be extended and adapted to different configurations with minor modifications. As shown in figure 23, the redundancy condition is generally satisfied by two boilers that work in conjunction with an internal combustion cogeneration unit. These three components will satisfy internal (pre-heating process) and external (DHN) needs. One single TE is considered in the reference optimization problem.
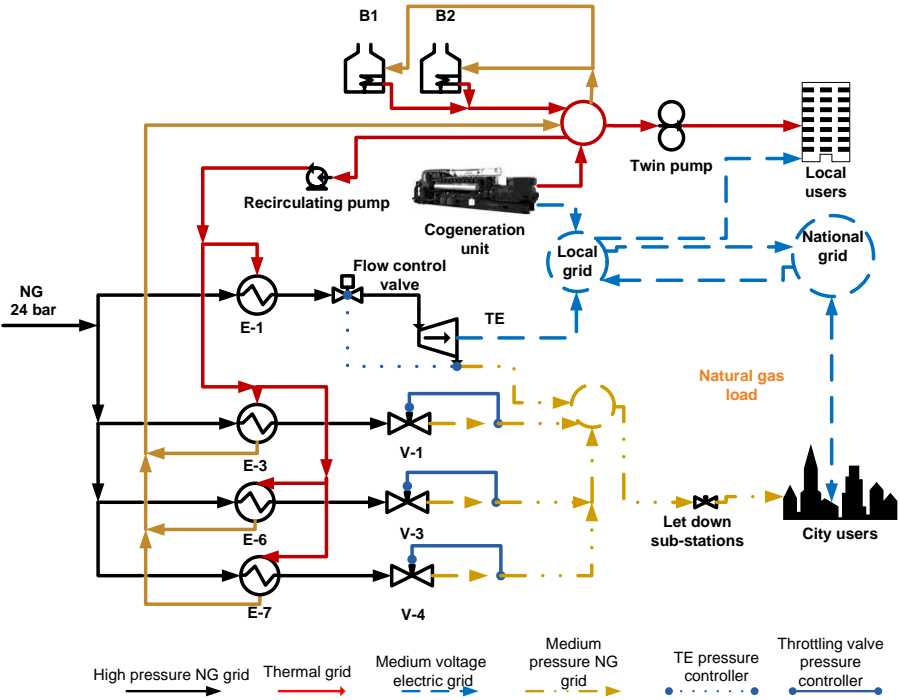
Figure 23. Reference system configuration.

3.3.3. Problem statement

The problem objective function is expressed as:

$$\min\{LCOE\} \tag{2}$$

subjected to the following constraints.

Heat balance for equipment sizing

The heat balance for the equipment sizing is defined as:

$$Q_{b1} + Q_{b2} + Q_{chp} - \xi P_{TE} = Q_{ext\_user}^{MAX} + Q_{valve}^{p.h.\_MAX} \tag{3}$$

where Q_{b1}, Q_{b2} and Q_{chp} are, respectively, the nominal sizes of the two boilers and the CHP, and P_{TE} represents the turbo expander nominal electric power. For simplicity, the heat power ratio ξ is considered constant for this model. Normally, the heat power ratio varies between 0.95 and 1.1 depending on the operating conditions and the system characteristics [4]. The heat power ratio is defined as:

$$\xi = \left(\frac{q_{TE}^{preheating}}{P_{TE}^{ref}} \right) \frac{1}{\varepsilon_{HE} \eta_{alt} \eta_{inverter}} \tag{4}$$

where ε_{HE}, η_{alt} and $\eta_{inverter}$ are, respectively, the effectiveness of the heat exchanger linked to the TE, the effectiveness of its generator and the DC/AC

90

inverter efficiency. The $q_{TE}^{preheating}$, instead, is the TE preheating need at the reference nominal power P_{TE}^{ref}. This ratio, as a first approximation, will be considered as constant for this model.

The terms $Q_{ext\_user}^{MAX}$ and $Q_{valve}^{p.h.-MAX}$ in Equation 3 represent the maximum expected external thermal load (DHN or other integrated process) and the maximum throttling-valve-preheating needs. The over dimensioning by considering these values as constant before and after the TE implementation will further ensure safe system operations for the case scenarios in which the system has to work under certain extreme operating conditions of NG flow peaks or temporary TE faults.

Redundancy

Heat production must always be ensured in case of component faults. Otherwise, methane hydrates will suddenly occur. Thus, the redundancy condition is defined as:

$$Q_{b1} - Q_{b2} = 0 \tag{5}$$

Overall thermal energy balance

The thermal energy balance is defined as:

$$Q_{b1}h_{b1}^{f.l.} + Q_{b2}h_{b2}^{f.l.} + Q_{chp}h_{chp}^{f.l.} - \xi P_{TE}h_{TE}^{f.l.} - Q_{vlv} = E_{user}^{MAX} \tag{6}$$

where E_{user}^{MAX} represents the average daily maximum thermal energy required by external users, and Q_{vlv} represents the average throttling-valve-preheating need expected after the retrofit. For this reason, it will depend on the type and size of the

implemented TE, which is a variable of the optimization problem, for instance, considering the *Honeywell* TE models [5] and given the PRS conditions:

$$\begin{cases} 550 \leq P_{TE} \leq 450 \Rightarrow Q_{vlv} = Q_{vlv,a} \\ 450 < P_{TE} < 160 \Rightarrow Q_{vlv} = Q_{vlv,b} \\ P_{TE} \leq 160 \Rightarrow Q_{vlv} = Q_{vlv,c} \end{cases}$$

Therefore, $Q_{vlv,a}$, $Q_{vlv,b}$ and $Q_{vlv,c}$ are the values of throttling-valve-preheating needs for different TE sizes and the given PRS. The terms $h_{b1}^{f.l.}$, $h_{b2}^{f.l.}$, $h_{chp}^{f.l.}$ and $h_{TE}^{f.l.}$, respectively, represent the average optimal number of operating hours per day at full load for boilers 1 and 2, CHP and TE. For a given time length, the product between the optimal nominal sizes, the respective optimal average number of operating hours per day and the number of expected operating days will result in the OEP.

Natural gas balance

The overall recoverable energy balance is defined as:

$$n P_{TE} h_{TE}^{f.l.} \leq N_{tot}^{recoverable} \tag{8}$$

where n is the number of days per year that the TE is expected to work considering system stops for maintenance, and $N_{tot}^{recoverable}$ represents the amount of average energy that might be recovered within the n days of work considered. The Q_{vlv} cannot be considered as a continuous function. The $N_{tot}^{recoverable}$ is strictly related to the NG flow and varies with the TE size, since each TE has different technical constraints upon the admissible peak NG volume flow. Then:

$$
\begin{cases}
550 \leq P_{TE} \leq 450 \Rightarrow N_{tot}^{re\,cov\,erable} = N_a \\
450 < P_{TE} < 160 \Rightarrow N_{tot}^{re\,cov\,erable} = N_b \\
P_{TE} \leq 160 \Rightarrow N_{tot}^{re\,cov\,erable} = N_c
\end{cases}
$$

where N_a, N_b and N_c are the quantities of the average recoverable energy for different TEs under certain PRS conditions and time lengths.

TE synchrony

In the case of a low-temperature system configuration where a double-stage expansion process is used, the power and operation synchrony constraints between the TEs must be added to the mathematical problem formulation, such as:

$$
h_{TE1}^{f.l.} - h_{TE2}^{f.l.} = 0 \tag{7}
$$

$$
\tag{8}
$$

$$
P_{TE}^{I} - P_{TE}^{II} = 0
$$

where P_{TE}^{I} and P_{TE}^{II} are the nominal powers of the first- and second-stage expansion turbines in the low-temperature configuration, respectively.

3.3.4. Model limitations and enhancements

Some minor limitations must be underlined for the proposed approach. The abovementioned OEP does not consider the effect of efficiency at partial loads for

each component. For this purpose, the efficiency must be considered as a reference value to properly address the system optimal control. Finally, the application of this model might be time consuming for non-expert users since it requires a preliminary effort to assess the N_a, N_b and N_c values, as well as the $Q_{vlv,a}$, $Q_{vlv,b}$ and $Q_{vlv,c}$. This requires long-term estimation, which is necessary to properly identify what the future NG flow rates are for the considered period of assessment [

3.3.5. Design optimization in brief

Energy recovery from a pressure reduction in natural gas networks was addressed through a structured retrofitting approach aimed at optimal design. The scope of this methodology is to drive the entire retrofitting process and enable project success. The developed method was demonstrated to maximize energy savings and reduce the complexity and calculation time [6]. The architecture of the proposed method is quite different from the current design techniques that are either heuristic or computationally demanding. The novel formulation of a non-smooth constrained optimization problem based on the LCOE minimization allows managing variable boundary conditions. Moreover, the innovative technological impact of the SRA method enables the exploitation of situations for which the current design does not allow and for which only an optimized size can recover waste energy.

The proposed case study reported in [6], demonstrated that the SRA optimization technique permits identifying the best system configuration in the PRS retrofit, particularly with regard to the turbo expander model and heat supplier technology. All the different issues of the integrated system design are addressed with the optimization technique. The turbo expander design provides helpful recommendations concerning the number and size of the machinery. Moreover, the effect of varying the natural gas flow patterns on the optimal results can be

evaluated to address the uncertainty. Optimization can be maintained along the system life for variable operating conditions by proper system operation management, which can be easily addressed using the OEP index.

Similar to previous studies, it has been confirmed that the combined heat and power technologies are not suitable for all retrofitting scenarios. The actual benefits are intimately linked to the natural gas flow in the station. If the flow is too low, the implementation of the technology is not justifiable. Furthermore, the repercussions of increasing fuel costs on the optimal results were evaluated. The results for the case study proposed in which all thermal supply technologies (boilers and cogeneration unit) were fed by natural gas showed that the eventual costly operating scenarios are disconnected from the optimization problem in the sense that no consequence on the diminishing component was observed. However, this situation might be different for multi-fuel-based systems, and for those cases, the optimization results might be different.

Finally, this study highlights that optimal retrofit interventions are challenging to design due of their sensitivity to calculation scenarios and boundary conditions. The lack of appropriate design tools leads to incomprehension and underestimation of the actual benefits in terms of energy savings and carbon emission reductions of PRS retrofitting, thus limiting the diffusion of this smart, energy-saving technology. Instead, through an effective optimization tool such as the SRA, it is possible to achieve the effective exploitation of the waste energy recovery potential from natural gas transportation and distribution networks.

Nomenclature

$E_{total}^{recoverable}$ Total energy recoverable for the assessment period (kWh)

E_{user}^{MAX} Maximum daily thermal energy required by external users (kWh)

F_t Fuel expenditure in the year t (euros)

$h_{b1}^{f.l.}$	Boiler 1, average optimal number of operating hours per day at full load (h)
$h_{b2}^{f.l.}$	Boiler 2, average optimal number of operating hours per day at full load (h)
$h_{chp}^{f.l.}$	Cogeneration unit, average optimal number of operating hours per day at full load (h)
$h_{TE}^{f.l.}$	Turbo expander, average optimal number of operating hours per day at full load (h)
I_t	Investment expenditure in the year t (euros)
M_t	Operation and maintenance in the year t (euros)
$N_{tot}^{recoverable}$	Effective amount of energy recovered (kWh)
N_a	Potential recoverable energy case a (kWh)
N_b	Potential recoverable energy case b (kWh)
N_c	Potential recoverable energy case c (kWh)
P_{TE}	Turbo expander nominal electric power (kWe)
P_{TE}^{ref}	Turbo expander reference nominal power (kWe)
P_{TE}^{I}	First stage turbo expander nominal electric power, low temp. confi. (kWe)
P_{TE}^{II}	Second stage turbo expander nominal electric power, low temp. confi. (kWe)
$q_{TE}^{preheating}$	Turbo expander preheating need at the reference nominal power (kWe)
Q_{b1}	Gas fired boiler 1 nominal size (kW)
Q_{b2}	Gas fired boiler 2 nominal size (kW)
Q_{chp}	Cogeneration unit nominal thermal size (kW)
$Q_{vlv,a}$	Throttling valve preheating energy case a (kWh)
$Q_{vlv,b}$	Throttling valve preheating energy case b (kWh)
$Q_{vlv,c}$	Throttling valve preheating energy case c (kWh)
$Q_{valve}^{p.h.\_MAX}$	Maximum throttling valve preheating thermal need (kW)
Q_{vlv}	Throttling valve preheating energy (kWh)

$Q_{ext\_user}^{MAX}$	Maximum external user thermal load (kW)
r	Interest rate (%)

Greek letters

ε_{HE}	Heat exchanger effectiveness
ξ	Heat power ratio
η_{alt}	Alternator efficiency (%)
$\eta_{inverter}$	Inverter efficiency (%)

Abbreviations

CHP	Combined heat and power
COP	Coefficient of performance
DHC	District heating and cooling
DHN	District heating network
ESCo	Energy service companies
RR	Internal rate of return
LCA	Lifecycle assessment
LCOEel	Levelized cost of electricity, (euros/kWh)
LCOEth	Levelized cost of thermal energy (euros/kWh)
NG	Natural gas
NPV	Net present value
OEP	Optimal energy production
PI	Profitability index
RS	Pressure regulation station
SRA	Structured retrofitting approach
TE	Turbo expander
WER	Waste energy recovery

REFERENCES

[1]   S. Sanaye and A. M. Nasab. Modeling and optimizing a CHP system for natural gas pressure reduction plant. Energy 40; pp. 358:369, (2012).

[2]   C. A. Frangopoulos, M.R. Von Spakovsky, E. Sciubba. A brief review of methods for the design and synthesis optimization of energy systems. International Journal of Thermodynamics 5.4; pp. 151:160, (2002).

[3]   CESLIUS project, available online: http://celsiuscity.eu/ (accessed 10/10/2017)

[4]   D. Borelli, F. Devia, E. Lo Cascio, C. Schenone.Energy recovery from natural gas pressure reduction stations : Integration with low temperature heat sources. Energy Convers Manag 2018; 274:283-159.

[5]   Gas expansion Turbine, available online: https://www.honeywellprocess.com/en-US/explore/products/gas-measurement-and-regulation/gas-expansion-turbines/Pages/default.aspx (accessed 06/08/2017).

[6]   Lo Cascio, Ermanno, Marc Puig Von Friesen, and Corrado Schenone. "Optimal retrofitting of natural gas pressure reduction stations for energy recovery." Energy 153 (2018): 387-399.

3.4. Water temperature reduction strategies

As reported in [1], the typical pressure ratio (β) value is almost 5 but, in some cases, β ranges from 8 to 12, up to a maximum of 15. Some of these characteristic operating ratios enable the possibility to split the expansion process in two stages, and allow to lower the overall process temperature. In this way, due to the typical pressure operating ranges and geographical positioning, energy recovery from PRSs represents a key opportunity for eco-industrial parks development [2] and low temperature thermal process integration e.g. industrial micro-grid networks [3] and 4th generation district heating networks [4]. Moreover, the opportunity to lower the water temperature of the process enables the possibility to employ a wider range of heat production technologies, such as geothermal heat pumps or thermal solar panels.

In general, the integration with district heating networks or waste heat sources in urban areas offers a noticeable opportunity of a coupled energy recovery. Moreover, PRSs operating schedule is directly linked to the NG users' demand, which leads to a spontaneous load matching between supply and demand in buildings heating thus making the integration among PRSs and district heating networks even more favorable. This integration of NG network with urban thermal grids, as well as the exploitation of a part of the large waste heat amount available inside cities, is a smart opportunity to improve urban energy recovery and to achieve a more effective energy use.

But this smart and novel technology for diffused energy saving requires a further step in terms of system analysis and modelling, since the management of the low temperature heat coming from DHN or WER needs the plant to be adapted and controlled in a new way compared to the common integration with a CHP system.

In [5], the authors study the integration of PRSs with low temperature heat sources. Energy performance of a typical low temperature PRS configuration was analyzed though numerical dynamic simulations. Results have been compared to high temperature ones and energy benefits for a typical winter day were estimated. Further, system fault tolerance was evaluated and time-to-hydrates was assessed by considering Motiee et al. [6], Mokhatab et al. [7] and Kidnay et al. [8] analytical predictive formulations.

3.4.1. System configurations

At a first glance, energy recovery from gas expansion seems to involve positive aspects only, and a large diffusion could be expected. Nevertheless, only few plants are currently in operation. Enthusiasm for this technological solution often collides with technical constrains and economic problems, mainly due to two different needs: the risk of hydrates formation and the costs increase costs for the retrofit

intervention. Therefore, this kind of energy recovery system becomes less convenient not only from an energetic viewpoint, but even from operating and economic ones. The opportunity to reuse waste energy or exploit existing heat facilities can move the balance towards a more efficient utilization of the NG pressure drop, fostering in this way the diffusion of the expansion technology. In this sense, research on integrating low temperature heat sources in the PRSs energy recovery systems represents a key issue, which deserves to be deepened and well analyzed.

As known, one of the constraints that one must faces to design an energy recovery system based on NG pressure drop is methane hydrates formation. Solidification of methane hydrates occurs when water molecules form a cage-like structure around smaller guest molecules (e.g. methane, ethane, propane, iso-butane, normal butane, nitrogen, carbon dioxide, and hydrogen sulfide) [9]. Many studies have been focused on methane hydrates formation in natural gas pipelines. Considering the NG composition shown in table 3 and a pressure of about 5 bar, three different mathematical correlations have been considered in order identify methane hydrates formation temperature. More precisely, by considering Motiee et al. [6], Mokhatab et al. [7] and Kidnay et al. [8] correlations, methane hydrates formation respectively occurs at temperatures of about -4.47ºC, -2.67ºC and -2.23ºC.

In general, this is a very challenging limit. Nevertheless, in urban areas or wherever possible, when properly managed it does not reduce the possibility of integrating a DHN or even an industrial waste energy source with the PRS to recover waste heat (also at low temperature) in order to reach a higher level of efficiency.

Table 3. NG composition at standard conditions.

Chemical	weight composition [%]
Methane	92.347
Ethane	4.646
Carbon dioxide	0.568
Normal butane	0.133
Iso-butane	0.102
pentane	0.031
Iso-pentane	0.028
Helium	0.017
Propane	0.8
Nitrogen	1.319
Other hydrocarbons	0.009

Anyway, it must be noticed that integration between the TE, which generates electricity from NG expansion, and the low temperature heater requires the adaptation of the system configuration in order to optimize its functioning and, ultimately, its control. For the purpose of analyzing the system behavior for different operating conditions and to find an effective set-up, two different plant configuration have been analyzed and compared. A traditional set-up was studied, with a single TE like the one installed in the city of Genoa within the framework of the EU project CELSIUS (Combined Efficient Large Scale Integrated Urban Systems), hereafter called "GE1 demonstrator" (Fig. 24). Then a low temperature

integrated system was modelled. At this stage, it is worth to recall that CELSIUS is a project in the Smart Cities framework co-funded by European Union's Seventh Framework Programme for research, technological development and demonstration (grant agreement № 314441). The GE1 demonstrator consists in a TE, capable of delivering a nominal power of 550 kW_e, whose design working flow rate is 22500 Sm^3/h, a slightly lower value than the average hourly flow rate of the PRS. The TE processes the NG from the national transport network, at a pressure of 24 bar_g, reducing its pressure to 5 bar_g.

Figure 24, shows a picture of GE1 demonstrator, while figure 25a-b represents a simplified schematization of high and low temperature PRS configurations. Referring to the high temperature configuration, the WER is achieved by means of a TE line. The NG is preheated with a process water temperature of about 85ºC by means of a shell and tubes heat exchanger (H). The thermal energy is provided by means of two, standard, gas-fired boilers, which produce the hot water necessary to accomplish the NG preheating process. Looking upstream the TE, there is a flow control valve that enables NG mass flow regulation. A single phase Direct Current generator (DC) converts the mechanical power into electricity, that is consequently transformed in Alternate Current by means of an inverter (AC). The AC is cooled by the cold NG, which comes from the TE. This arrangement has the double benefit of cooling the AC and helping to prevent the formation of hydrates in the NG stream. In the conventional expansion lines, each throttling valve (V1, V2 and V3 in figure 25) is provided with a twin one called "monitor" whose scope is to lock the line in case of downstream fault. Here, the preheating process is achieved by means of shell and pipes heat exchangers as well (H1, H2 and H3). Referring to the low temperature configuration, the process temperature is lower due the second TE implemented in series. In this way, the total NG pressure drop is split into two stages, so that the thermal preheating need at each expansion is lower. In this case, as described for the high temperature configuration, the NG is used as a vector for

AC unit cooling process. Referring to TEs sizes and geometry, for the case study considered, the TEs are the same for both system configurations.
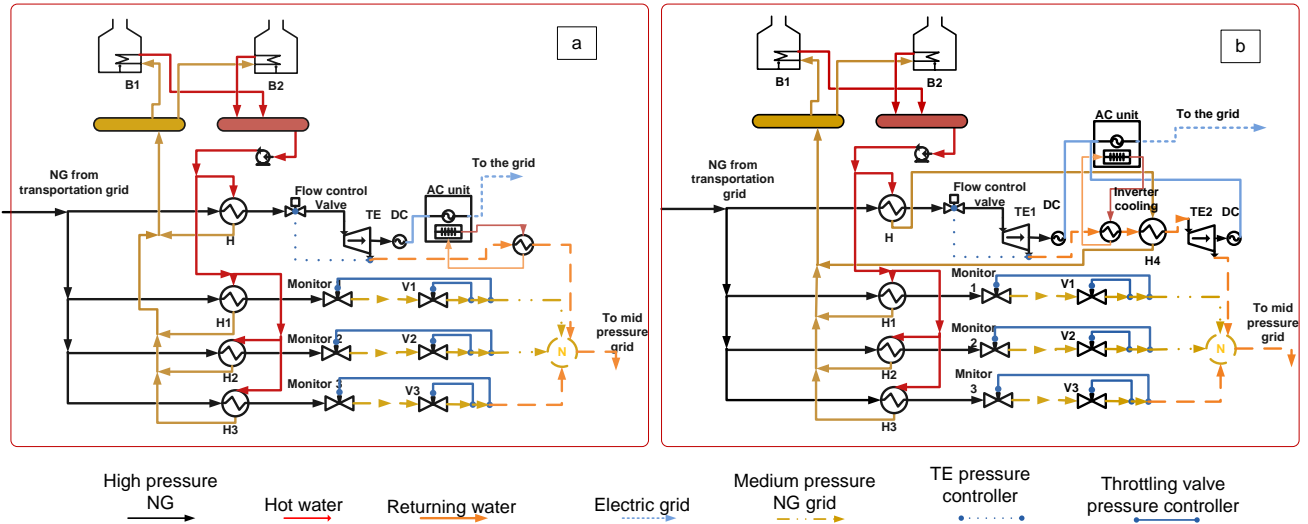

Figure 24. GE1 demonstrator.

Figure 25. System configuration: a) High temperature; b) Low temperature.

3.4.2. Numerical model setup

The two previously described configurations have been numerically modeled by means of Honeywell *UniSim Design Suite®* software [10]. Figure 25 shows the sketch of the High Temperature Configuration, on the left (a), and, on the right (b), the novel Low Temperature Configuration, named respectively HTC and LTC. For both cases, the NG inlet temperature and pressure were set at 15ºC and 25 bar with an expansion ratio of about 5 respectively which is, as mentioned in the previous section, the most typical operating condition for NG distribution for PRS located in urban areas. Heat losses of pipes and components were not considered for simplicity in the model. Pressure transients take an important role in operation of a letdown station. For this reason, the NG networks, which are directly connected to the TE, are modeled by considering a plenum of about 20 m^3, which corresponds to the volume of the closest part of the network. Analogously, the water thermal inertia was modeled by considering a 25 m^3 plenum. Valves and heat exchangers characteristics have been implemented and modeled according manufacturers' technical sheets [11], TEs characteristics are shown in figure 26. The preheating heat exchanger which serves the TE has an overall heat transfer coefficient (UA) of about 1.94 kW/K. The circulating pumps flows are about 60 and 40 m^3/h for throttling valves and TE lines respectively, for both system configurations. Standard gas fired boilers have been modeled by means of two heaters whose heat flows are regulated through PID controllers with proportional, derivative and integrative coefficients of about 5, 1, 0.001 respectively.
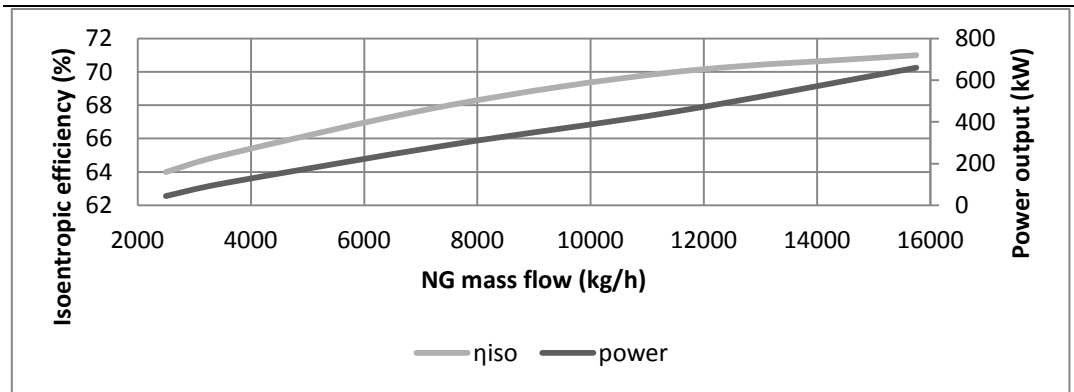
Figure 26. Turbo expander characteristics.

3.4.3. System transient analysis

The distribution of NG to the lines, which feeds the network, i.e. to the TE and the throttling valves, is made by the fine regulation of the set-point of each of them. Throttling valves set points are chosen in order to give priority to WER. The three throttling valve lines openings are proportionally regulated through a pneumatic system in a sequential manner: each set point is chosen in order to let just one line open for standard NG flow scenarios. For higher NG loads, the second and the third line will sequentially open following downstream pressure. For the high temperature system configuration, the TE and valves set points are represented in table 4.

Table 4. Model set points.

Configuration	TE (kPa)	2nd TE (kPa)	V1 (kPa)	V2 (kPa)	V3 (kPa)
High temp.	560	-	500	450	400
Low temp.	1100	520	500	450	400

In the low temperature configuration, the throttling valves control logic is defined similarly to the one used for the high temperature configuration. However, in this case two TEs will be implemented in series in order to split the NG expansion process in two stages. For this purpose, an intermediate pressure that maximizes the specific work of the entire expansion process has been used. As described in table 4, this corresponds to 11 bars.

In the following sections, numerical results of the above mentioned high and low pressure system configuration are presented. The configurations have been analyzed for different NG flow scenarios and boundary conditions, in dynamic regime. As a first, a typical winter day NG flow scenario has been analyzed in order to identify the main parameters of the process: TE energy production and outlet NG pressure and temperature, thermal energy needs and boilers dynamics behavior and, consequently, throttling valves dynamic response. This critical NG flow scenario has been selected due to its particular trend and peaks because, among all NG possible flows which take place along a year, it allows to observe the TEs and throttling valves parallel operation. In fact, by considering typical summer NG flows scenarios, it might be possible to not observe the dynamic behavior of the throttling valves due the lower NG volume flows involved.

3.4.4. High temperature configuration

Figure 27 represents a standard NG flow scenario and figure 28 represents the correspondent TE power production. As shown in figure 29, the TE's NG inlet and outlet temperature are stable to values of about 71 ºC and 5 ºC respectively with slight differences in transients phases that do not affect system safety and operation. The same consideration would be valid for TE's NG pressures of figure 30. For the same NG flow scenario, during NG demand peaks, the boilers will achieve a thermal power output of about 800 kWth as shown in figure 31. Finally, referring to figure 32, as described in the previous section, each valves, V1, V2 and V3, will proportionally open depending on the NG mass flow with a sequential dynamics. Valves outlet temperatures are shown in figure 33. The water flows for the preheating process are about 40 and 60 cubic meter per hour for TE and valves lines respectively.
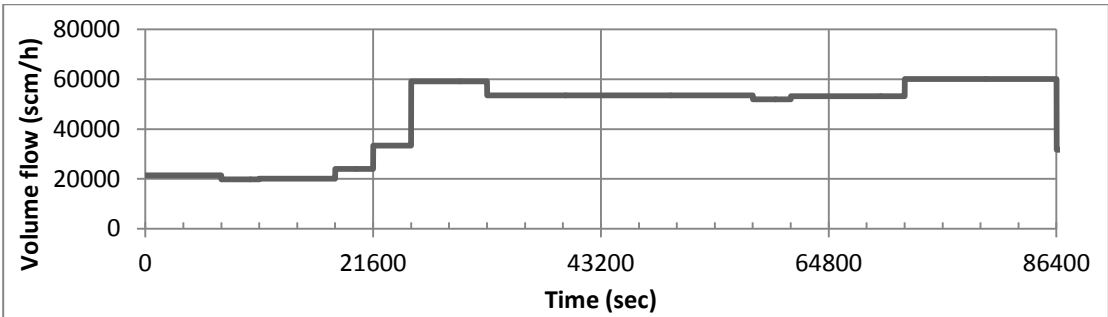
Figure 27. NG standard daily flow scenario (model input).
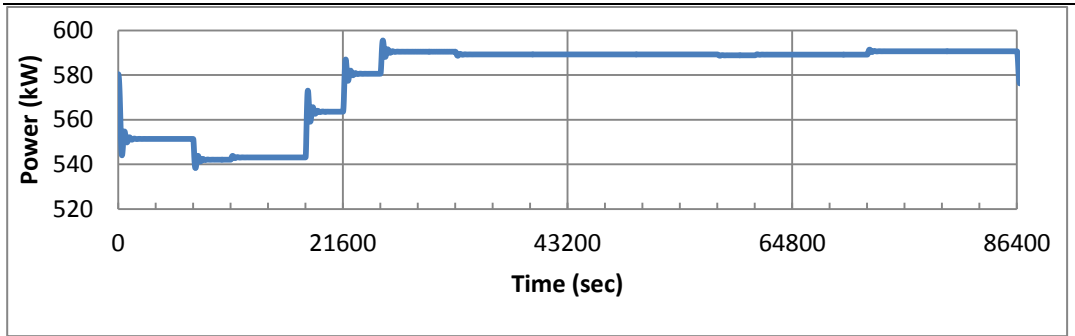
Figure 28. TE mechanical power production
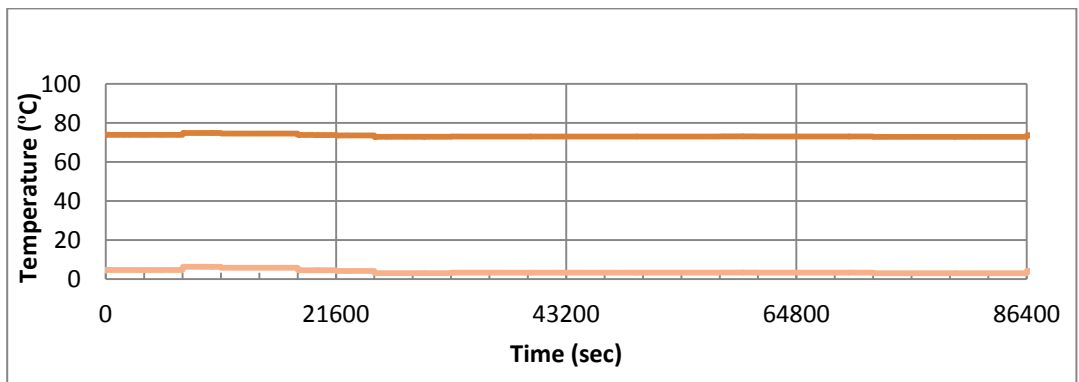
Figure 29. TE, NG inlet and outlet temperatures
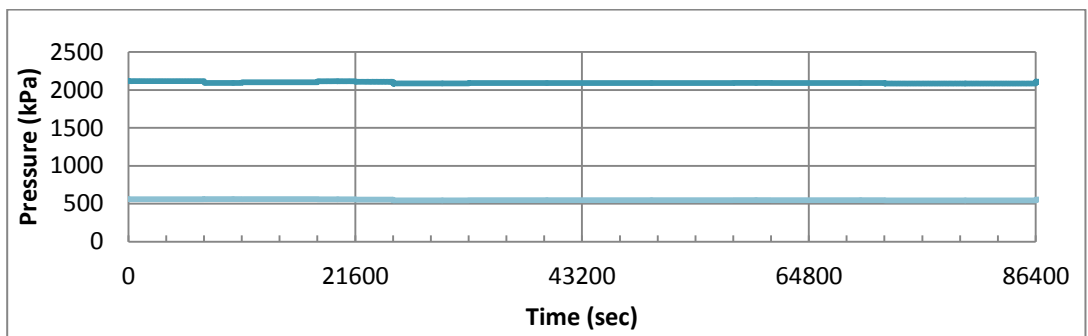
Figure 30. TE, NG inlet and outlet pressures
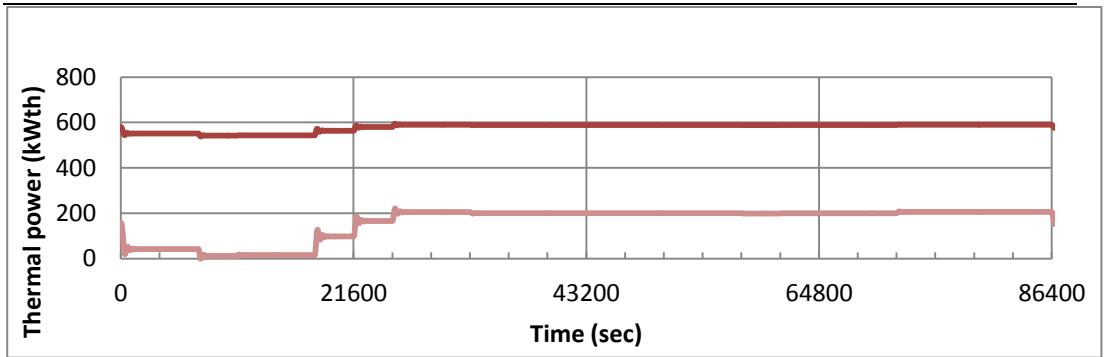
Figure 31. Boilers thermal production
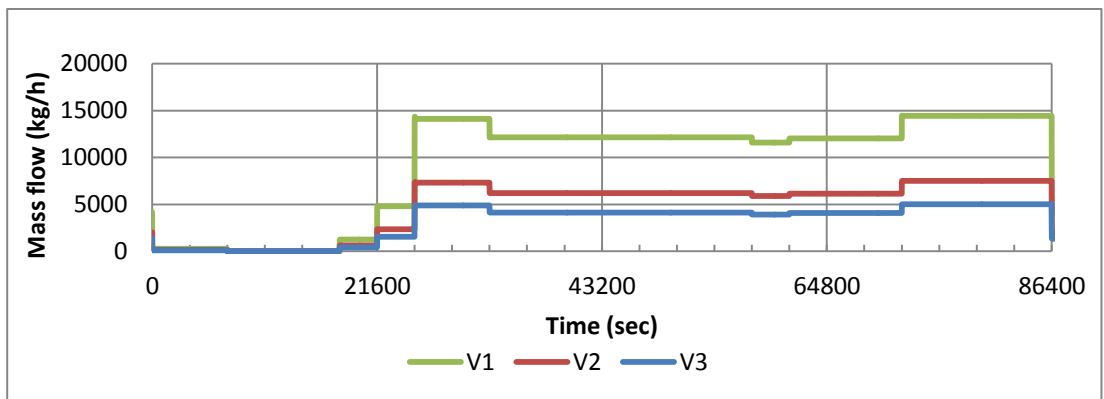
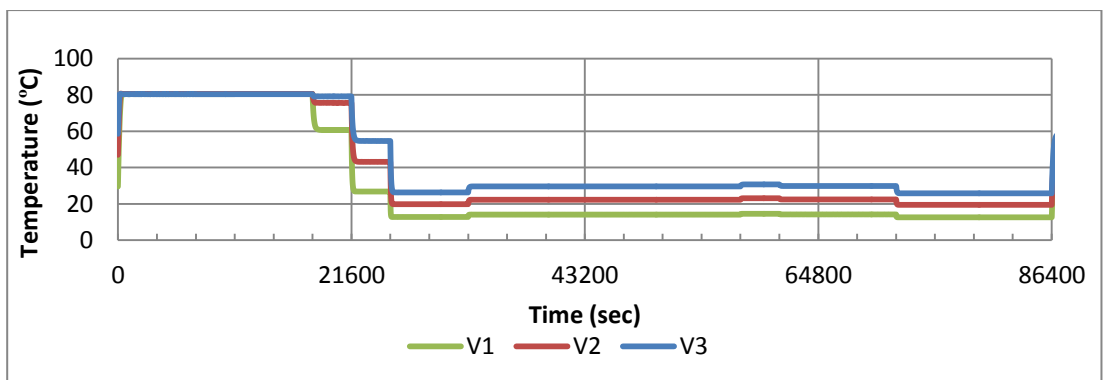Figure 32. Throttling valves, NG mass flows

Figure 33. Throttling valves, NG outlet temperatures

3.4.5. Low temperature configuration

Same NG flow scenario of figure 27 has been simulated for the PRS low temperature configuration. In this case, process water temperature set point has been set to 55 ºC for boilers. The pressure set point is designed to give priority to the recovery line i.e. the highest set point is implemented in the TE and following valves will sequentially open as it happens for the high temperature configuration. Results for TEs mechanical power are shown in figure 34. It is possible observe that, with the selected intermediate pressure, power generation is almost equally subdivided on both the first and second stages. Figure 35 show the effect of the transients on the first and second stage TE outlet pressures. Here it is possible to appreciate that the NG pressure regulation is performed with high stability also when NG flow transients occur. Instead, figure 36 represent the outlet temperatures at the first stage and at the second stage of the TEs. Referring to figure 37, during NG demand peaks, the two boilers will achieve a thermal power output of about 650 kWth. As modeled for the high temperature configuration, the preheating process water flows are about 40 and 60 cubic meter per hour for TE and valves lines respectively. Finally, figures 38 and 39, represent the throttling valves' NG mass flow and outlet temperatures respectively.
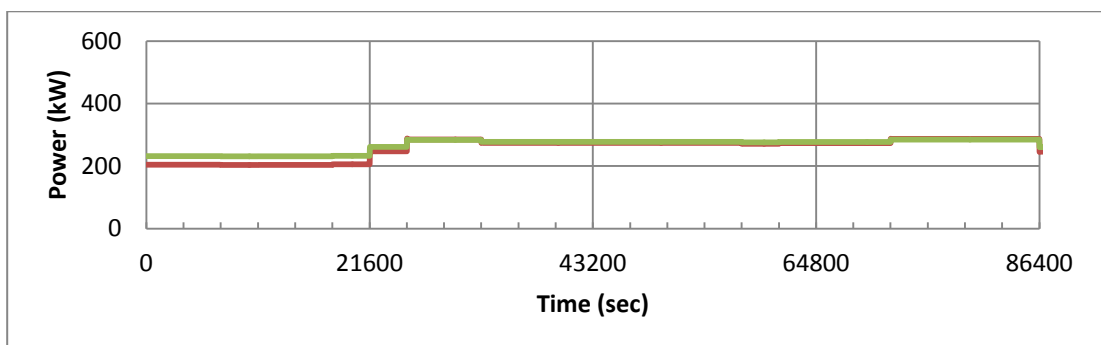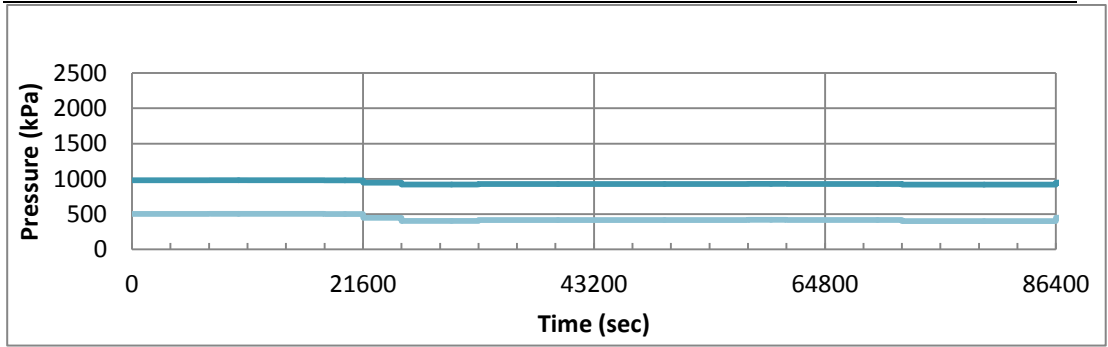

Figure 34. TEs mechanical power

110
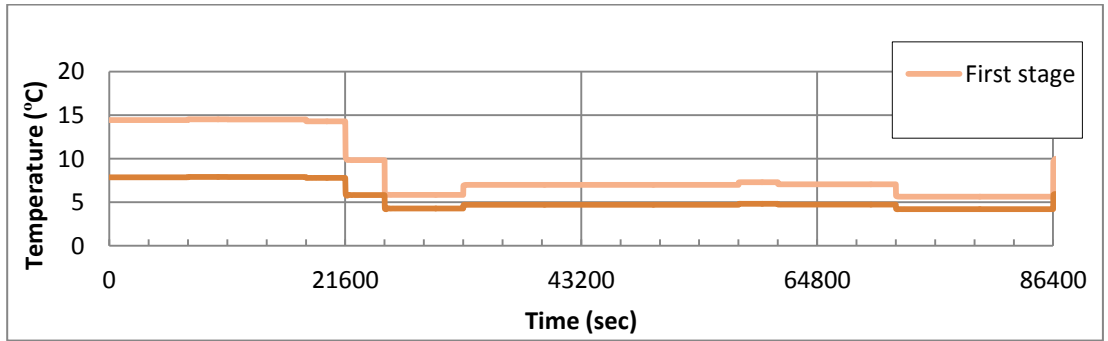
Figure 35. TEs, oulet pressures
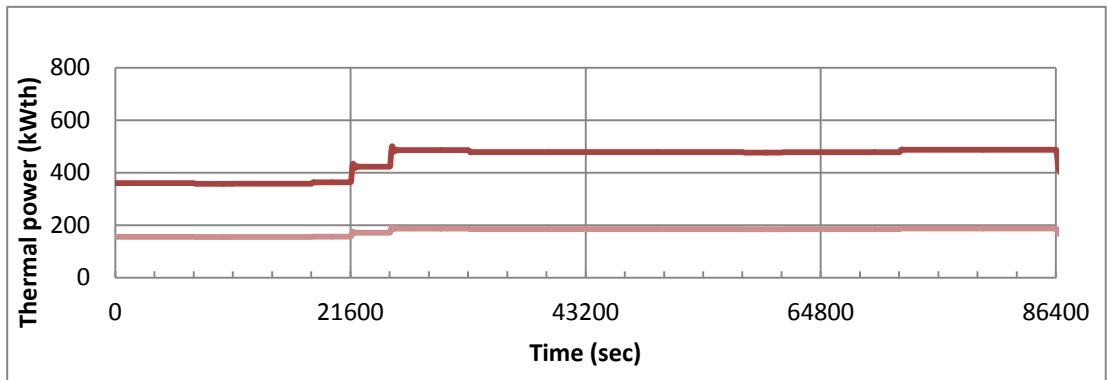

Figure 36. TEs, NG outlet temperatures

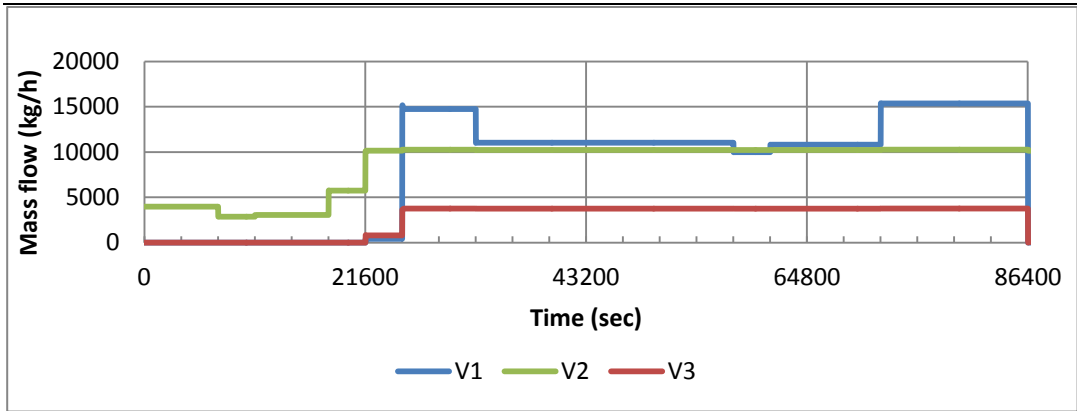Figure 37. Boilers thermal production

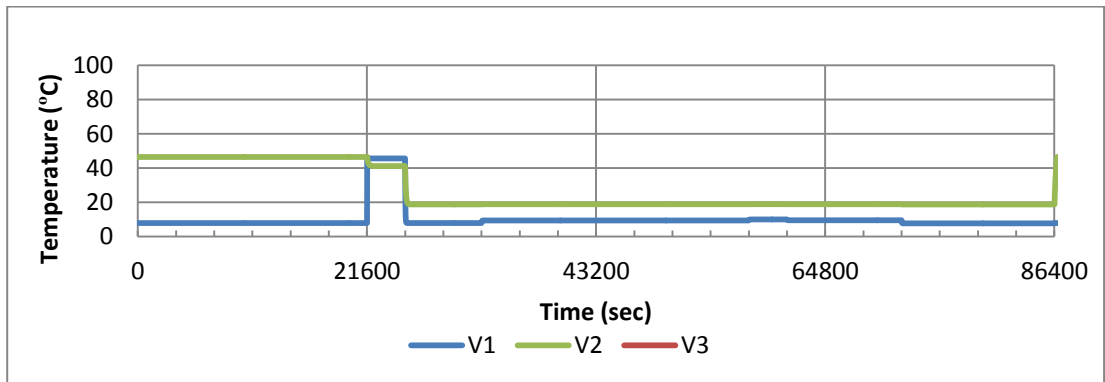Figure 38. Throttling valves, NG mass flow

Figure 39. Throttling valves, NG outlet temperatures

3.4.6. Time-to-hydrates

The conditions set introduced in Section1 was used as a reference base, that is 5 bar and 15°C, for which the methane hydrates formation occurs in the range -2 / - 5°C. The low temperature configuration has been analyzed for different operational conditions in order to estimate the minimum water process temperature set point before methane hydrates formation might occurs. More precisely, referring to figure 40 the entire dynamic simulation refers to time length of about 33 minutes where, the NG inlet temperature and the user demand have been kept constant at 15 ºC and 20000 kg/h respectively. The initial boilers set points were fixed at 55 ºC

112

and they have been sequentially changed at minutes 1 and 10 to lower values of about 50ºC and 45ºC respectively. After 20 minutes, boilers have been shut off.
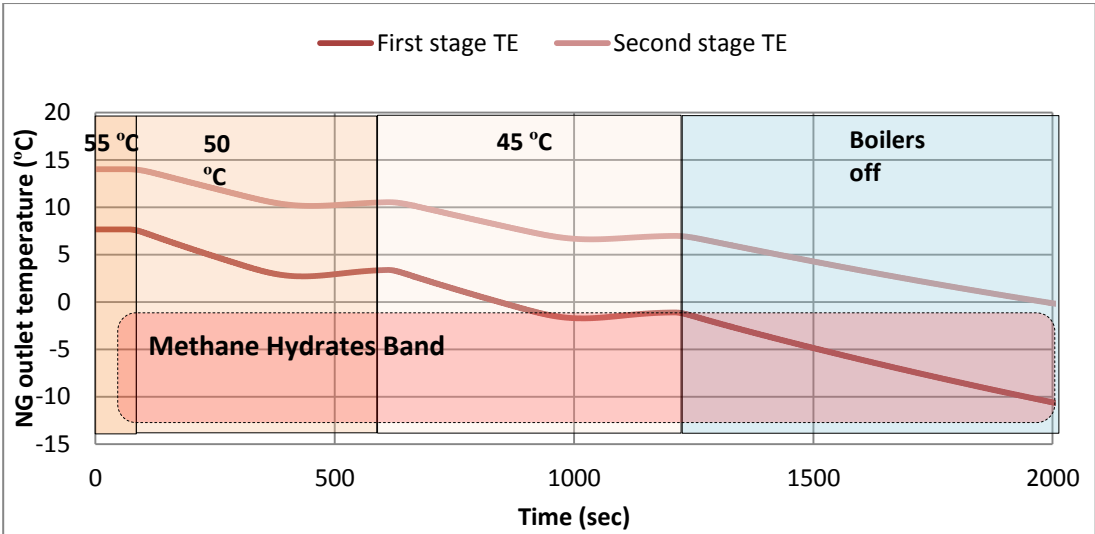

Figure 40. TEs' NG outlet temperatures for different set points

3.4.7. Discussion and applications

A large set of components is currently available on the market for the exploitation of the high pressure of the national distribution grid, in very large plants characterized by very high mass flow rate. The complexity of the TE plant for a NG PRS is linked to safety issues and, hence, only a small set of TEs is available in small sizes because they would be too expensive in most of the applications. Currently, there is not any known application of double expansion system for low-size PRSs.

Nevertheless, it is important noticing that, due to its configuration complexity, the power produced by a double stage expansion processes is comparable with those produced by a single-stage one and that, in most of the operating conditions, the LTC gives only slighter reduction, if any. The analysis of the results, which are

shown in the previous section, confirm the hypothesis of gathering a considerable amount of work from a double expansion process in a PRS.

Most of the plants, which generate the pressure drop from the national and transnational grid to the local one, are provided with conventional boilers to prevent NG cooling beneath the temperature threshold, at which hydrates formation takes place. Currently, a large interest is devoted to the revamping of the PRS with TE, in order to recover the energy otherwise dissipated in the throttling valves.

3.4.8. Advantages of the thermal integration

A set of interesting advantages are hidden behind the temperature reduction strategy in PRSs. This advantages are mutually connected and all of them gravitate towards the possibility to reduce carbon emissions in urban areas (figure 41). In fact, first of all, reducing the temperature would open the possibility of exploiting lower and lower enthalpy heat sources introduces more and more efficient solutions and renewable as well. For instance, it is possible to recall some of them in an approximately temperature descending order: condensation boilers, CHP, high temperature heat pumps and solar heaters.

Moreover, PRSs temperature reduction benefit not only consists in the implementation of more efficient primary energy conversion components or renewable, since there are more advantages that is important to highlight. In fact, the LTC, is potentially characterized by a phenomenon of self-induced economic and financial sustainability. This means that, by reducing the temperature, we would be able to integrate also with, for instance, 4th generation DHN [12] enabling economic sustainability due the aided income generated by the thermal energy sold by the PRS. At this stage, it is worth to recall that, the initial investment price of the LTC could increase of about 30-40% with the respect to

HTC case. This opportunity enables the possibility to let PRS retrofit investments feasible.

Finally, it is important to highlight that, to carry out an economic analysis of the novel configuration would be surely fundamental to understand the feasibility of such implementation, however, intuitively, investment sustainability is related to a series of local factors. This means that it would be easy to lead to too specific assessment or, better, to too vague conclusions about the financial and economic issues of PRSs retrofits. For this purpose, the author believe that this kind of projects requires *ad hoc* economic and financial analysis or, at least, more in-depth studies but, this is not the scope of such article.

Finally, last but not least, with the proposed LTC it would be possible to reduce the heat losses through pipelines and, for northern countries, where low outside temperatures boost the heat exchange with external environment, this would led to not negligible energy saving.

For this reason, it is important to analyze the performance of the plants feed by a low temperature heat source. Comparing one by one figures 27-33, which present the HTC performance, with the corresponding figures 34-39, which contains the LTC ones, it is possible to see that the novel configuration is able to operate correctly in the selected scenario. Because of this comparison, it is possible to conclude that the novel LTC, which preheats NG to 50-55°C only, properly matches the normal daily transient as well as the HTC.

As obvious, a crucial aspect is also related to the whole system control. As demonstrated in [13], it is possible to achieve a 17% energy saving by implementing an appropriate control in this type of system. Moreover, the thermal integration with external users, would require even more attention to this issue since, more efficient primary energy conversion could be achieved by implementing appropriate optimization algorithms. However, generally speaking,

we would feel confident to say that, typical city gate PRSs' NG load profiles have an natural matching with thermal and electrical ones making integration even more easy and, for well designed systems, the implementation of thermal or electrical storages might be avoided.
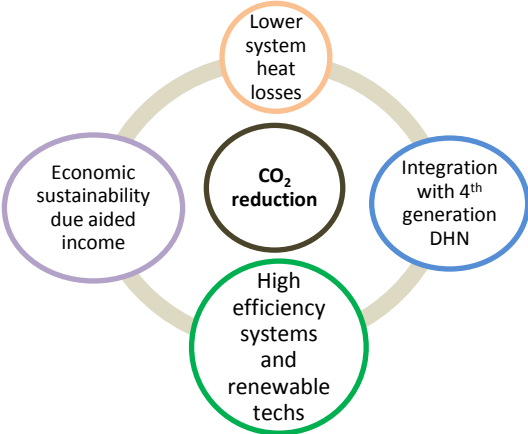

Figure 41. Representation of low temperature configuration advantages.

3.4.9. Discussion and conclusions

Figure 42 represents the dynamics variation of the thermal need reduction for low temperature system configuration. Here, the performance analysis show how, for low temperature configuration, it is possible to achieve an average reduction of about 14% on the specific thermal production with the respect to high temperature system configuration, for a typical winter day. For the same NG flow scenario, figure 43 shows a comparison between the ratios of the specific heat consumption and power outputs for low and high temperature configurations respectively: differently from the HTC, the LTC enables an higher energy ratio. That might suggest the possibility to achieve more performing operation in LTC with the respect to HTC.
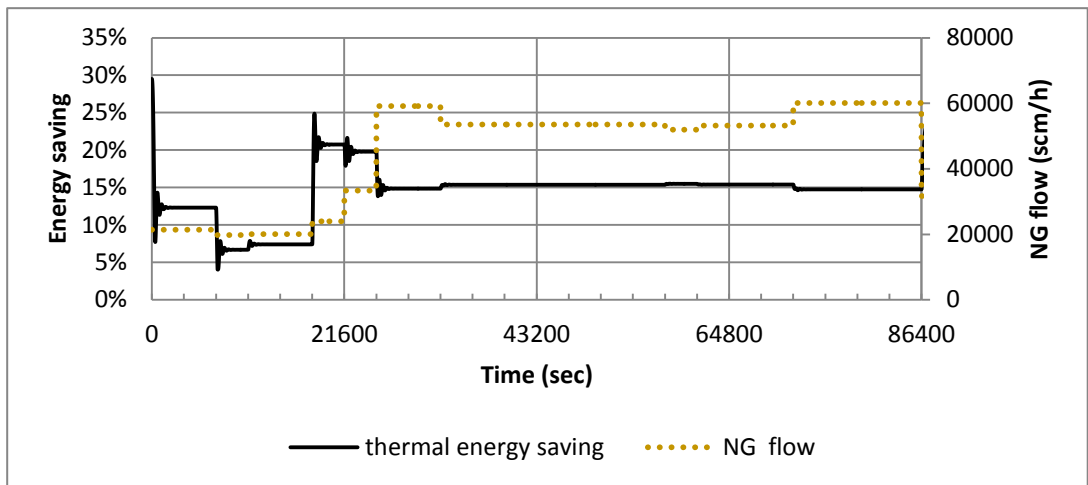
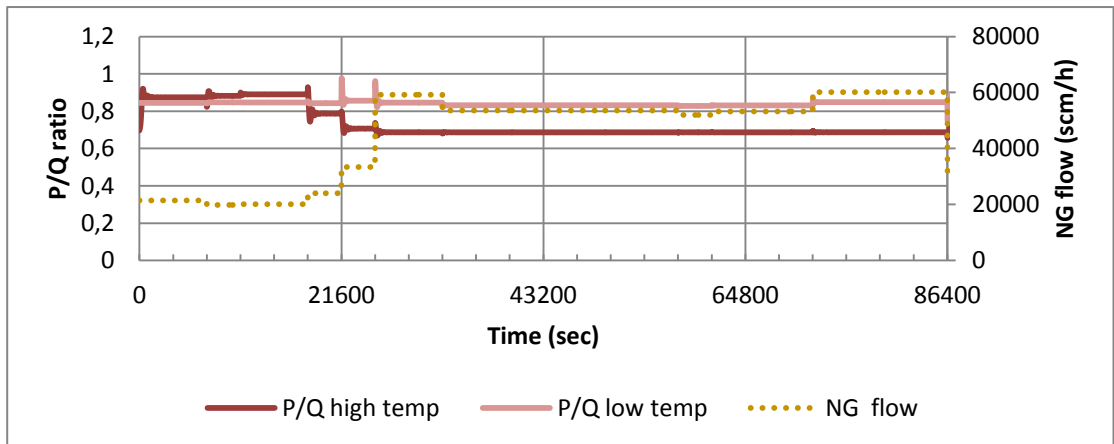Figure 42. Percentage thermal need reduction between systems.

Figure 43. Energy ratios comparison between two system configuration.

Finally, the dynamic model of the LTC is able to assess the dynamic behavior of the plant in case of fault of the heat source. The large thermal capacity of the components of HTC and the value of the temperature of their thermal supplier give rise to a long transient that can be managed by the operators. In this frame, it is interesting to study the dynamic behavior, in case of fault, of the LTC because, due to its lower temperature set point, it could generate shorter transients that could lead, in a too short time, to unsafe conditions. For this reason, a dynamic simulation of the LTC, in case of fault of the thermal supplier, has been carried out and the results are reported in figure 40. It is possible to see that the time which takes to the hazardous conditions of hydrate formations, is more than 15 minutes. In fact, the temperature at the first stage outlet, that is the lower one, drops below -2°C about 1000 s after the beginning of the event. This is a further assessment of LTC, because the existing control system can easily manage such a long time response. Instead, in order to avoid hazardous operations that would easily lead in expensive system damage after few minutes, redundant TE's supervision system is strongly recommended for isolated and unsupervised stations where the personnel time-to-intervention is longer than the abovementioned threshold.

Concluding, there are many advantages in reducing the process water temperature of natural gas pressure regulation systems with energy recovery system implemented. This advantages are mutually connected and all of them gravitate towards the possibility to reduce carbon emissions in urban areas. These consist in the possibility to exploit low enthalpy heat source (waste heat), to implement more efficient system configurations (condensing boilers, geothermal heat pumps etc), to thermally integrate the system with 4th generation district heating network generating in this way, an added income which would balance the higher investment cost of the novel configuration proposed. These factors push authors to analyze the possibility of reducing the process water temperature in PRS from the energy point of view by considering a double stage expansion process i.e. two

turbo-expander in series. As commonly known, water process temperature is normally set to 85 ºC. With the proposed novel configuration, temperature can be reduced up to 55ºC. However, working with this conditions, makes the risk of methane hydrates formation even higher since it becomes easier to fall down in the hydrates zone in shorter time. For this purpose, within this study, an accurate transient analysis was carried out for a typical winter scenario which can be considered the most suitable for this purpose. To achieve reliable results, we based our analysis by using a numerical model which has been built and validated basing on the existing plant located in the city of Genoa. Results of the analysis demonstrate that the proposed novel configuration does not led to hazardous system operations i.e. the risk of methane hydrates formation is ward off in normal operating conditions. Moreover, extreme conditions were analyzed. In fact, the system behavior in case thermal production and turbo expander supervision fault was studied. More precisely, the simulation covered a time length of about 33 minutes. Considering the low temperature configuration, we calculated the time-to-hydrates including system thermal inertia. In this scenario, as inlet conditions, a natural gas flow of about 20000 kg/h at 15 ºC was considered. The starting process water temperature was about 55 ºC. This set point was dynamically lowered after 1 minutes to 50 ºC. Here no hydrates formation as been detected. However, after 10 minutes the water set point was lowered at 45 ºC. In this case, within 6.5 minutes the hydrates zone would be reached. More in general, we would feel confident saying that, starting from the initial set point of 55 ºC, if fault occurs, the system would fall in the hydrates zone within 15 minutes. In this case, human intervention is essential to avoid system disasters. So, for those isolated stations, where human intervention is naturally slower, redundant security systems is strongly recommended instead. Finally, the energy performance of the two configurations were compared. In this case, results show that the low temperature configuration could achieve higher energy performance reaching a average energy saving of about 14% for typical winter operating conditions. Concluding, the novel proposed

system configuration has many advantages in terms of opportunity of exploiting low enthalpy heat sources, high efficient primary conversion technologies utilizations, integration with renewable sources. Moreover, the novel configuration, with an appropriate control logic, could easily achieve higher energy performance with the respect to the high temperature one, increasing carbon emission reduction in urban areas and keeping safe system operations.

REFERENCES

[1]   SNAM. Available online http://www.snam.it/ (accessed 14/07/2017) .

[2]   S. H. Chae, S. H. Kim, S. Yoon, and S. Park, "Optimization of a waste heat utilization network in an eco-industrial park," Applied Energy 87(6); pp. 1978:1988,(2010).

[3]   C. Marguerite, R. Schmidt, and N. P. Garcia, "Concept development of an industrial waste heat based micro DH network" *CISBAT*, pp. 597:602, (2015).

[4]   H. Lund, S. Werner, R. Wiltshire, S. Svendsen, J. Eric, F. Hvelplund, and B. Vad, "4th Generation District Heating (4GDH) Integrating smart thermal grids into future sustainable energy systems," Energy 68, pp. 1:11, (2014).

[5]   D. Borelli, F. Devia, E. Lo Cascio, C. Schenone.Energy recovery from natural gas pressure reduction stations : Integration with low temperature heat sources. Energy Conversion Management 159; pp. 274:283, (2018).

[6]   Motiee M, *Hydrocarbon Process*, Int Ed, pp. 70: 98, 1991.

[7]   B.F. Towler, S. Mokhatab, "Quicky estimate hydrocarbon formation conditions in natural gases", Hydrocarbon Processing 84; pp.61:62,(2005).

[8]   Kidnay, Arthur J., William R. Parrish, and Daniel G.

McCartney. Fundamentals of natural gas processing. Vol. 218. CRC Press, 2011

[9]   Sloan Jr, E. Dendy, and Carolyn Koh. *Clathrate hydrates of natural gases*. CRC press, 2007.

[10]   www.honeywellprocess.com.   Available   online: https://www.honeywellprocess.com (accessed on 08/03/2017).

[11]   Pietro Fiorentini. Available online: https://www.fiorentini.com/it/ (accessed 14/07/2017)

[12]   H. Lund, S. Werner, R. Wiltshire, S. Svendsen, J. Eric, F. Hvelplund, and B. Vad. 4th Generation District Heating (4GDH) Integrating smart thermal grids into future sustainable energy systems. Energy 68, pp.1:11,(2014).

[13]   E. Lo Cascio, D. Borelli, F. Devia, and C. Schenone. Future distributed generation : An operational multi-objective optimization model for integrated small scale urban electrical, thermal and gas grids. Energy Conversion and Management,143; pp. 348–359,(2017).

3.5. RETs Integration

The integration of PRS with RETs was first analyzed by Farzaneh-gord in [1], where a case study located in Birjand city was presented. A non-controllable solar flat-plate collector array integrated with a fossil-fuel-based heater was considered to heat-up the NG. This case study was further enhanced in [2]. In fact, the same system configuration was analyzed through including an automatic control and the results were compared with the case where no TE was implemented. The local solar irradiation has been estimated by considering solar engineering formulation in both cases [3]. These studies, conducted in Iran, where solar irradiance conditions

are definitely favorable, revealed that the integration with solar energy is a strategic action for carbon emissions reduction in PRS operations.

Thus, solar-boosted PRSs might be a great option for smart transition to a sustainable and clean energy scenario for other contexts as well. However, the use of flat-plate collectors in EU countries does not ensure that the required NG preheating temperature (normally about 75-85ºC for a TE-based system) would be reached, especially in northern countries [4]. Differently from flat-plate collectors, parabolic trough solar collectors (PTSC) are capable to deliver energy at a higher temperature [5],[6],[7],[8]. This key aspect would open the possibility to accomplish the NG preheating based on a 100% renewable process, enabling near-zero carbon emission for PRSs operations. In the reality, the opportunity to drastically reduce carbon emissions is a challenging objective in PRSs. In fact, considering that most of the PRSs are located near urban areas, a wide number of physical and technical constraints could be found during PRSs retrofitting intervention if on-site space available. For this purpose, in [9], the possibility to employ a new PRS system configuration coupled with an appropriate PTSC size and thermal storage unit (TS) is investigated. In [9], the system dynamic behavior and performance were examined based on the information of a real plant located in the city of Genoa [10]. The analysis was conducted for those typical average intense days for each season. The analysis was then further extended at different latitudes considering appropriate EU cities. An in-depth dynamic analysis of the most hazardous scenarios was also carried out in order to evaluate the possibility to achieve near-zero carbon emissions in PRSs operation. Energy, environmental and economic performance of the new system was presented in comparison with the conventional PRS where no PTSC was implemented. In order to achieve a better understanding of the performance and the characteristics of this kind of retrofit intervention, study [9] is further detailed.

3.5.1. System description

The PRS configuration considered in this study is shown in Fig. 44. The plant is constituted by a TE [11] which operates in parallel to three lines equipped with JT valves (VLV1-3) [12]. The TE mass flow rate is controlled by a variable-inlet guide vanes (VIGV) based on the downstream pressure, through a proportional-integral controller (P-I). The heat exchangers (HE1-4) enable upstream NG preheating and the amount of energy required varies based on the type of process involved. The return water streams converge in a header (HDR) before entering the TS. The hot water flow rate is controlled by variable speed pumps (P1-5). The hot water is stored in the TS which is fed by a boiler unit (BO) and a Sun-tracking PTSC through dedicated counter-current flow heat exchanger (HE5). The dimension of the PTSC is subjected to the area available for the panels positioning. Normally, most of the PRSs are located in the urban areas. This aspect makes it difficult to find more space than the area available on the PRS building roof. These buildings are normally characterized by construction standards, which foresees a roof area of about 350 square meters. These push authors to consider an appropriate configuration with a maximum of 4 panels for a total caption area of about 333.6 square meters. The BO unit power output is regulated based on the outlet temperature by a proportional controller (P). The PTSC module characteristics are determined based on the manufacturer catalogue [13]. The PTSC modules are assembled in parallel since a relatively low preheating temperature of about 85 ºC is needed for the process. The high-temperature fluid (HTF) used in the PTSC is a diathermic oil and its characteristics can be found in [14]. The NG inlet and outlet pressures are set to 25 bars and 5 bars respectively which are the common

operating values of the NG distribution nodes [15]. More details are summarized in Table 5.

Table 5. System characteristics.

| Component	Value	Component	Value
Number of JT lines [-]	3	BO, nominal power [kW]	1100
HE1-3, overall UA [kW/K]	1.5	BO, steel and water mass [kg]	1998;950
HE4, overall UA [kW/K]	16	BO, steel [kJ/kgK]	502
HE5, overall UA [kW/K]	3	BO, P gain [kg/s]	9e-4
TE, model	*H-MTG550*	PTSC, model	*SF-Skytrough®*
TE, nominal mechanical power [kW]	550	PTSC, number of modules	4
TE, P-I gains [m]	3.16e-5;2.71e-8	PTSC, aperture area [m^2]	333.6
TE, set point [bar]	5.1	ST, volume [m^3]	17.6
VLV1-3, set points [bar]	5;4.9;4.8	ST, cond. heat transfer area [m^2]	25.9
P1-3,4,5,6,7, mass flow rate [kg/s]	8;11.1;10;0.45;11	ST, overall UA [W/K]	10.36
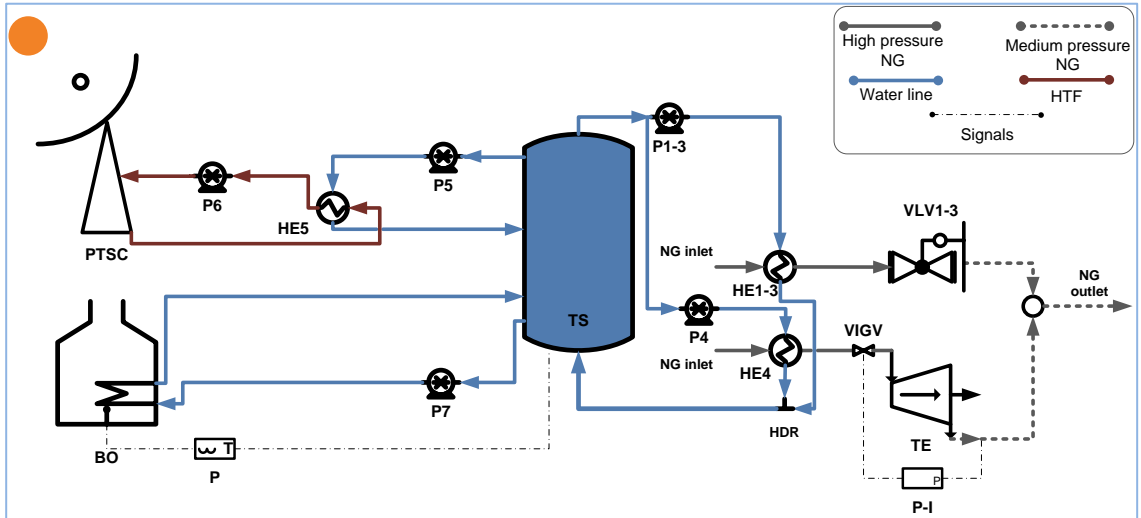
Figure 44. A layout of the simplified system configuration.

3.5.2. Simulation scenarios

The assessment was conducted for a typical average intense day in January, April, July and November. The system behavior and its performance were evaluated at latitudes: Latitude 44º24' North, Longitude 8º56' East (Genoa), Latitude 40º51' North, Longitude 14º14' (Naples) and Latitude 52º22' North, Longitude 4º53' (Amsterdam). The solar irradiance and ambient temperatures were taken from *Joint Research Centre* database [17]. As a Sun-tracking PTSC was considered, the direct solar irradiance (DNI) was used in the simulations (Fig. 45). The BO efficiency, the TE's iso-entropic efficiency and the NG normalized flow rates are reported in Fig. 46. For simplicity, the NG composition considered in this study was characterized by pure methane. Thus, according to Motiee et al. [16], the methane hydrated formation was about -4.5 ºC to -2.2 ºC. For this purpose, an operational scenario as "risky" if the NG temperature was considered as around 0ºC, ± 10%.

The NG upstream and downstream pressures were fixed at a constant value of 25 bars and the regulator set points were adjusted in order to give the operation priority to the TE. The relative amount of methane flowing through the JT valves can be deducted by the definition of the recovery factor (R) defined in Equation (1).

$$R = \frac{\dot{m}_{TE}}{\dot{m}_{tot}} \tag{1}$$

where, $\dot{m}_{TE}$, $\dot{m}_{tot}$ are respectively the amount of NG flowing through the TE and the total amount of NG entering the PRS. The initial conditions considered in all simulations are presented in Table 6.

Table 6. Simulation initial conditions.

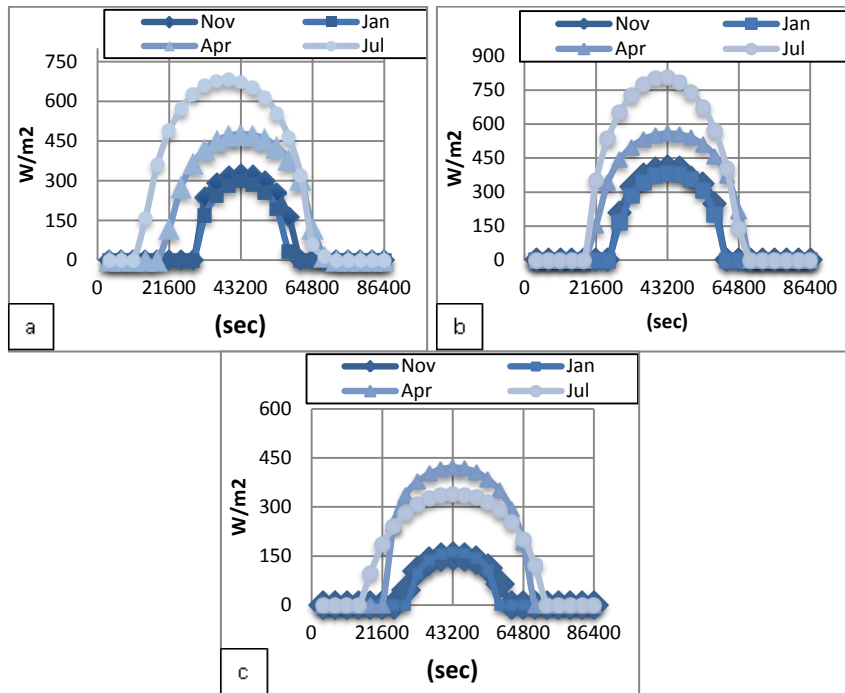| Process variable	Value
Thermal storage temp. (K)	350
Downstream NG pressure (bars)	5
BO outlet temp. (K)	350
HTF outlet temp. (K)	350
Starting time (h)	01:00 AM
VLV1-3 opening (%)	0

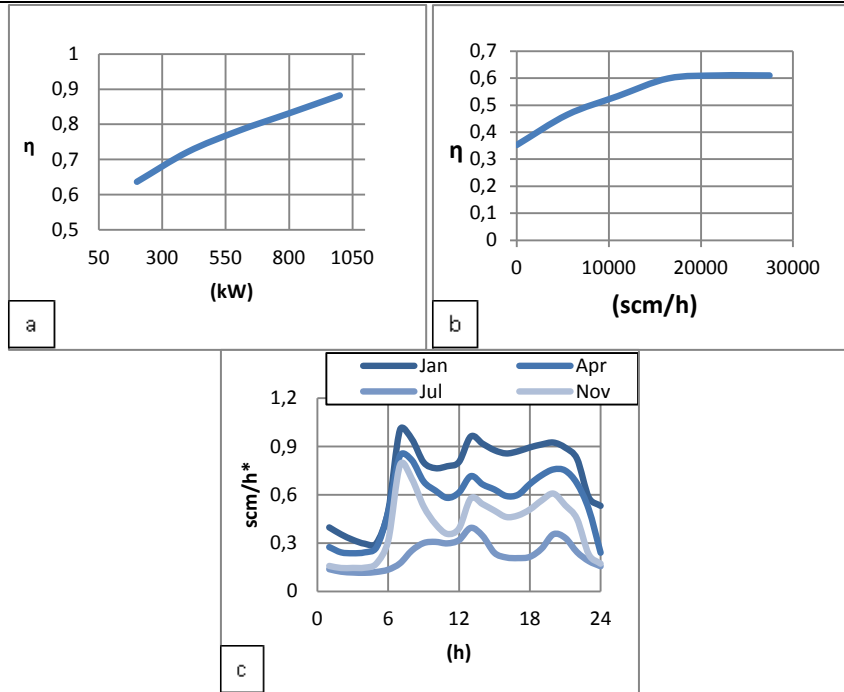Figure 45. Direct normal irradiance: (a) Genoa; (b) Naples; (c) Amsterdam.

Figure 46. Simulation characteristics**:** (a) Boiler efficiency; (b) TE iso-entropic efficiency; (c) NG normalized flow rates.

3.5.3. Results

In Fig. 47, the percentage reduction of the operational cost is presented in comparison with the percentage reduction of the PQ ratio and the carbon emissions factor. During summer time, at 12.00 PM, a carbon emissions reduction of 33% and 31% for the Naples case and Genoa case was achieved with the respect to the conventional case. For the Amsterdam case, this value was calculated to be 15%. The same results were valid for the operational cost reduction.
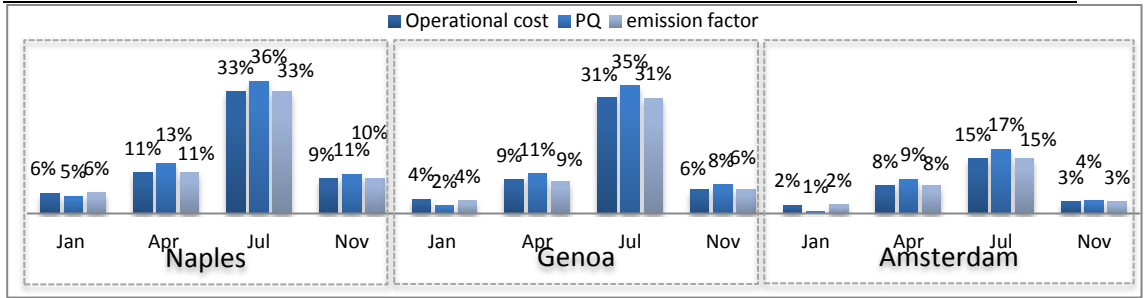
Figure 47. Percentage operational costs, PQ ratio, CO_2 reduction

3.5.4. Hazardous operations

Despite the physical constraint related to the dimension of the collectors that drastically reduced the opportunity of carbon-free operations, the use of PTSC coupled with TS is a strategic choice since it opens the possibility to achieve zero carbon emissions. However, this is possible only under certain operating conditions. In fact, during the summer season, in clear sky conditions, the PRS operation could be conducted by using the PTCS only and the load shifting capability of the TS. This means that carbon-free process can be achieved. However, this might result in hazardous operations due to the following reasons: while the PTSC is feeding the TS, if an NG peak occurs, the risk to open an operating window with too low NG temperature is quite consistent. This is due to the fact that the BO start-up takes few minutes before the water temperature in the TS reaches a secure set-point. This can be observed in Fig. 48. Here, the simulation conditions are referred to the Genoa case with a clear sky condition in July. In this simulation, the BO set-point was 62 ℃, the TS's initial conditions was 76.8 ℃ and the R-value was 1. Following this scenario, the BO started in the early morning for a few hours before the PTSC started (Fig. 48g). Then the entire process was conducted only with the PTSC until the second NG peak load occurred in the evening. Here the BO start-up again but the responsiveness of the system was to slow due to the system thermal inertia. A dangerous operating window was opened

(Fig. 48e). The NG temperature drastically dropped to -13.15 ℃. The TE's local control system must stop the TE operations before it happens. If it does not occur in a responsive manner, air moisture would rapidly condensate and froze on the TE's external surface causing dangerous perturbation on the downstream sensors, while the methane hydrates would take place inside the pipes. The system might be seriously damaged. Thus, this system management approach must be avoided and operators have to renounce the possibility to achieve a carbon-free process. However, the possibility to purse the zero-emissions objective from PRS process was not completely lost as demonstrated in Fig. 49. In fact, by using an appropriate control strategy, it is possible to maintain the BO units completely off. This can be achieved by controlling the TE's power output which must be conducted only in concomitance to the PTSC heat gain at a partial load. This would avoid the TE dragging down the NG temperature during peaks ensuring safe operations. Instead, the early morning NG load can be satisfied by using the JT valves which preheating heat required is sensibly lower than the TE one as commonly known. As shown in Fig. 19g, the minimum NG temperature did not exceed 2.5℃. With such approach, the methane hydrates formation was properly prevented and a 100% carbon-free process was achieved. However, this action implicates the R ratio to be reduced from 1 to 0.3 causing a 66 % reduction of the TE's energy harvesting i.e. 3.6MWh lost on 5.5MWh producible. Once again, by observing the dynamic results of such PRS, the need for proper optimization technique clearly emerges.
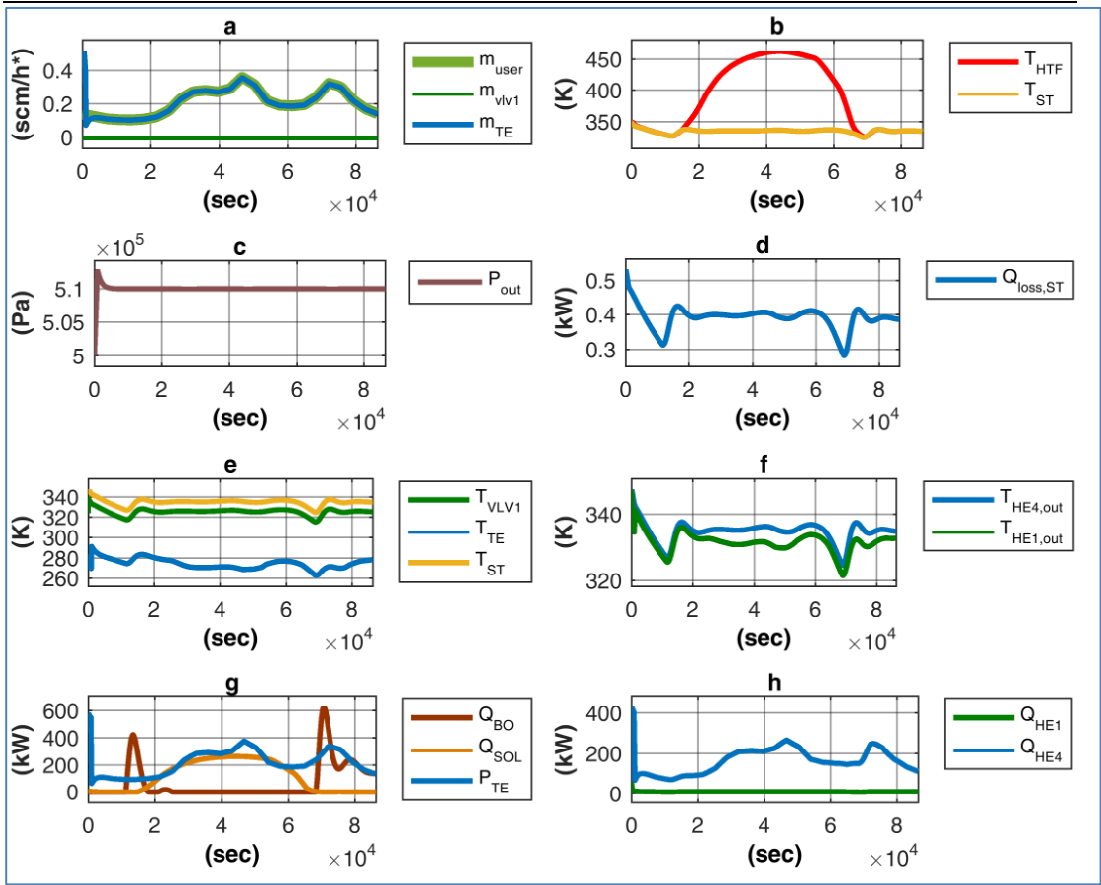
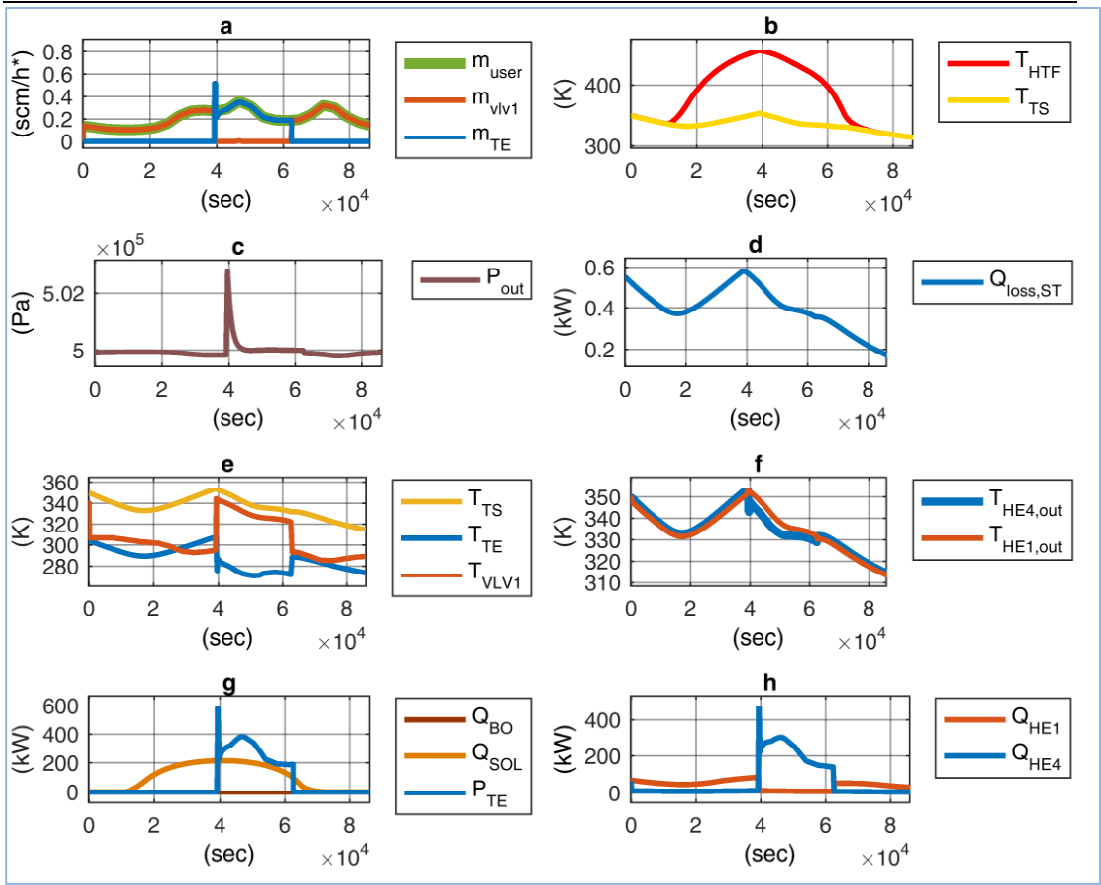Figure 48. In-depth transient analysis: non optimized process.

Figure 49. In-depth transients simulation: optimized operations.

3.5.5. PRS and RETs in brief

In this research, the possibility to employ parabolic trough solar collectors and thermal storage tank in the so-called natural gas pressure reduction stations designed for energy harvesting was numerically investigated. A dynamic model built in the *Matlab-Simulink*® environment based on a real plant operations records was developed and used for performance assessment. Based on the typical average intense days conditions, the energy and environmental performance of the proposed system at different latitudes for the city of Genoa, Naples and Amsterdam was evaluated. The R indicator was introduced to deduce the operational state of the

system. For the proposed case scenarios, the novel configuration enabled a maximum carbon emissions reduction of 33% and 31% and 15% for the city of Naples, Genoa and Amsterdam respectively, in comparison with a conventional plant without solar boosters. The corresponding characteristics average daily emission factors associated to the plant operations calculated were $0.238\frac{kg_{CO2}}{kWh}$, $0.243\frac{kg_{CO2}}{kWh}$ and $0.261\frac{kg_{CO2}}{kWh}$. For these cases, the system state was characterized by an R-value equal to 1. The risk of methane hydrates formation can be practically excluded under these conditions. During winter season, the case related to the city of Amsterdam did not revealed to be energetically effective, thus, operation and maintenance costs might be higher than the effective primary energy consumption reduction. Thus, parabolic trough solar collectors might be a favorable solution for carbon reductions only in clear sky conditions during winter. The possibility to achieve zero-carbon operations in pressure reduction stations was then investigated. The results demonstrated that starting from the 44° parallel, during summer season, this objective is possible to be purse. However, a proper management of the turbo-expander power output must be conducted in order to avoid hazardous operational windows openings. Practically speaking, this foresee a plant conduction characterized by an average R-value of 0.3 which corresponding energy harvesting loss of about 66% with the respect to the fossil-fuel supported case. By observing the dynamic behavior of the system under different operating conditions, the necessity to employ novel accurate algorithm to enable optimal control of the system clearly emerges. In conclusion, the adoption of parabolic solar trough collectors coupled with thermal storage to reduce carbon emissions linked to the European natural gas distribution network is a strategic retrofit measure that policymakers should consider in a responsive manner in order to conduct an intelligent transition to a more sustainable energy scenario.

REFERENCES

[1] M. Farzaneh-gord, A. Arabkoohsar, M. D. Dasht-bayaz, and V. Farzaneh-kord, Feasibility of accompanying uncontrolled linear heater with solar system in natural gas pressure drop stations, Energy 41; pp. 420–428, (2012).

[2] A. Arabkoohsar, M. Farzaneh-gord, M. Deymi-dashtebayaz, and L. Machado, A new design for natural gas pressure reduction points by employing a turbo expander and a solar heating set, Renew. Energy 81; pp. 239–250, (2015).

[3] Duffie JA, Beckman WA. Solar engineering of thermal processes. 2nd ed. New York: Willy; 1991

[4] F. Jafarkazemi, and E. Ahmadifard. Energetic and exergetic evaluation of flat plate solar collectors, Renewable Energy 56; pp. 55-63, (2013).

[5] A. De Risi, M. Milanese, and D. Laforgia. Modelling and optimization of transparent parabolic trough collector based on gas-phase nanofluids. Renewable Energy 58; pp. 134-139, (2013).

[6] F.A. Al-Sulaiman, F. Hamdullahpur, and I. Dincer, Performance assessment of a novel system using parabolic trough solar collectors for combined cooling, heating, and power production, Renewable Energy 48; pp. 161-172, (2012).

[7] S. A. Kalogirou, S. Karellas, V. Badescu, and K. Braimakis, Exergy analysis on solar thermal systems : A better understanding of their sustainability, Renewable Energy 85; pp. 1328–1333, (2016).

[8] P. Michel, Exergy analysis of solar collectors, from incident radiation to dissipation, Renew. Energy 47; pp. 194-202, (2012).

[9]   Lo Cascio, E., Z. Ma, C. Schenone. Performance assessment of a novel natural gas   pressure reduction station equipped with parabolic trough solar collectors. *Renewable   Energy 128; pp.* 177-187, (2018).

[10]   D. Borelli, F. Devia, M. M. Brunenghi, and C. Schenone, Waste Energy Recovery from Natural Gas Distribution Network : CELSIUS Project Demonstrator in Genoa, Sustainability 7 pp. 16703–16719, (2015).

[11]   Honeywell MTG 550, available onlin: https://www.honeywellprocess.com/en-US/explore/products/gas-measurement-and-regulation/gas-expansion-turbines/Pages/turboexpander-mtg.aspx. (Accessed 12/12/2017).

[12]   Pietro Fiorentini, available online: https://www.fiorentini.com/it/it/prodotti/prodotti/regolatori_azione_pilotata. (Accessed 18/12/2017).

[13]   Skytrough, available online: http://www.skyfuel.com/products/skytrough/ . (Accessed 18/12/2017).

[14]   Heat transfer fluid, available online: https://www.paratherm.com/heat-transfer-fluids/paratherm-nf-heat-transfer-fluid/. (Accessed 18/12/2017).

[15]   Redelivery points - SNAM. Available online: http://www.snamretegas.it/en/services/New_Delivery_Redelivery_Points/ (accessed 18/12/2017).

[16]   Motiee M, *Hydrocarbon Process*, Int Ed, pp. 70: 98, 1991.

3.6. Enhanced Flexibility: The Gas Bagging

In [1], the authors introduce and analyze the possibility of employing a novel technique called gas bagging to shift the energy harvesting schedule to night hours or, in general, to a different moment. Gas bagging is based on control of the downstream distribution pressure that can be dynamically regulated as it occurs in the transportation pipeline where, the so-called gas-line-packing [2] technique is used to store the natural gas in the pipeline itself for service continuity, optimization, and speculating purposes. In addition, a set of additional advantages is hidden behind this approach. In general, the added flexibility that is generated facilitates optimal coordination with other processes or resources. For instance, gas bagging might become strategic for coordination with renewable resources, enabling optimal control in smart grids. In addition, gas bagging could unlock the service continuity issue of power-to-gas applications, enabling overnight hydrogen production for hybrid vehicles [3]. Gas bagging enables operational flexibility that could become strategic for optimal electric-vehicle charging scheduling [4] and in a market environment [5]. Furthermore, the increase of the downstream pressure leads to a proportional decrease in the process temperature i.e. the gas-preheating temperature is lower. As described in [6], the temperature reduction in pressure reduction stations is a strategic action for thermal system integration with low temperature heat sources. Thus, gas bagging can also be utilized for system thermal integration purposes. In general, gas bagging is constrained by the physical characteristics of the distribution system and safety measures, generally linked to the infrastructure location, topology and volume, pipeline geometry and type, and second-stage interconnections. Moreover, the typical pressure dynamics characterizing gas bagging should be managed by an appropriate system-control

architecture in order to ensure safe operations excluding the risk of methane-hydrate formation.

3.6.1. System description

In Figure 50, a schematization of the overall system architecture is presented. For the sake of simplicity, a simplified configuration is considered in this paper but more complex systems might also be taken into consideration. Indeed, the proposed system consists of a high pressure (HP) transportation pipeline, a pressure reduction station equipped with a TE working in parallel to a Joule-Thomson valve, a single straight pipe as medium pressure (MP) distribution system and, finally, a set of low pressure regulators (LPR1-3) whose scope is to bring the natural gas at lower pressure (LP) for delivery to end-users e.g. 0.5-0.04 barg. Finally, the electric output of the station can be used for local power demand e.g. to charge electric vehicles or, differently, it can be injected into the electricity grid. However, in most cases, the distribution system could be more complex than the one proposed for this research. For instance, the network topology might include nodes and interconnections that generate concentrated pressure losses enabling, for given downstream volume, a different response in the pressure transient with the respect to a straight pipeline system. In any case, it is possible to define an equivalent straight pipeline system. In addition, for a given distribution network system, there might multiple pressure reduction stations; thus, the need of coordination between redelivery points should be properly considered during gas-bagging operations (as it is done during conventional ones). Demonstrating the effects of the interactions with other redelivery points in the presence of concentrated pressure losses is not within the scope of this research. However, the proposed simplifications have been chosen in order to use a reference system configuration, generally close to real system ones, with the final aim of demonstrating the feasibility and the performance of gas bagging.
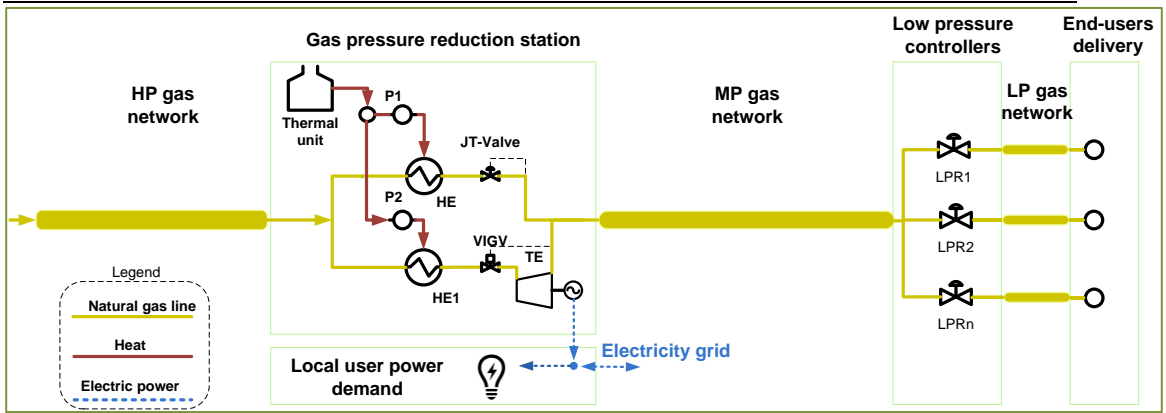
Figure 50. Network structure and subsystem schematization.

3.6.2. Theoretical and technical analysis

Gas bagging is designed to increase the flexibility of energy harvesting from natural gas distribution networks. It can be performed in those pressure reduction stations equipped with TE technology. In general, gas bagging is characterized by two typical modes as described in Figure 51: the *bagging* mode and the *un-bagging* mode. These refer to the operations performed at pressures higher and lower than the conventional set-point respectively. The maximum operating pressure during the *bagging* mode is established by the technical characteristics and safety constraints of the distribution system as will be further detailed below. The same consideration is valid for the maximum *un-bagging* pressure but, for given natural gas flow rate, pressure losses through the pipeline must be accurately considered to ensure a proper natural gas end-user delivery. In the following sections, an insight of the novel gas bagging technique is provided. Issues concerning safety and technical constraints are explored and, finally, advantages and potential applications of gas bagging are presented.
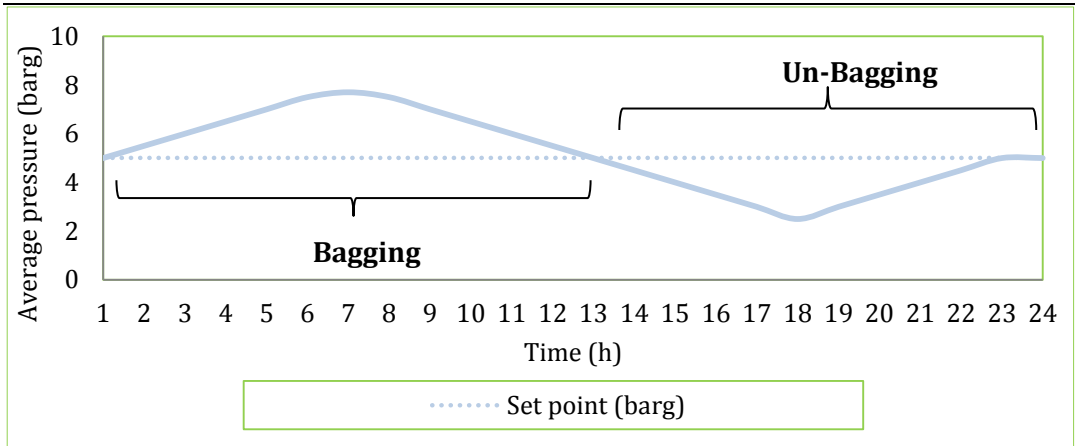
Figure 51. Gas bagging mode representation.

The relevant case scenarios considered in this study are linked to typical flow patterns for a natural gas distribution system located in Italy [7]. As shown in Figure 54, July and January flow patterns for gas-bagging proof of concept purposes are considered. This is because the most hazardous operations (methane hydrates formation) could normally emerge during these periods where the natural gas flows are at their respective bounds. This scenarios have been simulated in a Matlab Simulink environment through a dynamic regime model and further details can be found in [1]. Furthermore, for each scenario, two sets of simulations were performed: one related to the conventional operation where the TE's power output is driven by the natural gas flow rate and the equivalent simulations for the gas-bagging-based operation. The latter were carried out by imposing a power production schedule on the TE and on the Joule-Thomson valve (figure 52). To maintain the TE's power production schedule during downstream pressure transients, a PID controller was used. This, acting on the VIGV of the TE, enables proper power production. For each set of simulations, different control architectures were considered for the thermal unit outlet temperature: constant set-point, PID optimized set-point, and linearized MPC (figures 53). Finally, in order to assess the effectiveness of gas bagging, for a daily time frame, the same energy

139

production was imposed in the conventional simulations. In Table 7, the component design characteristics are reported, while in Table 8, the simulation initial conditions, which were kept equal in both the conventional and gas-bagging simulations, are detailed.
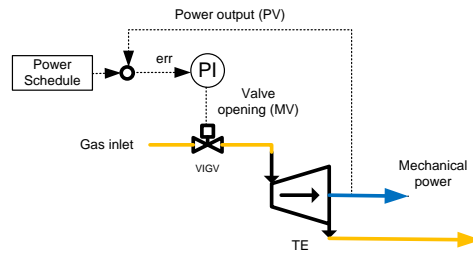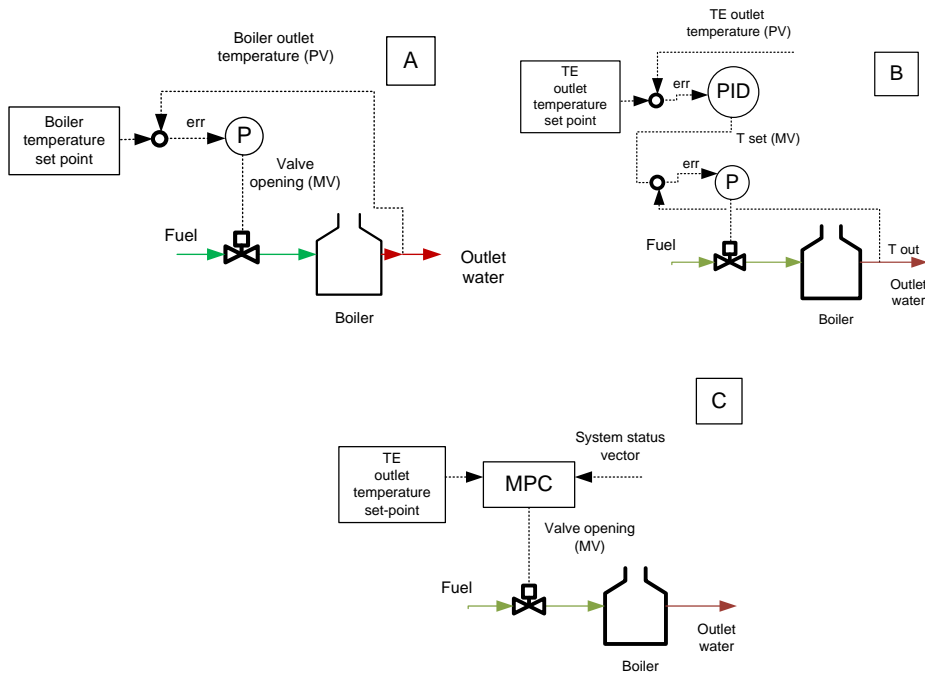

Figura 52

Figure 53. Control architecture: (a) Constant temperature; (b) PID Optimization; (c) MPC optimization.
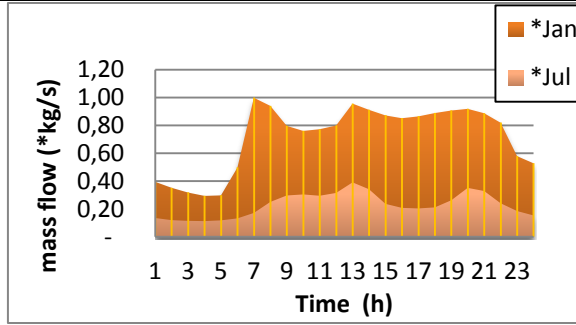
Figure 54. Natural gas (*normalized flows).

Table 7. Components details.

Component	Value	Component	Value
Number of JT lines [-]	1	TE, power tracking PI gains (gas bagging)	1e-4;5e-5
HE overall UA [kW/K]	1.5	BO, nominal power [kW]	1500
HE1, overall UA [kW/K]	16	BO, steel and water mass [kg]	1998; 950
TE, model, *Honeywell*	*MTG550*	BO, steel [kJ/kgK]	502
TE, nominal mechanical power [kW]	550	BO, fuel, P gain (conventional) [kg/s]	9e-4
TE, VIGV, PI gains (conventional) [m]	3.16e-5; 2.71e-8	Hydraulic circuit volume [m^3]	17.6
TE, set point (conventional) [bar]	5.1	Hydraulic circuit heat transfer area [m^2]	25.9
JT-Valve set point (conventional) [bar]	5	Hydraulic circuit overall UA [W/K]	10.36
JT-Valve plug diameter [cm]	5	Downstream pipe diameter [mm]	500
P1, P2, mass flow rate [kg/s]	8; 11.1	Downstream pipe length [km]	118

141

Table 8. Initial conditions of the simulations.

Component	Value	Component	Value
Boiler outlet temperature (K)	360.15	HP pipeline redelivery pressure (barg)	25
MP pipeline inlet pressure (barg)	5	Hydraulic circuit temperature (K)	360.15

Thus, for the conventional winter case (Figure 55a-d), in 24-hour operation, the total energy harvesting is about 12 MWh. As shown in Figure 55d, the energy production is concentrated in diurnal hours due to the typical patterns that characterize natural gas distribution. As shown in figure 55a, the TE reaches its maximum power output for most of the day. The delivery pressure considerably decreases to a minimum of about 1 barg while the MPC controller does not lead to constraint violations for the TE's outlet temperature i.e. the risk of methane hydrates can be excluded (Figure 55b-d). The same energy output, can be shifted to night hours with the gas bagging (Figure 55e-h). In this case, a maximum bagging pressure of about 8 barg is achieved. Following figure 55d, in order to compensate the downstream-pressure increase, the TE's PID controller gradually increases the gas flow rate during the *bagging* mode without overstepping the maximum inlet gas mass flow rate of the TE. The minimum pressure achieved (Figure 55f) in the gas *un-bagging* mode is about 0.75 barg. This is enough to guarantee a proper operation for the low-pressure regulators. However, the risk of achieving too low delivery pressures can be attenuated by opening the Joule-Thomson valve, enabling pressure increase. Finally, the gas temperature at the outlet of the TE remains close to the set-point thanks to the MPC controller, i.e. the risk of formation of methane hydrates is avoided.
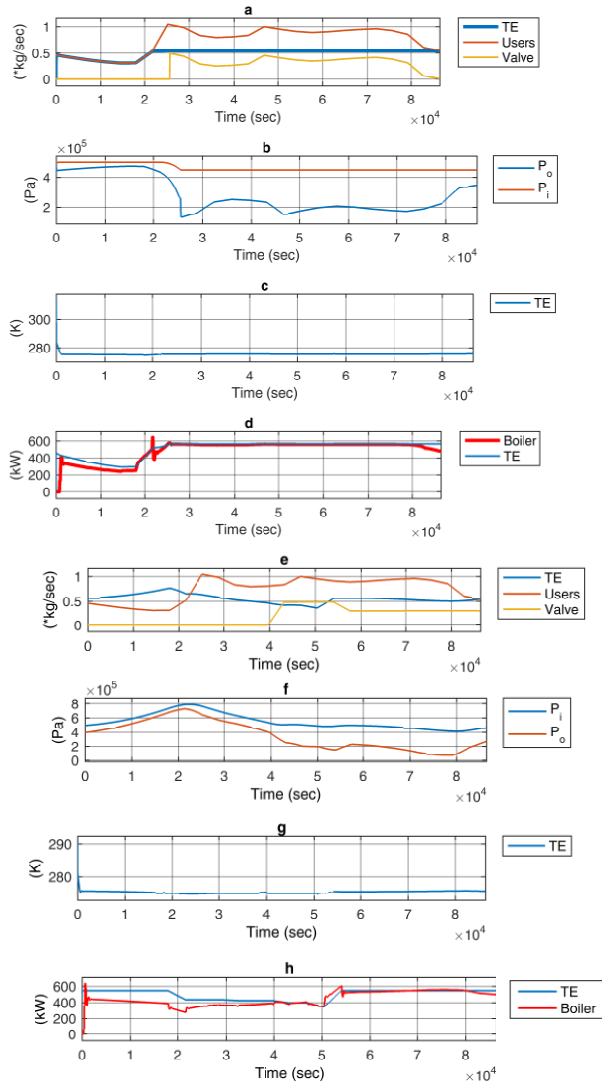
Figure 55. Winter scenario: (a-d) Conventional; (e-h) gas bagging.

In figures 56a-d, it is possible to observe the dynamic behavior of the system for the conventional operation in a typical summer scenario. More precisely, the total TE energy production is about 5 MWh per day. The minimum gas delivery pressure at the end of the pipeline segment is relatively high due to the lower mass flow with respect to the winter case. No hazardous operations are detected in this

case. Furthermore, in figure 56e-h, the dynamic behavior of the system for the bagging operation is presented. Here, a maximum bagging pressure of about 9 barg is achieved, while the modest gas flow rate involved does not seem to significantly affect the delivery pressure at the end of the pipeline. Finally, no violation of the TE's outlet gas temperature was observed thanks to predictive control.
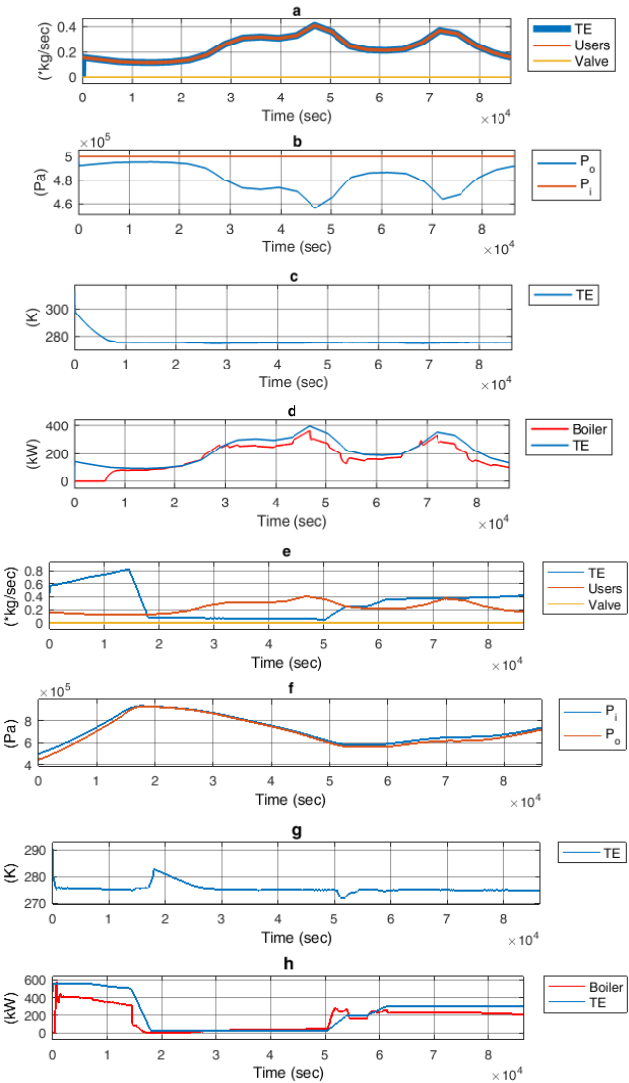

Figure 56. Summer scenario: (a-d) Conventional; (e-h) gas bagging.

In table 9, the operational performance of the system for the gas-bagging mode are reported in comparison to the conventional mode for the winter and the summer case scenarios. For each of them, three different control architectures have been tested for the thermal unit control. Namely, constant temperature, PID, and MPC. Following, the fuel cost, calculated as the fuel mass consumed multiplied by a reference constant price (€0.8/kg) is reported together with the gross income calculated as the difference between the income generated by the electricity production (€0.15/kWh) minus the operational cost. In addition, the value of the average isentropic efficiency of the TE and the average boiler thermal efficiency are shown in table 9. These are calculated as the integral over the 24-hour operations. Furthermore, with reference to the thermal unit control, the possibility of observing unstable behavior of the controller might arise. This is specially verified when employing PID controller. To address this issue, a qualitative index named boiler behavior has been defined as reported in table 9. When oscillation occurs, frequent step changes, ranging from the lower to the upper bound were observed. This behavior might be difficult to avoid even with a proper tuning of parameters. Thus, being not physically acceptable, this kind of behavior must be avoided. Furthermore, the average outlet temperature of the gas is reported in table 9. This is calculated as the integral over the 24h operation. Finally, in the last column of table 9, the risk of methane-hydrate formation is presented. A hazardous operation occurs when the natural gas temperature leaving the TE goes below 2°C during system operations. Differently, the operation can be considered safe. In addition, for the given case scenario, the application of gas bagging to those systems with smaller downstream distribution system is possible for pipeline networks longer than 88.125km (0.5m in diameter) with an energy penalization of about 25.8%. For smaller distribution networks, it is highly recommended to limit the power production schedule in order to reduce the daily energy production.

Finally, for the case study presented, it was possible to perform the gas-bagging operation and the MPC control architecture turned out to be the most appropriate option which guaranteed cost-effective system operations for this case study. Gas-bagging operations result to be more economically convenient with respect to the conventional mode. This is due to the complex system dynamics involved which, in general, foresee different operations of the TE and the Joule-Thomson valve. At this stage, it is worth recalling that it might be possible to determine the optimized operating schedule i.e. optimal bagging and un-bagging pressure, which could lead to even better performing operations.

With reference to table 9, for the gas-bagging simulations, for the winter case scenario, a modest decrease in the operational costs can be observed for the conventional mode for constant set-point, PID, and MPC-based thermal unit control respectively. This issue is linked to the Joule-Thomson valve opening which occurs with different dynamics between the two modes. In any case, MPC ensures a safe operation in both simulation scenarios. Moreover, MPC enables a stable behavior of the thermal units compared to PID control, which tends to generate undesired thermal load oscillations. With reference to the gas-bagging summer scenario of table 9 instead, MPC is capable of significantly reducing the operational cost by 23.3% per day with respect to the constant temperature control, while ensuring safe operating conditions. This operational cost reduction is more emphasized during summer than winter since, for a given temperature set-point for the control of the boiler unit, at lower gas mass flow rate, a thermal overproduction occurs. This means that the natural gas is excessively preheated before entering the TE. As a result, the outgoing natural gas will be uselessly, relatively hot. Thus, an optimized control has shown that it enables significant energy saving.

Table 9. Gas bagging versus conventional.

case	Mod.	Control	Fuel cost (euro)	Gross Income (euro)	TE output P (kWh)	Average TE isentropic efficiency	Thermal unit energy output Q (kWh)	Average thermal efficiency	Boiler behavior	P/Q (-)	Average outlet temp. (K)	Operation
January	Gas Bagging	Const. T	816	505.10	12010	0.54	11050	0.73	No Oscillations	1.09	278	Haz
		PID	800	521.10	12010	0.54	10825	0.73	Oscillations	1.11	277	Haz
		Lin. MPC	800	520.00	12000	0.54	10800	0.73	No Oscillations	1.11	275	Safe
	Convention	Const. T	850	470.00	12000	0.54	11640	0.75	No Oscillations	1.03	278	Safe
		PID	767	564.00	12100	0.54	10330	0.73	Oscillations	1.17	271	Haz
		Lin. MPC	848	437.90	12100	0.54	11690	0.74	No Oscillations	1.04	275	Safe
July	Gas Bagging	Const. T	430	157.95	5345	0.48	5320	0.65	No Oscillations	1.00	298	Safe
		PID	387	200.95	5345	0.48	4763	0.63	No Oscillations	1.12	289	Safe

	Lin. MPC	330	256.30	5330	0.45	4000	0.62	No Oscillations	1.33	275	Safe
Conventional	Const. T	414	175.82	5362	0.50	4893	0.64	No Oscillations	1.10	282	Safe
	PID	377	210.62	5342	0.52	4700	0.63	Oscillations	1.14	280	Safe
	Lin. MPC	365	218.00	5300	0.50	4320	0.63	No Oscillations	1.23	276	Safe

3.6.3. Gas bagging in brief

The degree of flexibility of gas bagging is strongly dependent on the technical characteristics and the safety constraints of the pipeline system. The risk of conducting hazardous operations can be properly managed by employing a model predictive controller for the boiler units. In addition, a model predictive controller enables operational cost reduction. Thus, from a reference case scenario consisting of a pipeline of 118 km, the authors have demonstrated through numerical dynamic simulations that gas bagging allowed to completely shift the energy production to night hours while maintaining safe operations i.e. no risk of methane hydrates formation. Furthermore, the results highlight that, for the proposed case study, a daily decrease of about 6% of the operational cost in the winter operations can be achieved with gas bagging. Similarly, in summer periods, the operational cost reduction was about 10%. In addition, for given power production schedule, the effectiveness of gas bagging for pipeline lengths smaller than 25%, 50%, and 75% was assessed. Results demonstrated that the 25% reduction did not affect the gas-bagging effectiveness or the energy production. At the same time, gas bagging can be performed safely without any system-constraint violation. This condition is verified by reducing the pipeline length by 50%. In this case, the system operates at its maximum tolerable conditions and an energy loss of about 25.8% has been recorded with respect to the initial case scenario (117 km of pipeline). For smaller distribution volumes, in order to perform gas bagging, the power production schedule must be limited in order to reduce the energy production. Finally, gas bagging can be performed at different levels but accurate analysis and tests must be conducted before implementation. Concluding, gas bagging has revealed itself to be a strategic method to increase energy harvesting flexibility from natural gas distribution networks enabling better integration into smart grids contexts. Future research steps should involve an in depth analysis of the environmental

performance of the gas bagging compared with the conventional operations. Further, simulations using computational fluid dynamics for an in-depth understanding of downstream distribution phenomena under variable boundary conditions and optimal scheduling should be consider as well.

REFERENCES

[1]   Lo Cascio, E., De Schutter, B., Schenone, C., Flexible energy harvesting from natural gas distribution networks through line-bagging. *Applied Energy 229*, pp. 253-263, (2018).

 [2]   Ríos-Mercado, Roger Z., C. Borraz-Sánchez, Optimization problems in natural gas transportation systems: A state-of-the-art review, Applied Energy 147, pp. 536-555, (2015).

[3]   F. Alavi, E.P. Lee, N. van de Wouw, B. De Schutter, Z. Lukszo, Fuel cell cars in a microgrid for synergies between hydrogen and electricity networks, Appliel Energy 192, pp. 296-304, (2017).

[4]   L. Luo, S. Zhou, H. Huang, S. Gao, J. Han, X. Dou, Optimal planning of electric vehicle   charging   stations comprising multi-types of charging facilities**,** Applied Energy, 226,   pp. 1087-1099, (2018).

[5]   T. K. Kristoffersen, K. Capion, P. Meibom, Optimal charging of electric drive vehicles in a   market environment, Applied Energy 88, pp. 1940-1948, (2011).

[6]   Borelli, Davide, F. Devia, E. Lo Cascio and C. Schenone, Energy recovery from natural gas pressure reduction stations: integration with low temperature heat sources, Energy Conversion and Management, 159, pp. 274–283, (2018).

[7]   E. Lo Cascio, Z. Ma, C. Schenone, Performance assessment of novel natural gas pressure reduction station equipped with parabolic trough solar collectors, Renewable Energy 128, pp. 177-187, (2018).

4. Guidelines to digitaliazation

In this section, the author will provide the guidelines to digitalisation for integrated natural gas distribution system highlighting the key categories and factors involved in the process.

4.1. Key categories and factors

Following, the critical factors involved in the digitalisation process are reported. In general, these factors can be divided in four categories (figure 57-58) namely related to the area of the *process optimisation*, predictive *operation and maintenance* (O&M), *integration and interaction* with external processes or users for coordination purposes and, finally, *safety area*. The process optimisation area involves those factors necessary to conduct local optimisation of the process. To be more precise, local optimisation should be performed by considering external processes and factors (when those factors exist). As previously highlighted, the process optimisation task requires that all the process thermodynamic variables to be monitored. All these variables define the process status at every time step. Also, digital twin can be employed as decision support and management tool. Digital twin consists of a digital deterministic dynamic model of the local process. This can be used for online or offline process control. At this stage, it is worth to recall that the digital twin, might involve the use of load forecasting technique to simulate the performance of the process for upcoming time slots.

Predictive analytics solutions enable an optimal maintenance activity which is directly linked to an operational cost reduction and, in most case, to a safety increase. Also, state-of-the-art analytic software is capable of monitoring unusual

151

changes in the equipment and technology behaviour before the failure occurs. In this way, undesired downtimes could be avoided or reduced. According to the most recent experiences [1], these advanced analytics solutions can identify problems days, weeks or even months before they occur [1]. The predictive analytics tools enable personnel to understand how non-performing operations impact on the financial performance of the processes.

Concerning the GE1 experience [2], the vibration of the turbo expander is one of the critical parameters to be monitored to enable optimal O&M. This is because most faults were recorded on this equipment. To be more precise, this would involve the power shaft functioning [3].

The interaction with complementary external processes, e.g. the natural gas compressor stations is crucial to be managed appropriately especially for gas bagging application previously introduced. On one side, this would require direct communication and coordination between the PRS and the compressor station for natural gas pressure optimisation for transportation purpose. On the other hand, a set of critical parameters must be monitored at low-pressure regulation level. This aspect will be further detailed.

PRS location usually is naturally suitable to host electric vehicles recharging stations due to their area characteristics. This means that the recovered energy can be further exploited locally by electric vehicles; thus, avoiding grid injection. To achieve sustainable coordination and local system optimisation, electric vehicles should be capable of communicating their arrival time, and energy needs to the PRS controller. Similarly, the PRS controller should be able to express the availability for charging electric vehicles (two-way communication). For this purpose, geofencing technologies could be employed.

Last but not the least, the digitalisation process should adequately transform the safety issue as well. How would digitalisation impacts the safety in PRS operations

and management? The main problems are related to the monitoring of three main parameters: the natural gas leaks, the TE's vibration and the environmental noise. Besides, a smart smoke detector should be employed. The vibration monitoring is necessary both for predictive maintenance but also to detect imminent equipment failures like the power shaft problem previously mentioned. This is quite risky since when the failure happens, the internal rotor hit the machine's case internally; thus generating the risk of fires and blasts. For this reason, prediction algorithms should be employed to detect hazardous operations. Finally, noise monitoring is also crucial when using turbo expander technologies: in some operating conditions which depend on the velocity of the natural gas leaving the turbo-expander and the geometry of the pipeline, generates swirling dynamics in the fluid behaviour which in translated in operations characterised by the dangerous noise level.
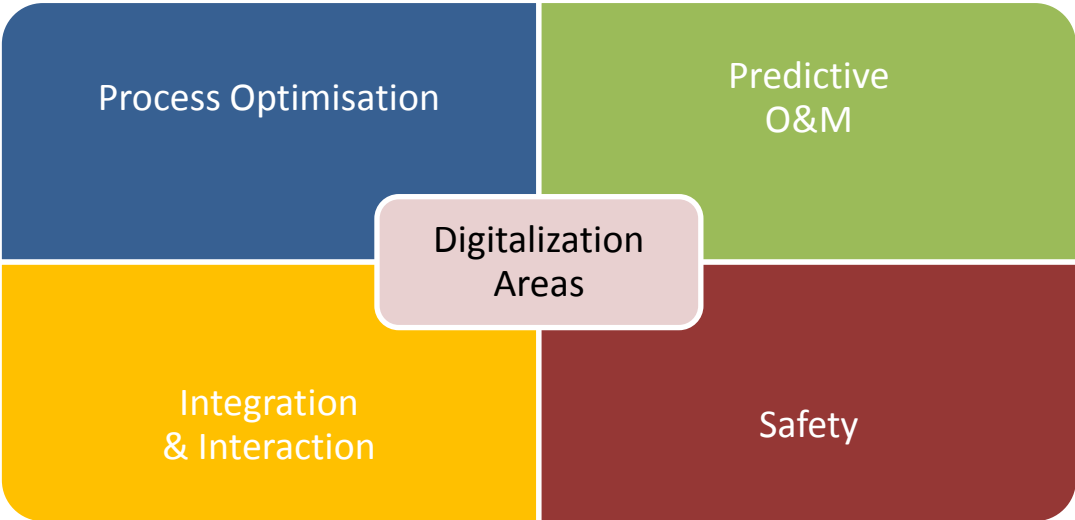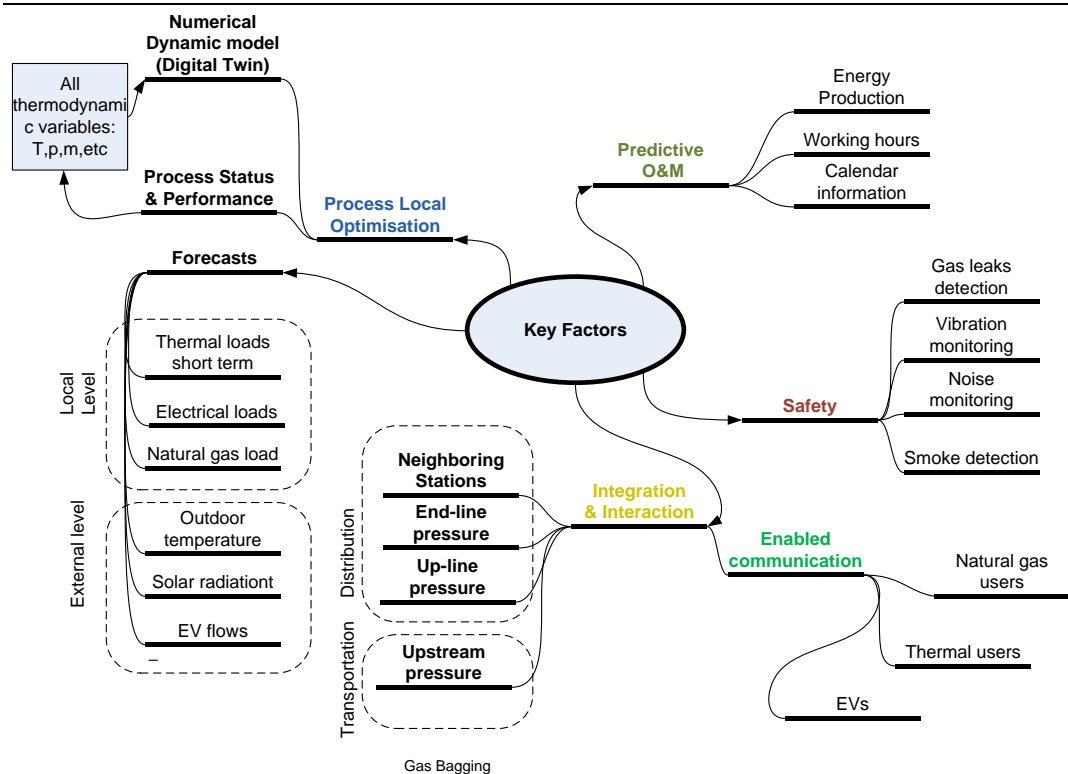

Figure 57. Digitalisation areas.

Figure 58. Digitalisation key factors.

4.2. ICT architecture

The overall ICT architecture is represented in figure 60. All the data flows are used to enable the near-optimal coordination employing cloud computing technology [4]. This data flow management approach, open up the possibility to achieve an effective system control at higher level; thus, avoiding disaggregated optimisations processes which might lead to non-effective system performance, i.e. higher carbon emissions. Also, the cloud computing technology becomes essential at the problem optimisation stage due to the complexity of the optimisation problem itself, in fact, cloud computing are characterized by higher computational power which would enable faster optimisation problems.

To be more precise, concerning figure 60, the communication infrastructure foresees a series of data to be acquired from upstream to end-users. The communication infrastructure starts with the enabled communication between the compressor stations, where the natural gas transportation pressure is established, and the cloud computing service. The researchers in the past have deeply analysed the optimal transportation pressure problem that impacts on the natural gas transportation cost. However, in a digitalisation perspective, new challenges arise if a cooperative approach between the transportation and the distribution is adopted. In fact, the optimal pressure issue can be transformed into a cooperative optimisation problem where a game-theory-based control approach can be utilised. Practically speaking, if a new business model is employed, the economic income deriving by the energy harvested by the PRSs (which depends also on the delivery pressure) can be shared with the transportation company (which manage the delivery pressure). In this perspective, the economic transactions between the transportation and the distributor could be dynamically adjusted by intervening on the delivery pressure of the natural gas. As known, at higher pressures corresponds higher operating costs for the transportation (higher work for compressor stations) and higher potential income for the distributor (the expansion ratio decreases the specific work of the turbo expander increases). For the two players, a Naish equilibrium [5] might exists; thus, this would be translated into a more efficient process for the these two sub-sectors of the gas chain. If a Naish equilibrium does not exists, at least, the flexibility of the system could be further enhanced by manipulating the natural gas transportation pressure. In any case, to achieve this objective, it would be necessary to set-up an ICT structure enable the required monitoring and control.

The local control of the PRS also monitors the upstream pressure since it is necessary information for the local optimisation problem. More precisely, this information becomes fundamental when a gas bagging application, previously

described, is implemented. Similarly, the gas bagging application, requires the constant monitoring of the up-line pressure and the down-line pressure of the distribution pipeline, to maintain safe system operations and reliable gas delivery service. Of course, the monitoring of these parameters is essential also for conventional processes, for safety and reliability purposes as well.

In addition to these parameters, also the two-way communication is enabled with other PRSs connected to the same distribution branch. This is necessary in order to coordinate the gas bagging operations as previously appropriately described.

End-users should also communicate their actual gas consumption to the central cloud-based-system to perform a proper loads coordination during online system control or for optimal scheduling of the energy production. For this purpose, the implementation of the smart meters becomes crucial (figure 59). In Italy for instance, the first implementation process of the smart meters, generally known as the "roll-out", for electricity distribution has been already completed in 2018. The Enel smart meter will be now substituted by the open smart meter which embeds advanced characteristic designed for metering, analysis and, the most important, communicate with home automation systems. Differently, the roll-out process of natural gas smart meters, with remote communication, is taking longer due to some factors mostly related to the state-of-the-art of the technology. More precisely, the main barrier that sharply limits the diffusion of such technology is related to the limited energy autonomy of this system which depends on the embedded battery. Of course, the use of AC is not allowed due to safety reasons. However, these technologies are essential to enable the smart-demand response.
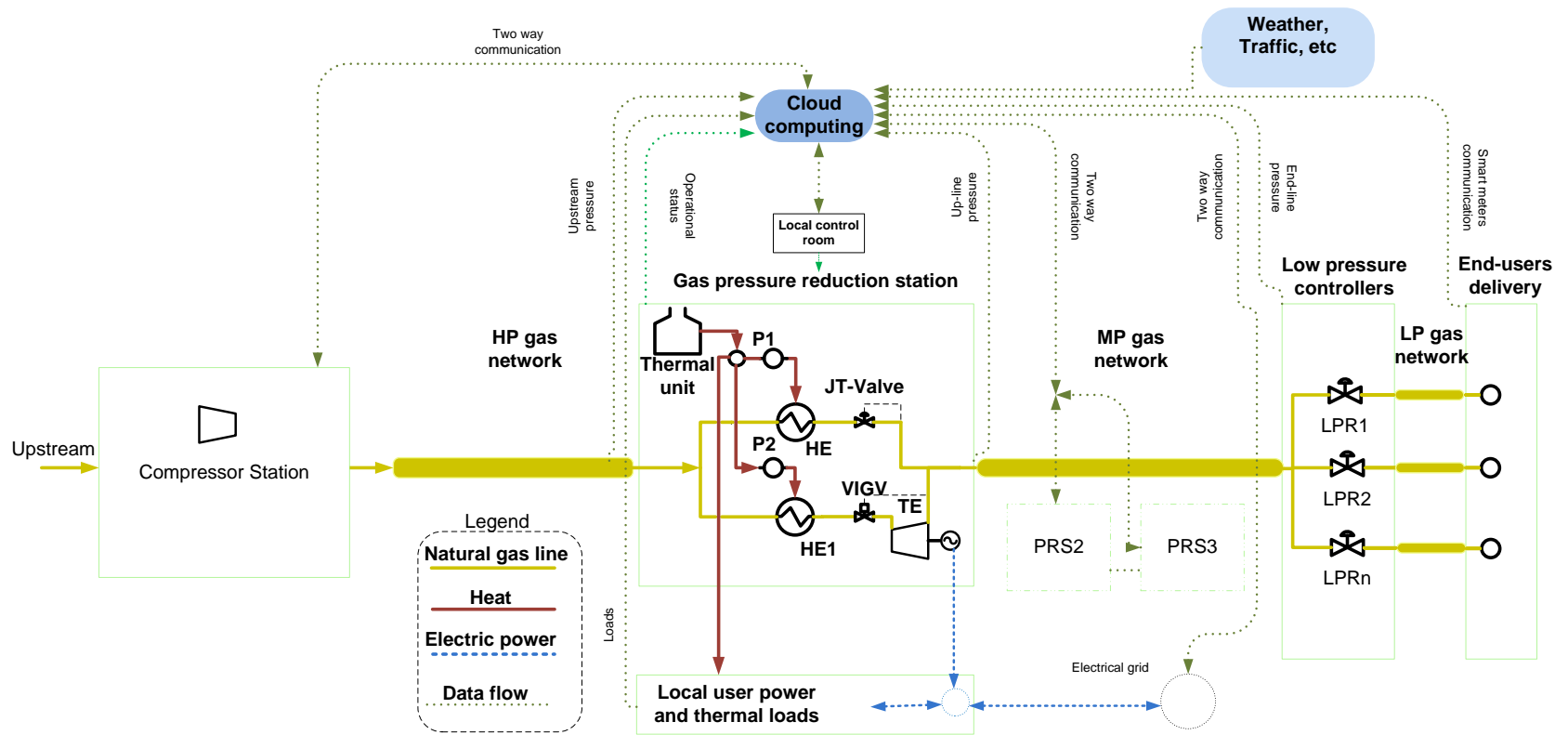

Figure 59. Smart gas meter [6].

157

Figure 60. ICT architecture.

4.2.1. Risks of the cloud computing

There are some security issues related to the could computing when applied to PRS and whole system control. These, are mostly associated with the volatility of the information stored and the data security. The risks can be summarised in two main points: data security and privacy, and service continuity.

In fact, for the first case, for end-users, to store personal data might represent a risk of violation of personal privacy. This becomes easy to imagine when one thinks about the data relatives to energy consumption. In fact, from these data, it would be theoretically possible to reconstruct people's habits when they are living at home. The degree of accuracy in users' behaviour predictions (user profiling) might be impressing if coupled with water, electricity and gas consumption metering at the same time. If employed, Wi-fi connections might be hacked, and data loss could occur. In a competitive and open energy market, this represents a risk for the industrial security.

At the design level, problems relative to the service continuity issues must be taken into consideration when could services are used. For this reason, redundant clouds are employed by established companies, but the problems could anyway emerge due to download and upload speed issues. Thus, a failure in the cloud service would be translated into a failure in the gas, electricity and thermal energy delivery services is a sort of "domino effect" dynamic. This aspect still requires a more in-depth investigation. In general, to define a unique strategy might not be the right approach to this problem since every system has its characteristics, i.e. different response to failure. For this reason, once again the use of a digital twin becomes essential. One solution could be the use of a passively induced local control based on on-site computers. This passive switch should ensure service continuity to the natural gas distribution and electricity as well. Of course, the optimal control and

the proper coordination of the system wouldn't be possible anymore during cloud service's failure.

4.3. Incentives design

An incentive mechanism, design ad-hoc for the energy recovery in natural gas pressure reduction station has not been defined in most European countries yet. For the power injection into the national transportation grid, usually, the energy produced by the turbo-expander is remunerated with a tariff derived from the cogeneration regulatory framework and adapted according to a bilateral agreement between the producer and the electricity transportation company. However, there might be many different scenarios where the regulatory framework does not provide a clear answer relative to the energy remuneration and incentives. The problem has been arisen by the author different researchers [7]. Just for instance, as highlighted in [7], the thermal energy for the natural gas preheating phase, could be provided by renewable resources, by conventional fossil fuels or by a hot mix, as it happens in [7] and [8]. The authors have investigated this problem in [7], and the solution might be relatively simple: the energy output should be weighted based on the thermal energy production and multiplied for the dedicated tariff.

Also, the limitation of the regulatory framework arises at a more higher level. In this sense, as highlighted by [9], the energy recovery process requires up to 5 times more thermal energy than the process based on the use of conventional Joule-Thomson valves. For this reason, the overall performance of the system must be verified and quantified based on the performance of a baseline thermal energy need that should be represented by that conventional process. This aspect is fundamental, and it should be taken into consideration during the regulatory framework design phase to enable reliable and adequate energy remuneration. To achieve this accurate performance monitoring, once again, the use of reliable digital twin would be an asset. For given boundary and operating conditions, the

digital twin would be capable of simulating a parallel process, based on Joule-Thomson valves, which is necessary to define the WER index clearly described in [9]. The WER index establishes the effectiveness of the process performed at every time step.

Of course, in this perspective, a further tariffs differentiation for injected and locally exploited energy should be foreseen.

4.4. Performance monitoring and post-validation

The objectives of the digitalisation process aim to improve the quality of the at different levels: process control, operation and maintenance, integration and integration and, of course, safety. However, the implementation of dedicated ICT infrastructures should justify the actual benefits regarding energy efficiency and flexibility that both lead to environmental emissions reduction. However, these two objectives should be appropriately monitored and validated: here, a new challenge starts.

The post validation process is a complex objective to be achieved. It depends on the characteristics of the energy system involved, the interactions with external users or processes and the overall benefits that might be achieved by these interactions. In reality, policymakers should be aware that digital technology could increase the energy consumption at the end of the story. For this reason, a post-validation process must be foreseen. Differently, the risk of the digital revolution, ending up only with a "...it was only good business for some companies..." becomes consistent. The primary objective of the digitalisation process of the energy industry is to reduce the overall carbon emissions attenuating the global-warming.

The simple question is: how it would be possible to validate the effectiveness of digitalisation in a such complex, multi-energy, integrated environment?

First of all, the monitoring of the effectiveness of the digitalisation should be undertaken at two levels: locally; thus, analysing the energy performance of the process like the PRS but also at higher level, to understand the impact of digitalisation at the global level. In any case, paradoxically, the digitalisation is the answer to the question. Once again, the use of advanced modelling tools might be useful.

At global level, when energy systems and process are locally integrated to enhance flexibility and energy efficiency, when the consumers become prosumers, when complementary sectors such as transportation are involved in the coordination and optimization process, e.g. electric vehicle recharging and/or vehicle to grid applications, the need of integrated assessment modeling clearly emerges. Integrated assessment modelling is a type of scientific modelling often used by the environmental sciences and environmental policy analysis [10]. The modelling is integrated because ecological problems do not respect the borders between academic disciplines [10]. Integrated assessment models, therefore, integrate knowledge from two or more domains into a single framework [10]. Integrated modelling is referred to as assessment because the activity aims to generate useful information for policy making, rather than to advance knowledge for knowledge's sake [10]. Integrated assessment modelling is that part of an integrated assessment that relies on the use of numerical models [10].

Instead, at local level, the performance assessment of the process can be verified locally using the digital twin previously described.

REFERENCES

[1]   https://blog.schneider-electric.com/industrial-software/2015/07/17/optimizing-operations-   maintenance-predictive-analytics/

[2]   CESLIUS project, available online: http://celsiuscity.eu/ (accessed

10/10/2017)

[3] Gas expansion Turbine, available online: https://www.honeywellprocess.com/en-US/explore/products/gas-measurement-and-regulation/gas-expansion-turbines/Pages/default.aspx (accessed 06/08/2017).

[4] Cloud Computing, available online: https://it.wikipedia.org/wiki/Cloud_computing, (accessed 02/10/2018).

[5] Naish Equilibrium, available online: https://en.wikipedia.org/wiki/Nash_equilibrium, (accessed 02/10/2018).

[6] Open Smart Meter, available online: https://www.webnews.it/speciale/enel-open-meter/, accessed (02/10/2018).

[7] Lo Cascio, E., Z. Ma, C. Schenone. Performance assessment of a novel natural gas pressure reduction station equipped with parabolic trough solar collectors. *Renewable Energy 128; pp.* 177-187, (2018).

[8] E. Lo Cascio, Z. Ma, C. Schenone. Performance assessment of a novel natural gas pressure reduction station equipped with parabolic trough solar collectors. Renewable Energy 128, pp. 177-187, (2018).

[9] E. Lo Cascio, D. Borelli, F. Devia, C. Schenone. Key performance indicators for integrated natural gas pressure reduction stations with energy recovery. Energy Conversion and Management 164,pp. 219-229, (2018).

[10] Integrated Assessment Modelling, available online: https://en.wikipedia.org/wiki/Integrated_assessment_modelling, (accessed 02/10/2018).

5. Discussion and Conclusions

In the first part of this research, the author presented a collection of his research contributions to the topic related to the energy management in natural gas pressure reduction station equipped with turbo expander technology. Furthermore, Starting from the state of the art and the authors' prior research contributions, the guidelines for digital retrofit for a specific kind of distributed energy system, were outlined. More precisely, renewable integration, cogeneration, temperature reduction strategies, integration with external processes/users and, finally, the most recent system management techniques have been taken into consideration during the guidelines definition. Following, a discussion of the different aspect that gravitate around the digitalisation of gas distribution industry will be presented.

5.1. ICT, control and flexibility

From the conducted research, it clearly emerge the need to intervene at differently levels in order to properly enable a digitalisation process of integrated natural gas distribution systems. To be more precise, technically speaking, the digitalisation process does not require complex ICT systems. In fact, the implementation of few dedicated sensors and a digital infrastructure are the only retrofits required for this purpose. The digitalisation challenges are more related to the optimisation of the large-scale system, the data security and the regulatory framework. In fact, with reference to the optimisation task, the use of predictive algorithms and efficient optimization problem is required. When online optimisation is conducted, the computation of the optimal solution must be conducted in advance for every time slot, thus efficient computation and accurate forecasting algorithms are needed. For these prurposes, the use of digital twins would be recommended in order to perform control optimisation and prediction both online and offline. This represents a challenging task when complex large-scale systems are involved.

The ICT architecture and a proper system control would open up the possibility to increase the system flexibility by employing gas bagging management strategy. In a perspective of local energy exploitation, the gas bagging is strategic since the possibility to avoid electrical storages is enabled. For this purpose, once again it would be fundamental to design proper control algorithms in order to achieve safe operations and services continuity. In addition, the ICT architecture should be designed in order to enable a two-way communication with the compressor stations. This would open the possibility to find optimal delivery pressure of the gas transmission and distribution operators and coordinate gas bagging applications.

5.2. Data security & Domino Effects

The data security problem must be carefully considered. Hackers attacks must be prevented and dedicated protocols should be designed in order to protect and to handle these situations. Differently, the data kidnapping social phenomena could become even more frequent.

The reliability of the cloud computing service and the component failure, must be managed with accuracy and, for this reason, it would be necessary to employ analytics software for predictive O&M and assess the effect of a digital failure on the processes of the multi-carrier system; thus, excluding the possibility of a sort of digital domino effect that could emerge from the integration of the different systems. For instance, a fault on the turbo expander would be reflected on the other processes performance, thus, it is fundamental to assess resilience of the systems to components failures.

5.3. Regulatory framework and business models

The regulatory framework must be redesigned according the new paradox involved. At the current state, the regulatory framework represents a barrier to the digitalisation; thus, limiting the CO_2 saving potential deriving from a digital retrofit. New incentives must be properly designed especially for pressure reduction stations characterized by a renewable thermal energy production.

A new business model between the transportation and the distribution sectors of the natural gas should be considered in order to unlock the possibility to coordinate the two sectors in an optimal way basing on a game-approach; thus enabling an overall carbon emissions reduction from a part of the natural gas chain.

The post-validation of the digitalisation must be carefully considered due to the risk of higher energy consumption. For this purpose, the use of digital tools would be strategic.

Concluding, from this research, it clearly emerges that there are several issues at different levels that must be taken in consideration to achieve a proper digital intervention, e.g. ICT architecture design, energy management system creation, joint business models creation, flexible incentives design, cybersecurity, post-validation of the environmental performances of the whole digital retrofit. All these issues, from a specific point of view, make the digitalisation process an important challenge for policymakers, techs companies, industries and researchers. But, from another point of view, digitalisation represents an important element that, if it is

appropriately managed and contextualised, it will create new commercial opportunities; thus, boosting-up new and existing economies. In other words, digitalisation might represent a tool to partially manage the economy and the environmental crisis, helping to achieve Sustainable Development Goals but, of course, a proper orchestration will be needed. However, in author opinion, regarding the energy sector, one of the main problem of this emerging digital scenario consists in the risk of a speculative behaviour by techs companies that would be translated at the end in a good commercial affair rather than a strategic action for environmental and economic sustainability. In this perspective, policymakers should be paying attention to this aspect that represents a latent risk whose manifestation, whose damage, would not be possible to be metered (or detected) in the future because, in other words, the question would not be about "what has been made so far...". The question would be about "what has not been made so far...", which is rather than difficult to be quantified. Concluding, a set of integrated multidisciplinary research programs are required to address in a strategic way the digitalisation issue.

APPENDIX

Author research papers and prior contributions to the topic:

[1]   Lo Cascio, E., De Schutter, B., Schenone, C. (2018). Flexible energy harvesting from natural gas distribution networks through line-bagging. **Applied Energy**, 229, pp. 253-263.

[2]   Lo Cascio, E., Ma, Z., Schenone, C. (2018). Performance assessment of a novel natural gas pressure reduction station equipped with parabolic trough solar collectors. **Renewable Energy**, 128, pp. 177-187.

[3]   Lo Cascio, E., Borelli, D., Devia, F., Schenone, C. (2018). Key performance indicators for integrated natural gas pressure reduction stations with energy recovery, **Energy Conversion and Management**, 164, pp. 219-229.

[4]   Lo Cascio, E., Von Friesen, M. P., Schenone, C. (2018). Optimal retrofitting of natural gas pressure reduction stations for energy recovery. **Energy**, 153, pp. 387-399.

[5]   Borelli, D., Devia, F., Lo Cascio, E., Schenone, C. (2018). Energy recovery from natural gas pressure reduction station: Integration with low temperature heat sources, **Energy Conversion and Management**, 159, pp. 274-283.

[6]   Lo Cascio, E., Ma, Z., Borelli, D., Schenone, C. (2017). Residential building retrofit through numerical simulation: a case study. **Energy Procedia**, 111, pp. 91-100.

[7]   Lo Cascio, E., Borelli, D., Devia, F., Schenone, C. (2017). Future distributed generation: An operational multi-objective optimization model for integrated small scale urban electrical , thermal and gas grids, **Energy Conversion and Management**, 143, pp. 348–359.

[8]   Borelli, D., Devia, F., Lo Cascio, E., Schenone, C., Spoladore, A. (2016). Combined Production and Conversion of Energy in an Urban Integrated System, **Energies**, 9, pp. 1-17.

Acknowledgements to reviewer